

EVALUATION OF THE EFFECTS OF COLLAGEN-INDUCED ARTHRITIS AND METAL  
HYPERSENSITIVITY ON OSTEOLYSIS AND THE INFLAMMATORY RESPONSE TO  
WEAR DEBRIS IN THE MURINE AIR POUCH

A Thesis by

Nora M. Strong

Bachelor of Science, Kansas State University, 2006

Submitted to the Department of Biological Sciences  
and the faculty of the Graduate School of  
Wichita State University  
in partial fulfillment of  
the requirements for the degree of  
Master of Science

May 2014

© Copyright 2014 by Nora M. Strong

All Rights Reserved

EVALUATION OF THE EFFECTS OF COLLAGEN-INDUCED ARTHRITIS AND METAL  
HYPERSENSITIVITY ON OSTEOLYSIS AND THE INFLAMMATORY RESPONSE TO  
WEAR DEBRIS IN THE MURINE AIR POUCH

The following faculty members have examined the final copy of this thesis for form and content, and recommend that it be accepted in partial fulfillment of the requirement for the degree of Master of Science, with a major in Biological Sciences.

---

Paul H. Wooley, Committee Chair

---

William J. Hendry III, Committee Member

---

Ramazan Asmatulu, Committee Member

## DEDICATION

To my family and friends, and especially my dear husband

## ACKNOWLEDGMENTS

First, I would like to thank my mentor, Dr. Paul Wooley, for his tireless support and guidance throughout this project. His encouragement and direction were absolutely vital to the completion of this project. My gratitude extends to my committee members, Dr. William Hendry III and Dr. Ramazan Asmatulu for their support and willingness to devote their time to support my project.

I would also like to thank Dr. Stephen Miller for his suggestions and input on my project, as well as Zheng Song and Dr. Shuye Yang for technical assistance during the project. Last, but not least, I thank my husband for many hours of editing and providing another perspective to guide my writing, as well as patience and support throughout this project.

## ABSTRACT

The re-introduction of metal-on-metal joint replacements and their subsequent poor performance has increased interest in the biological response to metallic debris, particularly metal hypersensitivity and its relationship to osteolysis. Since the immune response is implicated in some implant failures, it is possible that other immune irregularities, such as rheumatoid arthritis, can affect survival of implants.

For this study, chromium hypersensitivity was induced in one group of DBA/1 mice, collagen induced arthritis was induced in another group, and a control group was sensitized to keyhole limpet hemocyanin, an irrelevant antigen. All mice then received air pouches with syngeneic bone implanted. Antibodies to chromium and collagen were measured to assess sensitization, and arthritis progression was assessed daily. The animals were divided into three groups, receiving saline, polyethylene, or cobalt-chromium particles injected into the pouch. The mice were sacrificed 26 days after particle injection. Pouch thickness, cell count, inflammation, lymphocyte infiltration, and bone density were assessed histologically.

The inflammatory responses differed based on the type of biomaterial, regardless of immunological sensitization. Polyethylene was consistently the most inflammatory debris. There were no significant differences in lymphocytic infiltration or bone resorption between groups. High variability was observed in responses, with some mice exhibiting little inflammation and lymphocytic infiltration and others showing severe inflammation and perivascular lymphocytic cuffing. Neither biomaterial appeared to alter the course of the arthritis.

Individual responses to immunological stimuli and inflammatory debris are complex and resulted in variability within the experimental groups. This finding mirrors the patient experience, but hinders investigations of precise factors affecting adverse biomaterial responses. The dominant responses to biomaterial debris were inflammatory, even in the presence of adaptive immunological sensitivity. Based on this research, rheumatoid arthritis is not expected to elicit biomaterial concerns during joint replacement surgery.

## TABLE OF CONTENTS

Chapter	Page
1. INTRODUCTION.....	1
1.1 Total Joint Arthroplasty.....	1
1.1.2 Wear Debris Production.....	4
1.2 Aseptic Loosening .....	5
1.2.1 Bone Metabolism .....	6
1.2.2 Innate Immune System .....	7
1.2.3 Pathogenesis of Aseptic Loosening .....	9
1.3 Adverse Response to Metal Debris .....	10
1.3.1 Adaptive Immune System.....	11
1.3.2 ARMD.....	13
1.4 Metal Hypersensitivity .....	16
1.4.1 Prevalence of Metal Hypersensitivities .....	16
1.4.2 Detection of Metal Hypersensitivity .....	18
1.4.3 Animal Model.....	19
1.4.4 Previous Animal Work .....	19
1.5 Rheumatoid Arthritis .....	20
1.5.1 Background.....	20
1.5.2 Autoimmunity.....	22
1.5.3 Disease Pathology .....	23
1.5.4 Osteoimmunology .....	25
1.5.5 Response to Debris.....	26
1.5.6 Animal Model.....	27
1.6 Animal Model of Inflammation.....	28
1.7 Research Plan.....	28
2. MATERIALS AND METHODS .....	30
2.1 Animals .....	30
2.2 Conjugate Preparation .....	30
2.3 Metal Hypersensitivity Induction and Assessment .....	31
2.4 Preparation of Arthritis Conjugate.....	32
2.5 Collagen Induced Arthritis Induction and Disease Assessment .....	32
2.6 Preparation of Sensitizer for Control Group .....	32
2.7 Control Group Injections.....	33
2.8 Air Pouches .....	33
2.9 Harvest.....	34
2.10 Metal Antibody ELISA .....	35
2.11 Collagen Antibody Assay.....	36
2.12 Molecular Analysis of Pouch Tissue .....	36
2.13 Paw Histology .....	37

## TABLE OF CONTENTS (continued)

Chapter	Page
2.14	Air Pouch Histology ..... 38
2.15	Bone Density ..... 41
2.16	Statistical Evaluation ..... 41
3.	RESULTS ..... 42
3.1	Metal Sensitization ..... 42
3.2	Collagen Sensitization ..... 44
3.3	Pouch Cytokine Levels ..... 45
3.4	Air Pouch Thickness Measurements ..... 46
3.5	Pouch Cell Counts and Inflammatory Percentages ..... 50
3.6	Lymphocytic Infiltration ..... 53
3.7	Implanted Bone Density ..... 63
3.7.1	Integrated Optical Density ..... 63
3.7.2	Osteoclastic Osteolysis ..... 67
3.8	CIA Progression ..... 71
3.9	Arthritis Histopathology ..... 73
4.	DISCUSSION ..... 83
4.1	Metal Sensitization ..... 83
4.2	CIA Induction ..... 85
4.3	Pouch Cytokine Levels ..... 86
4.4	Pouch Reactivity ..... 87
4.5	Bone Density Measurements ..... 91
4.6	Effects of Particles on CIA Progression ..... 92
5.	CONCLUSIONS ..... 94
	REFERENCES ..... 98

## LIST OF FIGURES

Figure	Page
1.1 A Total Hip Replacement .....	1
1.2 The Basic Components of MOP or Ceramic-on-Ceramic Total Hip Implants .....	2
1.3 The Components of a Total Hip Prosthesis .....	5
1.4 The Mean OD Ratios for the Chromium and Control Groups in the Pilot Study .....	20
2.1 An Example of the Pouch Thickness Measurements.....	39
2.2 An Example of the Cell Count Performed on Each Air Pouch .....	40
3.1 The Highest Normalized OD Ratios for All Animals in the Metal Hypersensitive Group .....	43
3.2 The OD Ratios for All Animals in the Metal Hypersensitive Group at Each Sampling Point, and Representative Animals from the Other Treatment Groups .....	44
3.3 The Collagen Antibody Level of Each of the Sensitized Animals at Each Sampling Time Point .....	45
3.4 The Mean Pouch Thicknesses of Each Experimental Group, with Positive and Negative Metal Sensitive Animals Separated .....	47
3.5 A Representative Animal from the PBS Groups.....	48
3.6 A Representative Animal from the UHMWPE Groups.....	49
3.7 A Representative Animal from the CoCr Groups .....	50
3.8 The Mean Cell Density for Each Study Group, with the Positive and Negative Metal Sensitive Animals Separated .....	51
3.9 The Mean Mononuclear and Fibroblastic Cell Percentage for Each Study Group, with the Positive and Negative Metal Sensitive Animals Separated .....	52
3.10 Mean Lymphocyte Infiltration Scores for Each Study Group.....	55
3.11 A Representative Air Pouch Scored as a 0 .....	56
3.12 A Representative Air Pouch Scored as a 1 .....	57

LIST OF FIGURES (continued)

Figure	Page
3.13 A Representative Air Pouch Scored as a 2 .....	58
3.14 A Second Representative Air Pouch Scored as a 2.....	59
3.15 A Representative Air Pouch Scored as a 3, the Maximum Level of Lymphocytic Infiltration .....	60
3.16 A Second Representative Air Pouch Scored as a 3.....	61
3.17 An UHMWPE Air Pouch Displaying Necrobiosis.....	62
3.18 A CoCr Air Pouch Displaying Necrobiosis.....	63
3.19 The Mean IOD Values for Each Study Group, with the Positive and Negative Metal Sensitive Groups Separated .....	65
3.20 A Representative Section Showing Demineralization and Resorption of the Implanted Bone .....	66
3.21 A Second Representative Section Showing Demineralization and Resorption of the Implanted Bone .....	67
3.22 A Representative Section Showing Several Multi-Nucleated Cells Consistent With the Morphology of Osteoclasts, Attached to an Eroded Area in the Implanted Bone .....	68
3.23 A Second Representative Section Showing Several Multi-Nucleated Cells Consistent With the Morphology of Osteoclasts, Attached to an Eroded Area in the Implanted Bone.....	69
3.24 A Representative Section Showing a Multi-Nucleated Cell Consistent with the Morphology of an Osteoclast Next to an Area of Bone Resorption .....	70
3.25 A Representative Section Showing Several Multi-Nucleated Cells Consistent With the Morphology of Osteoclasts .....	71
3.26 The Mean Paw Scores by Particle Group of the Arthritic Animals by Study Day.....	72
3.27 The Mean Number of Affected Paws by Particle Group of the Arthritic Animals by Study Day .....	73

LIST OF FIGURES (continued)

Figure	Page
3.28 The Percentage of Total Paws Affected in Each Group Throughout the Study .....	73
3.29 The Mean Histopathological Scores for Each Particle Group.....	75
3.30 A Representative Section of a Normal Animal Scored as a 0 .....	76
3.31 A Representative Section of an Animal Given an Overall Score of 1 .....	77
3.32 A Representative Section of an Animal Given an Overall Score of 2 .....	78
3.33 A Representative Section of an Animal Given an Overall Score of 3 .....	79
3.34 A Representative Section of an Animal Given an Overall Score of 4.....	80
3.35 A Possible Germinal Center Adjacent to Eroded Bone.....	81
3.36 A Representative Section of an Animal Given an Overall Score of 5 .....	82

## LIST OF TABLES

Table	Page
2.1 The Study Groups.....	34
2.2 Study Timeline .....	34
2.3 The Scoring System Used for the Arthritis Paw Histopathology.....	37
2.4 The Lymphocyte Infiltration Scoring System for the Air Pouch Histopathology .....	40
2.5 Mice Positive for Chromium Hypersensitivity and the Highest Normalized OD Ratios .....	44

## LIST OF ABBREVIATIONS

°C	Degrees Celsius
µg	Micrograms
µg/L	Micrograms per Liter
µl	Microliter
µm	Micrometer
ALVAL	Aseptic Lymphocyte-Dominated Vasculitis Associate Lesion
ANOVA	Analysis of Variance
AOI	Area of Interest
APC	Antigen Presenting Cell
ARMD	Adverse Response to Metal Debris
BCA	Bicinchoninic Acid
BMP	Bone Morphogenetic Protein
CD4	Cluster of Differentiation 4
CD8	Cluster of Differentiation 8
CIA	Collagen Induced Arthritis
CoCr	Cobalt-Chromium
Co	Cobalt
Cr	Chromium
CrCl <sub>2</sub>	Chromium(II) Chloride
DMARD	Disease Modifying Anti-Rheumatic Drug
EDC	1-Ethyl-3-(3-dimethylaminopropyl) Carbodiimide Hydrochloride
EDTA	Ethylenediaminetetraacetic acid

## LIST OF ABBREVIATIONS (continued)

ELISA	Enzyme Linked Immunosorbent Assay
F <sub>c</sub>	Fragment Crystallizable
GM-CSF	Granulocyte-Macrophage Colony-Stimulating Factor
GSH	Glutathione
H&E	Haemotoxylin and Eosin
HCl	Hydrochloric Acid
HLA	Human Leukocyte Antigens
HRP	Horseradish Peroxidase
H <sub>2</sub> SO <sub>4</sub>	Sulfuric Acid
IFN- $\gamma$	Interferon Gamma
IgE	Immunoglobulin E
IgG	Immunoglobulin G
IL-1	Interleukin-1
IL-4	Interleukin-4
IL-6	Interleukin-6
IL-8	Interleukin-8
IL-12	Interleukin-12
IL-13	Interleukin-13
IL-17	Interleukin-17
IL-21	Interleukin-21
IOD	Integrated Optical Density
KLH	Keyhole Limpet Hemocyanin

## LIST OF ABBREVIATIONS (continued)

LSD	Least Significant Difference
M	Molar
M-CSF	Macrophage Colony-Stimulating Factor
MCP-1	Monocyte Chemoattractive Protein-1
mg/kg	Milligrams per Kilogram
mg/ml	Milligrams per Milliliter
MHC	Major Histocompatibility Complex
ml	Milliliter
mM	MilliMolar
MOM	Metal-on-Metal
MOP	Metal-on-Polyethylene
N	Normal
NaOH	Sodium Hydroxide
NF- $\kappa$ B	Nuclear Factor Kappa-B
Ni	Nickel
nm	Nanometer
OD	Optical Density
OPG	Osteoprotegerin
PAMP	Pathogen-Associated Molecular Pattern
PBS	Phosphate Buffered Saline
PGE <sub>2</sub>	Prostaglandin E2
PMMA	Polymethylmethacrylate

## LIST OF ABBREVIATIONS (continued)

PRR	Pattern-Recognition Receptors
RA	Rheumatoid Arthritis
RANK	Receptor Activator of Nuclear Factor Kappa-B
RANKL	Receptor Activator of Nuclear Factor Kappa-B Ligand
RSA	Rabbit Serum Albumin
TCR	T-Cell Receptor
T <sub>H</sub>	T-Helper Cell
THA	Total Hip Arthroplasty
TLR	Toll-Like Receptor
TJA	Total Joint Arthroplasty
TMB	3,3',5,5'-Tetramethylbenzidine
TNF- $\alpha$	Tumor Necrosis Factor Alpha
UHMWPE	Ultra-High Molecular Weight Polyethylene

## CHAPTER 1

### INTRODUCTION

#### 1.1 Total Joint Arthroplasty

Total joint arthroplasty (TJA) is a very common and very successful surgical procedure which involves the replacement of all articulating surfaces in a joint with a prosthetic device. In the hip, this involves the ball of the femur and the acetabular cup in the pelvis. This procedure can restore mobility and reduce pain for many patients suffering from osteoarthritis, rheumatoid arthritis (RA), osteonecrosis, traumatic injury, or other causes of joint pain and damage. Current implants are composed of titanium or cobalt-chromium alloys with one of three major types of bearing surfaces: ceramic-on-ceramic, metal-on-metal (MOM), and metal-on-polyethylene (MOP) [1-3]. Figure 1.1 shows a well-positioned total hip replacement, and Figure 1.2 shows the basic components of a hip prosthesis.

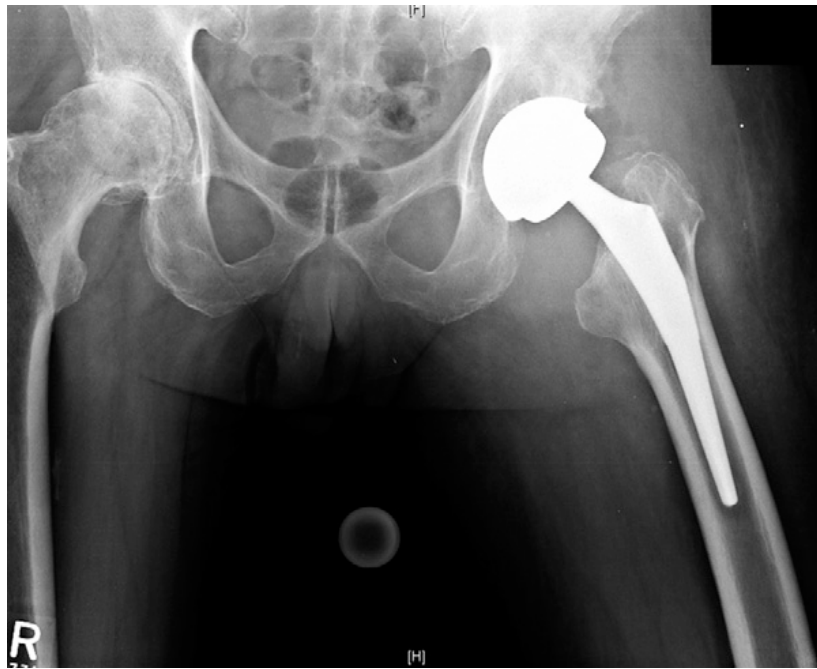


Figure 1.1: A total hip replacement [4].



Figure 1.2: The basic components of MOP or ceramic on ceramic total hip implants. In a metal-on-metal implant, the insert is also metallic [5].

The first hip prostheses used metal-on-metal bearing surfaces. High failure rates due to dislocation of the femoral head [1], high friction and locking of the bearing surfaces, and concerns about metal wear debris led to the addition of a polyethylene liner in the acetabular cup to articulate with the metal femoral head [6]. The majority of hip implants today use an ultra-high molecular weight polyethylene (UHMWPE) liner due to the lowered frictional wear debris production [2,6,7].

Originally, TJA was mainly performed in elderly patients, but the great success of the procedure has led to its use in younger, more active patients. This new patient base requires the development of longer lasting, wear resistant implants, to avoid multiple revision surgeries required to replace worn out implants. To this end, ceramic-on-ceramic implants were introduced along with the reintroduction of metal-on-metal implants [6-8]. Unfortunately, some of the new metal-on-metal implant designs have proven less wear resistant than expected. One particular design, the DePuy ASR hip implant, was recalled due to high failure rates. The design

of the implant left it prone to edge loading, in which the load is concentrated at the edge of the acetabular cup, causing greatly increased wear rates in improperly aligned prostheses [9-11]. The proper hip anteversion angle range was much smaller than that of most other implants, and many surgeons were unable to achieve the appropriate angle when implanting the ASR [10-14]. With the extremely high wear rates, new and previously less common failure modes are being observed [11-17]. Langton et al. found a failure rate of 48.8% for the ASR total hip at only six years post-implantation [9].

In order to improve future implant designs, a thorough understanding of the failure modes is essential. Many potential causes of failure exist, both mechanical and biological. Mechanical causes include edge loading leading to increased wear, brittle failure due to high impacts (specific to ceramic bearing surfaces), surgical implantation angle errors, impingement of the femoral and acetabular components, and joint dislocation [9,11,12,18]. Biological failures can result from infection, periprosthetic fracture, pseudotumors, aseptic loosening, pain, metal hypersensitivity, and adverse responses to metal debris (ARMD) [7,9,11,12,14-22]. A primary factor in adverse biological responses to implants is the production of wear debris by the implant [2,3,7,8,14,19,22]. Since many of the biological failures occur due to the functions of the patient's immune system, uncertainty exists concerning the longevity of implants in the presence of immune abnormalities occurring with autoimmune disorders, particularly RA, since it is a common factor leading to the need for TJA. The prevalence of TJA in RA patients has decreased in recent years due to the high effectiveness of biological response modifiers used to treat RA.

The focus of this work will be on aseptic osteolysis, metal hypersensitivity, and ARMD in the presence of metal hypersensitivity or a model of RA.

### **1.1.2 Wear Debris Production**

All articulating surfaces will produce particulate wear debris as a result of movement. The volume of debris produced depends on several factors, including bearing material, design, damage to articulating surfaces, and patient activity level. On average, the polyethylene liner in a well-functioning hip implant loses about 0.1 mm in wear each year [22], compared to 0.016 mm in ceramic-on-ceramic [23] and 0.0025 mm in a MOM implant [23]. Based on analysis of periprosthetic tissues in patients with failed implants, the polyethylene debris generated is about 0.23-1  $\mu\text{m}$  in diameter, significantly larger than the 0.05  $\mu\text{m}$  ceramic and metal debris typically observed [22].

Ceramic bearing surfaces wear quite slowly compared to MOP implants but good surgical technique is vital to avoid damaging the articulating surfaces and causing high wear rates. In addition, ceramic materials are brittle and there is concern that high impacts could crack the articulating surfaces [2], leading to some surgeon reluctance to implant them. While polyethylene bearing surfaces were introduced to decrease the level of metal debris generated by the joint, concerns about the high volume of wear produced by polyethylene liners led to the re-introduction of metal-on-metal implants, which, if properly implanted, are more durable and wear more slowly than polyethylene [19,22].

All joint implants contain some metal with two forms of metal being released into the body: particulate debris and corrosion products. Any metal implanted in the fluid environment inside the human body will undergo corrosion, leading to the release of metal ions. The small size of the particulate debris released from metal-on-metal bearings provides a significantly greater surface area for corrosion than the implant surface alone, greatly increasing the amount

of metal released in comparison to other bearing surfaces [1,12,14,19,24-26]. Current hip implants are modular (Figure 1.3), with interchangeable femoral heads and necks, allowing intra-operative customization by the surgeon and decreasing the amount of on-site inventory required to provide equivalent customization with solid implants. This modularity results in the existence of additional joints which can undergo corrosion and release metal into the periprosthetic tissue. In current implant designs, the Morse taper which connects the femoral head to the neck and stem of the femoral component is responsible for the majority of the non-articular corrosion due to both fretting and crevice corrosion [9,10,12]. Additionally, osteoclasts are known to cause pitting of metallic surfaces *in vitro* releasing corrosion products [27]. All of these sources of metal release into the body can contribute to complications, including aseptic osteolysis, metal hypersensitivity, and ARMD.

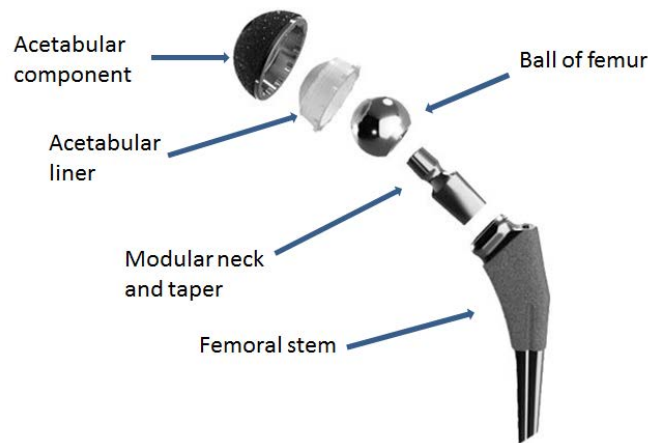


Figure 1.3: The components of a total hip prosthesis. This example is a metal on polyethylene bearing system [28].

## 1.2 Aseptic Loosening

The most common reason for implant failure is aseptic loosening, which causes more than 75% of all implant failures [22]. In aseptic loosening, a chronic inflammatory response

occurs due to the presence of any type of particulate wear debris and in the absence of infection, leads to resorption of the bone surrounding the implant. The bone resorption decreases the stability of the implant and weakens the surrounding bone. This leads to pain, loss of function, implant failure, and possible periprosthetic fracture, making revision surgery more challenging or impossible [22]. The response to debris has a direct correlation with the amount of debris present in the periprosthetic tissue, and debris generation is the major limiting factor of the lifespan of a prosthetic joint. Macrophages have long been recognized as a large player in osteolysis surrounding total joint implants, and a positive relationship exists between wear particle number and macrophage number in periprosthetic tissue [7]. To illustrate the process of aseptic loosening, bone metabolism and the innate immune system will now be discussed.

### **1.2.1 Bone Metabolism**

Bone is not a static structure. It is constantly being remodeled, resorbed by osteoclasts and formed by osteoblasts. Bone loss occurs due to an imbalance between the two processes, with the rate of resorption exceeding that of formation. Bone has many functions in the body, including definition of the body's primary structure, provision of muscle attachment sites to allow movement, and protection of internal organs, but the highest priority in the body is maintenance of calcium homeostasis. In response to hypocalcemia, bone resorption increases to raise the calcium level in the blood and bone formation slows. Unfortunately, formation occurs much more slowly than resorption [29].

Osteoblasts begin formation of bone by laying down bone matrix, or osteoid, containing collagen, which is subsequently mineralized [30]. Osteoblasts become trapped within the bone as it forms, becoming osteocytes [31]. Many factors promote bone formation: bone

morphogenetic proteins (BMP), intermittent parathyroid hormone exposure, mechanical loading, estrogen, and testosterone [29].

Osteoclasts are multinucleated cells that secrete various degradative factors to break down bone matrix and resorb the remnants. During bone resorption, the osteoclast attaches to bone, and forms a seal to create a microenvironment, which is then acidified. This results in demineralization of the bone matrix, and subsequent degradation by cysteine proteinases and matrix metalloproteinases. Finally, the remnants are phagocytosed by the osteoclast [32]. Osteoclasts are formed from monocyte/macrophage precursors, which fuse in response to the correct stimuli, most often macrophage colony stimulating factor (M-CSF) and binding of the receptor activator of nuclear factor-kappaB ligand (RANKL). M-CSF is required for survival of osteoclast precursors, and the receptor activator of nuclear factor kappaB (RANK) is a protein on the surface of the precursor, which binds RANKL on the surface of support cells such as osteoblasts and fibroblasts. RANK/RANKL binding and intracellular signaling promotes osteoclast differentiation and induces bone resorption. This process is inhibited by osteoprotegerin (OPG), a decoy receptor for RANK, also produced by osteoblasts, B-cells, and T-cells [30,32].

### **1.2.2 Innate Immune System**

The first line of defense against pathogens is the innate immune system. The defense elements include the skin, antimicrobial peptides (including lysozyme in tears), and cells of the innate immune system [33,34]. Some of the key cells include neutrophils and macrophages, which are phagocytic cells able to destroy pathogens through phagocytosis and reactive oxygen species or degradative enzymes. In the case of large targets that cannot be phagocytosed, reactive oxygen species and enzymes may be expelled extracellularly, potentially damaging

healthy tissue. A foreign body response may result from debris that is not easily degraded and removed from the area, such as large implant wear debris [35]. This response is characterized by fusion of macrophages to form multinucleated giant cells, theoretically in an effort to phagocytose large objects [35,36]. During the inflammatory process, there is a local increase in vascular permeability and expression of adhesion molecules by endothelial cells, which allows circulating white blood cells to extravasate from the blood into the affected tissue, facilitating infiltration by inflammatory cells and increased inflammation [36-38].

The innate immune system has no memory component and does not adapt to respond to new stimuli over time [34]. Instead, it responds to conserved molecular structures among pathogens, called pathogen-associated molecular patterns (PAMPs), which are not found in mammalian cells. Some of the more common examples include lipopolysaccharide and the peptidoglycan bacterial cell wall [39,40]. The patterns are recognized by pattern-recognition receptors (PRR), including Toll-like receptors (TLR) on macrophages [33,34,39,41]. TLR binding eventually leads to activation of the transcription factor NF- $\kappa$ B and subsequent production of inflammatory cytokines and heat shock proteins [34,39,41]. In response to the presence of a target, macrophages and other innate cells release IL-1, IL-6, TNF, M-CSF, and other cytokines, attracting and potentially activating more innate cells, as well as lymphocytes from the adaptive immune system. Macrophages and dendritic cells, another type of phagocyte, are termed professional antigen presenting cells (APCs), in that they are highly involved in activating cells of the adaptive immune system through antigen presentation [33]. Heat shock proteins are produced by cells during normal development and function, but expression increases during thermal, or other stresses. Some act as molecular chaperones to protect proteins and forming ribosomes from improper assembly [42].

Another component of the innate immune system is the complement cascade, a system of proteins and cleavage products, which mediates inflammation and destruction of pathogens. There are three major pathways for activation of complement, which lead to the formation of the membrane attack complex: a combination of cleavage products that attaches to the cell surface of a pathogen, an infected cell, or a cancerous cell, and lyse it. Complement can be activated by interaction with antibodies generated by the adaptive immune system, by microbial binding of plasma lectins, or directly by the pathogen. Various cleavage products can increase inflammation, and C3b can opsonize microbes and immune complexes to facilitate phagocytosis by macrophages [43].

### **1.2.3 Pathogenesis of Aseptic Loosening**

Although polyethylene debris is often associated with aseptic loosening, any particulate debris can cause inflammation around the joint and incite an innate immune response. The response to this wear debris is characterized by increased macrophage and osteoclast activity, leading to bone resorption [3,7,8]. Particles between 150 nm and 10  $\mu$ m are engulfed by macrophages, leading to the release of pro-inflammatory cytokines, including IL-1, IL-6, and TNF- $\alpha$ . In the presence of polyethylene, it is suspected that the cytokine production follows recognition of the particles by macrophage TLR4 [44]. TNF- $\alpha$  induces production of M-CSF by osteoblasts which will, in turn, attract more macrophages and osteoclasts to the area and further increase inflammation and bone resorption. As described previously, osteoclasts are formed by fusion of monocyte/macrophage precursors, and from macrophages present in the synovium. These cells can become osteoclasts in the presence of supporting cells, typically osteoblasts and fibroblasts. Not only does this response attract and activate macrophages and osteoclasts, the inflammatory mediators actually induce differentiation of osteoclast precursors in the

periprosthetic tissue [7]. As mentioned previously, the main osteoclast signaling pathway is the RANK/RANKL pathway. RANK is a cell surface protein found on mature osteoclasts and osteoclast precursors. It binds to its ligand, RANKL, which is present on osteoblasts and fibroblasts. When RANK binds to RANKL in the presence of M-CSF, the NF- $\kappa$ B signaling cascade is activated which initiates differentiation into osteoclasts and activates osteolysis. Expression of RANKL on osteoblasts is also upregulated by TNF- $\alpha$ , further increasing osteoclastogenesis [7,30].

In addition to the activation of macrophages and osteoclasts by particulate wear debris, appropriately sized non-degradable particles may also be phagocytosed by osteoblasts. This results in down-regulation of osteoblast proliferation, as well as the inhibition of collagen formation, the initial step of bone formation. Exposed osteoblasts also release IL-6, interleukin-8 (IL-8), MCP-1, and prostaglandin E<sub>2</sub> (PGE<sub>2</sub>). IL-6 and PGE<sub>2</sub> activate osteoclasts in the periprosthetic tissue, leading to bone resorption, while IL-8 and MCP-1 attract neutrophils and monocytes, respectively, increasing local inflammation. This elucidates a large role of the osteoblast in promoting and sustaining a localized inflammatory response in the periprosthetic tissue, potentially leading to aseptic osteolysis and eventual implant failure. When the cellular effects of particles of multiple implant materials were compared, metallic particles had a considerably greater inhibitory effect on osteoblasts than UHMWPE or polymethylmethacrylate (PMMA) cement. The responses to the particles were found to be dose dependent, further implicating excessive wear in premature implant failure [45].

### **1.3 Adverse Response to Metal Debris**

The biological response to metal debris and corrosion products differs from the response to UHMWPE, and may include the development of ARMD. This term describes joint failure

due only to the metal debris or corrosion product release from an implant [14]. An understanding of the adaptive immune system is necessary for a discussion of ARMD.

### **1.3.1 Adaptive Immune System**

While the innate immune response has no memory component, the adaptive immune response is directed toward a specific target and maintains an immunological memory of previously encountered targets to allow an enhanced response to subsequent exposures. The target of an adaptive immune response is an antigen, which is usually a foreign protein. The major effectors of the adaptive immune system are the lymphocytes: B-cells and T-cells. Each lymphocyte has surface receptors which recognize only one antigen, with great variability in the antigen binding region displayed among the cells. This variability is conferred by a process known as somatic hypermutation, in which highly error-prone polymerases and variable segment joining lead to nearly infinite receptor specificities. To prevent the maturation of self-reactive lymphocytes, cells with receptors which recognize self antigens undergo apoptosis during early development [46].

In an adaptive immune response, a foreign material is engulfed by a phagocytic cell, often a macrophage, and is processed into an actual immunological target, termed an epitope. The epitope is displayed on the surface of the cell in the context of a major histocompatibility (MHC) II molecule. The bound epitope can be recognized by the T-cell receptor (TCR) of a helper T-cell ( $T_H$ ) resulting in cellular activation. The activated  $T_H$  cell can then attract other T-cells, B-cells, and macrophages as well as activating B-cells with receptors bound to the specific antigen to secrete antibodies [46].

The B-cell receptor resembles an antibody attached to the cell surface. B-cell activation occurs when their receptors bind the appropriate antigen in the presence of co-stimulatory

molecules on  $T_H$  cells. Upon activation, B-cells multiply and become either plasma cells, which secrete antibodies with the same specificity as their receptors, or memory cells to enhance the response to subsequent encounters with the target antigen. All B-cells produced in this manner have identical receptors, so this process is known as clonal expansion. Circulating antibodies bind to the antigen and facilitate its destruction by activating complement or opsonization, which signals macrophages to phagocytose the bound antigen [46].

Whereas the B-cell is responsible for humoral immunity, the T-cells primarily act in a cell-mediated immune response. T-cells are classically divided into two types: helper T-cells ( $CD4+$ ) and cytotoxic T-cells ( $CD8+$ ).  $T_H$  cells are involved in the activation of B-cells and recruitment of macrophages and other T-cells, while cytotoxic T-cells initiate cell destruction by initiating apoptosis. In contrast to the B-cell receptor, T-cells require antigen to be processed into a specific epitope and presented in the context of a protein, either MHC-I or MHC-II. MHC-I is present on all nucleated cells, and displays processed antigen from within the cell. In a healthy cell, this antigen will be entirely “self,” and will be ignored by the immune system, in the absence of autoimmunity. If a cell is infected by a virus, or another event occurs to alter the status of the cell, the MHC-I may display a “non-self” antigen, which would target it for destruction via cytotoxic T-cells. The MHC-II molecule is present on APCs: fibroblasts, dendritic cells, macrophages, B-cells and others. These cells engulf pathogens or other “non-self” antigens, process them, and present them to  $T_H$  cells in the context of the MHC-II molecule. Activated T-cells release a variety of cytokines and chemokines to perpetuate the immune response. As with B-cells, activated T-cells undergo clonal expansion, producing memory T-cells in preparation for a subsequent encounter with the antigen [46,47].

After the infection is resolved, the memory lymphocytes remain in the body, to allow for an enhanced response to any subsequent exposures to the antigen. The initial adaptive immune response takes a few days to develop, so a full response will only occur on subsequent exposures. In order to develop a strong memory response, the lymphocytes must have a prolonged exposure to the antigen [8]. A joint prosthesis provides an ideal chronic exposure to implant materials.

### **1.3.2 ARMD**

As described earlier, metal debris in the body includes both particles and corrosion products. The mostly metal specific biological effects are termed adverse responses to metal debris (ARMD) [11,14]. These include metallosis, pseudotumors, and aseptic lymphocyte-dominated vasculitis associated lesions (ALVAL). ARMD can be diagnosed when a stable, well-functioning implant fails due to biological effects [11,14]. There is disagreement regarding the etiology of ARMD, with some researchers suggesting it is due to metal hypersensitivity, while others consider it to be cytotoxicity from the metal debris [10,12].

It is known that the metal debris and corrosion products do not remain localized in the periprosthetic tissue, as evidenced by increased levels of metal ions in patients' blood, suggesting that the debris has systemic as well as localized effects [6,12,22,25,49-51]. In some revision studies, patients with ARMD had higher average blood metal ion levels than patients with other reasons for prosthesis failure. In those studies, patients with higher metal wear were found to be at greater risk of ARMD [14]. Other studies have found no correlation with implant wear [19]. Metal ion levels in serum have been widely proposed as a method of monitoring wear of metal-on-metal bearings. It has been suggested that a serum level of  $< 7 \mu\text{g/L}$  of cobalt and chromium is associated with a properly functioning implant and a level  $> 20 \mu\text{g/L}$  is associated with a failing implant releasing enough debris to produce metallosis (defined below)

[9]. Other studies have proposed different ion cutoff points, and others have found little correlation between serum and whole blood metal levels and bearing wear. In response, Smolders et al. have proposed the use of multiple metal ion measurements to analyze trends as a more accurate measurement of implant functionality [51]. The significance of metal ion levels remains uncertain due to the abundance of environmental metal contamination, the variability between different implant systems, and the large variation noted between studies [49,50].

Metallosis is defined as the staining of periprosthetic tissue with metal debris, generally due to excessive wear or corrosion of the implant, and was originally a concern due to the potential misdiagnosis as severe tissue necrosis at revision [6,10,14]. As mentioned above, the presence of metallosis has been correlated with high metal levels in blood and serum.

ALVAL can occur in cases of both well-functioning joints and in joints exhibiting excessive wear [10]. The occurrence of ALVAL is not correlated with the metal levels in the blood and urine [6]. Common histological findings include histiocytes containing metal particles and areas of tissue necrosis, with perivascular lymphocyte cuffing [6,14]. ALVAL is primarily distinguished by the perivascular lymphocytic infiltrate since its other features are present in other tissue responses, including the foreign body response [6]. The lymphocytic infiltrate can also be observed with other diseases, including RA, contributing to the uncertain aetiology and diagnosis of adverse metal responses, including ALVAL [6]. Some researchers consider ALVAL to be the histological evidence of metal hypersensitivity [6].

A soft tissue response to debris that often causes considerable pain is the pseudotumor [6,14,17,52]. In some patients, mechanically well-functioning implants have been revised due to pain, with one researcher reporting a 27% revision rate for MOM implants due to a vaguely described “metal reaction” [53]. The exact description of a pseudotumor remains a topic of

discussion. They are generally considered soft tissue masses, either solid or cystic, associated with debris from an implant, which do not result from infection and are not malignant [6,14,17,52]. They have the potential to cause serious damage in the surrounding tissue, compressing nerves and blood vessels, and sometimes causing severe pain [6,54]. One case report describes a metal hypersensitive patient with a pseudotumor compressing the femoral vein and causing edema of the leg [53].

Pseudotumors were originally considered specific to metal debris from MOM implants, but further study has revealed their presence in patients with MOP implants and ceramic implants [17]. There remains uncertainty regarding the prevalence and risk factors of pseudotumors, although they are more common in women than men. Many studies have shown a correlation between high metal wear and elevated blood metal ion levels with an increased risk of developing pseudotumors, while others have found no change in pseudotumor incidence with degree of metal wear [17]. Matthies et al. found pseudotumors in 69% of patients undergoing revision for any reason, including asymptomatic patients with well-positioned and well-functioning implants [17]. A similar study found a prevalence of 59%. These high prevalences may potentially be due to the broad definition of pseudotumors, and the inclusion of asymptomatic patients in the screening [52]. In contrast, Beaulé et al. lists a prevalence of 0.10%, with other authors listing rates of 1% and 4% [54]. Beaulé et al. found a positive correlation with high wear as well as an earlier pseudotumor development with MOM than with MOP implants, and described bone destruction associated with the pseudotumor. Hart et al. found evidence of ALVAL in some, but not all, patients with pseudotumors, as well as in some patients without a pseudotumor, indicating that there may be some overlap of the two traits, but they are not necessarily the same process [52].

## **1.4 Metal Hypersensitivity**

Another metal-specific biological response is a metal hypersensitivity reaction. Metals are known to elicit hypersensitivity responses in susceptible individuals [48,55-57]. A hypersensitivity response is defined as an exaggerated and harmful immune response, often to a harmless antigen. Hypersensitivity responses are classified into one of four major types. Type I hypersensitivity is known as immediate hypersensitivity and is mediated by IgE antibody binding to mast cells and causing the release of histamine and other inflammatory mediators. Type II, antibody mediated cytotoxicity, results in cell destruction due to bound antibody. The type III response is known as immune complex hypersensitivity, and results in tissue damage due to circulating antibody-antigen complexes. Type IV hypersensitivity, also called delayed type hypersensitivity, occurs 48-72 hours after exposure to the target antigen. This response is characterized by involvement of macrophages and T lymphocytes [58]. Contact dermatitis is a common manifestation of a type IV response to implanted metals [55-57].

### **1.4.1 Prevalence of Metal Hypersensitivities**

Metals are well known for their potential to elicit hypersensitivity or allergic responses in humans. About 15% of the general population exhibits a contact dermatitis response to one or more metals, including chromium [55,58]. The prevalence of metal hypersensitivity increases in patients with metal-on-metal implants, even if the implant is stable and functioning well. In order to develop hypersensitivity, there must be multiple exposures to the target antigen, which must be of a sufficient size to elicit a response. Metal ions alone are too small to elicit an immune response. However, metal ions (haptens) can bind to body proteins (carriers) and produce a hapten-carrier complex, which is large enough for detection by the adaptive immune system [1,25,56,57,59].

There is a positive association between failing implants and hypersensitivity to one or more component materials of the implant. It is well established that loose or failing implants release much greater quantities of debris than stable implants, with a much higher metal concentration in the periprosthetic tissue. The long-standing question is whether exposure to this high level of debris from a failing implant induces metal hypersensitivity, or whether the patient developed the hypersensitivity prior to the failure and the elevated response increased osteolysis and thus caused failure of the implant [22,60]. This question will be a central focus of this investigation. If hypersensitivity leads to higher inflammation, pain, osteolysis, implant loosening, and potential early failure, then pre-operative hypersensitivity testing would be vital to the choice of implant type for each patient [25,62).

Metallic debris can cause failure in mechanically functional joint implants due to chronic inflammation and hypersensitivity. Mikhael et al. presented a case study of a bilateral metal-on-metal hip arthroplasty failure due to cobalt and chromium hypersensitivity. For 3 years following its implantation, the patient experienced periodic fevers, extreme hip pain, and required two canes in order to walk. The implants were stable with no osteolysis noted on radiographs. The patient had elevated serum levels of both cobalt and chromium and elevated inflammatory markers, including erythrocyte sedimentation rate, C-reactive protein, and blood leukocyte count. Periprosthetic tissue showed signs of a chronic inflammatory response. The patient had a known dermatological metal allergy, and his patch test for cobalt and chromium was positive. After ruling out infection, the patient underwent revision surgery to replace the cobalt-chromium acetabular liner with a highly cross-linked polyethylene liner and the symptoms resolved [62]. This case indicates that metal hypersensitivity can cause adverse responses even in the absence of loosening and indicates the importance of testing patients for

material sensitivities prior to arthroplasty to determine the most appropriate implant for each individual patient.

#### **1.4.2 Detection of Metal Hypersensitivity**

Metal hypersensitivity is difficult to confidently detect due to the questionable veracity of some testing methods and the lack of a universally accepted testing method [58,59]. The classic test is the patch test, in which the test material is applied to the skin for a set amount of time, and the skin response is measured based on redness and swelling. This test is controversial due to the potential of inducing sensitivity in the patient, as well as the uncertain relevance of a skin reaction to the reaction in a joint. The primary APCs in the skin are Langerhans cells, whereas the APC in the periprosthetic tissue remains undetermined [48,58]. *In vitro* tests are potentially more relevant, but have variable acceptance clinically [48]. One *in vitro* assay, the lymphocyte transformation test, measures the level of proliferation of lymphocytes cultured with and without particles, as a result of particle stimulation. This assay uses clonal expansion of lymphocytes recognizing specific particles and measures tritiated thymidine incorporation into the new cells during formation as a marker [27,58]. Other tests exist, including the leukocyte migration inhibition test, in which the random leukocyte motion leading to migration away from an area containing the test material is measured. A reduction of migration indicates that the test material provokes an immune response in the patient's white blood cells. Multiple factors, including migration inhibition factor, are produced during an immune response which function to retain cells at the site of the response [48].

The clinical long-term prospective studies of pre-operative and post-operative metal sensitivity are few in number and have produced somewhat conflicting results. Some patients with negative patch test results prior to the joint replacement surgery developed a positive

response several years after the surgery, suggesting sensitization. Other patients with positive patch test results pre-operatively tested negative after the replacement, suggesting a possible induction of immunological tolerance, or a pre-operative false-positive [25,62]. These seemingly contradictory results indicate how little is understood about the long-term effects of metal debris on the body.

### **1.4.3 Animal Model**

For this thesis, an animal model of metal hypersensitivity was required. Yang and Merritt developed a sensitization protocol for the induction of hypersensitivity to chromium, nickel, or cobalt in mice. Their study confirmed the haptenic potential of the metal ions when complexed with glutathione and rabbit serum albumin. Glutathione (GSH) was used due to its strong affinity for binding metal ions and rabbit serum albumin was used as the carrier protein, which allowed the mice to mount an immune response to the metal [56]. They also developed an ELISA to detect the presence of metal-specific antibodies in the serum of the sensitized animals [57]. The spleens of the sensitized animals were harvested and the splenocytes used to form hybridomas that produced monoclonal antibodies against the specific metal to which they were sensitized. They showed that the antibodies produced were specific to the glutathione-metal complexes and there was little cross-reactivity between the antibodies to each metal. The studies did not, however, investigate whether the sensitized animals would respond differently to metal particles such as wear debris [56].

### **1.4.4 Previous Animal Work**

For this thesis, a pilot study was performed using Balb/c mice, with the sensitization protocol described by Yang and Merritt. Eight mice were sensitized to chromium, and seven served as controls, receiving phosphate buffered saline (PBS) instead of the chromium conjugate.

Significant metal sensitization of the chromium group was achieved based on comparison of the level of metal antibodies using an enzyme linked immunosorbent assay (ELISA). Because some antibodies could bind to GSH without chromium, half of the wells were coated with GSH and chromium, and the other half with GSH only. The ratio of the optical density (OD) of wells coated with GSH and chromium to the OD of wells coated only with GSH was calculated to indicate successful sensitization to chromium. The mean OD ratio of the chromium group was significantly greater than the control group by one-way ANOVA ( $p < 0.017$ ). This success encouraged the continued use of this sensitization method. Figure 1.4 shows the results of the pilot study.

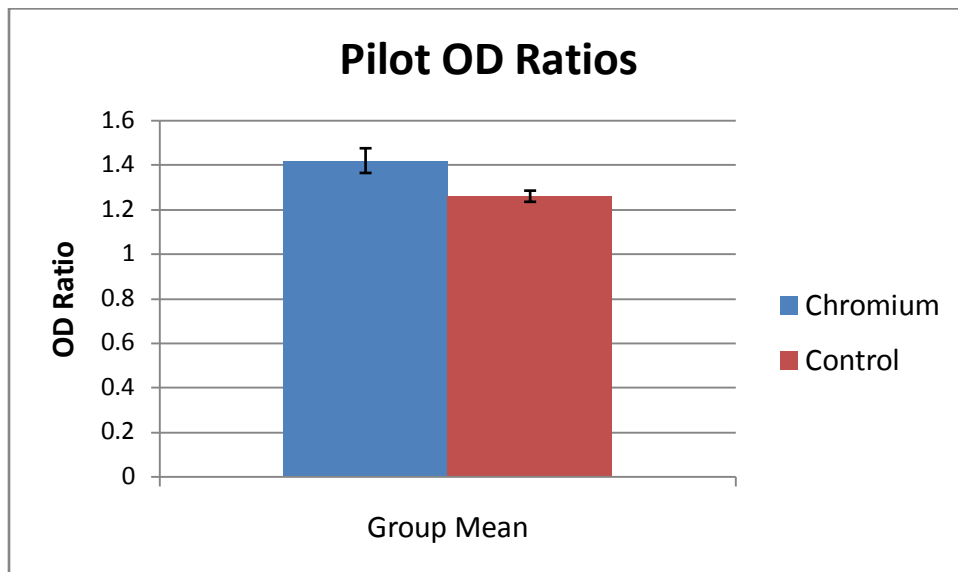


Figure 1.4: The mean OD ratios for the chromium and control groups in the pilot study. The error bars indicates the standard error.

## 1.5 Rheumatoid Arthritis

### 1.5.1 Background

Because end-stage RA is frequently treated by TJA, and patients with RA are more likely to receive a TJA than non-RA patients, it is important to understand how this autoimmune disorder could affect the body's response to implant wear debris. As many of the biological

responses to implants and debris involve the immune system, it is reasonable to expect that the alteration in immune function in RA could affect this response. This potential effect will be a focus of this investigation.

Rheumatoid arthritis is the second most common form of arthritis, affecting about 1% of adults worldwide [63-65]. It is a progressive autoimmune disorder in which chronic inflammation of joints leads to swelling and destruction of cartilage and bone, often causing permanent deformity of the affected joints. RA often affects the small joints of the hands, wrists, feet, elbows, knees, shoulders, and joints of the cervical spine [63]. As an autoimmune disease, RA can also produce extra-articular symptoms including fever, malaise, eye inflammation and damage, Felty's Syndrome, as well as heart and lung damage [63].

The cause of RA is unknown, but it appears to be multifactorial. There is a known genetic component of RA, related to the type of MHC genes, called human leukocyte antigens (HLA) in humans. Individuals expressing the HLA-DR4 antigen are at a 3.5 times greater risk of developing RA than other individuals [63]. This HLA antigen is suspected to affect antigen presentation to T-cells, contributing to perpetuation of the inflammatory process and activation of the adaptive immune system [66]. The genetic predisposition alone is insufficient to produce RA, however, based on studies of monozygotic twins in which only one individual developed RA [67]. A variety of contributing risk factors have been suggested, including viral infection leading to immune dysregulation. The major environmental risk factor for the development of RA is smoking, with a massive 21-fold increase in the risk of developing RA in smokers with the HLA-DR4 gene [68].

### 1.5.2 Autoimmunity

A critical requirement of the immune response is to distinguish “self” from “non-self” antigens. During development, lymphocytes with receptors that recognize “self” antigens are signaled to undergo apoptosis, thereby preventing autoimmunity. This system fails in the case of autoimmune diseases, including RA [32]. A theory exists which implicates chronic joint inflammation caused by the innate immune system in the development of autoimmunity. The innate immune system has also been implicated in the initiation of RA through TLR recognition of endogenous heat shock antigens expressed due to tissue damage and consequent induction of proinflammatory cytokine production by synovial cells and macrophages [41]. According to this theory, the local inflammation decreases the negative selection of autoreactive cells, leading to an adaptive autoimmune response [66].

A variety of autoantibodies can be found in RA patients, but their presence and abundance vary widely among patients. These include the Rheumatoid Factor and antibodies specific for type II collagen, heat shock proteins, and even glucose-6-phosphoisomerase [66]. In about 80% of patients, the Rheumatoid Factor is detectable in the blood [66,69]. The Rheumatoid Factor is an antibody which recognizes the fragment crystallizable (F<sub>c</sub>) region of the individual’s IgG antibodies [66,70]. The presence of this factor is an important risk factor for the development of RA [64,66]. The Rheumatoid Factor and other autoantibodies can contribute to the formation of immune complexes which embed into articular cartilage and fix complement. This leads to tissue destruction and the release of chemoattractants, increasing the number of leukocytes in the tissue [66]. The destruction of cartilage in the joints releases heat-shock proteins, leading to the activation of innate immune cells through TLR signaling [71]. Many endogenous antigens are also released during the tissue damage, including type II collagen and

proteoglycans [72]. These antigens can be processed and presented to T-cells in the joint, or can activate self-reactive B-cells, leading to activation of the adaptive immune system. The Rheumatoid Factor has also been found in patients with other autoimmune diseases and even in normal individuals, so it is not a specific indication of RA. There is evidence, however, that the presence of Rheumatoid Factor predicts more severe disease and a poorer prognosis [66,69].

More recently, antibodies to citrullinated autoantigens have been found in about 66% of RA patients. These antibodies are rare in non-RA patients, making them a more sensitive marker for RA than Rheumatoid Factor. The citrullinated autoantigens are found to be significantly more arthritogenic than the unmodified antigens. Citrullinated peptides are produced by deimination of arginine residues to form citrulline, which increases peptide binding to the HLA-DR portion of the MHC-II molecule on APCs in individuals with the genetic predisposition to RA [68]. This improved binding presumably contributes to greater presentation of these antigens to T-cells. The environmental risk factor of smoking acts synergistically in patients with the HLA-DR4 risk factor to dramatically increase the risk of developing RA. Klareskog et al. reported that citrullinated peptides exist in the lungs of smokers, but not in non-smokers, suggesting a causal relationship between the presence of the peptides and smoking [68]. There was also a strong dose-dependent effect of smoking on the levels of the antibodies. The presence of these antibodies has been shown to precede the development of clinical RA by several years, indicating a possible causal relationship [68].

### **1.5.3 Disease Pathology**

There appears to be both an innate and adaptive response in the pathogenesis of RA, with some authors suggesting that the innate response initiates the disease. This theory suggests that chronic inflammation in the joint leads to the development of autoimmunity [66]. RA presents

with a chronic inflammation of the synovial membrane surrounding the joint, called synovitis. There are two major types of synovial cells: macrophage-like and fibroblast-like. These cells have been implicated in the perpetuation of the inflammatory response due to production of several pro-inflammatory cytokines, including IL-1, IL-6, TNF $\alpha$  and granulocyte-macrophage colony-stimulating factor (GM-CSF). These cytokines attract and activate leukocytes, and also perpetuate the activation of the synovial cells in an autocrine manner. In response, the cells of the normally thin synovial membrane proliferate and are infiltrated by macrophages, T-cells and B-cells, forming an erosive pannus structure, which attaches to articular cartilage and leads to destruction of cartilage and underlying bone through release of metalloproteinases and other degradative enzymes, as well as osteoclast activation and differentiation [66,73]. It has been documented that the macrophage-like synovial cells can differentiate into osteoclasts in the presence of GM-CSF and RANKL, to directly destroy bone in the arthritic joint. This process is enhanced in the presence of TNF $\alpha$ , produced by macrophages and T-cells, which up-regulates the expression of RANKL on support cells, including fibroblasts, osteoblasts, and T-cells [32]. In addition to inducing cytotoxicity and osteoclast differentiation, TNF $\alpha$  also upregulates adhesion molecules on endothelial cells and enhances leukocyte extravasation into the inflamed tissue [65].

Angiogenesis is another important step in the development and perpetuation of RA, as it allows the infiltration of greater numbers of leukocytes from the bloodstream and oxygenates the massive synovial proliferation [74]. The heavy accumulation of inflammatory cytokines contributes to local and system inflammation, perpetuating the damage [73].

#### 1.5.4 Osteoimmunology

The realization that the immune system and bone metabolism are deeply interconnected led to the development of the field of osteoimmunology, which is critical to the understanding of RA. The T-cell is known to have a large role in RA. There are multiple types of helper T-cells ( $T_H$ ), with three major divisions:  $T_{H1}$ ,  $T_{H2}$ , and  $T_{H17}$ . Each type of T-cell expresses a different set of cytokines, which drive a particular immune response.  $T_{H1}$  and  $T_{H2}$  cells exert largely protective effects for bone and prevent osteolysis. Interleukin-12 (IL-12) signals T-cells to develop along the  $T_{H1}$  cell pathway and produce IFN- $\gamma$ , which inhibits osteoclastogenesis by disrupting the RANK/RANKL signaling axis. An IL-12 knockout mouse with induced arthritis was found to develop more severe disease than a wild type, confirming that IL-12 is involved in the prevention of osteolysis [32]. The  $T_{H2}$  cytokines IL-4 and IL-13 inhibit both the differentiation of osteoclasts and their activation by stimulating osteoblasts and endothelial cells to express OPG, a decoy for the RANK signaling pathway [32]. Recently, it has been discovered that the major T-cell instigator of the bone destruction process is the newly discovered  $T_{H17}$  T cell subset. These T cells release IL-17 and IL-21 [73] which are potent cytokines that increase the surface expression of RANKL on osteoblasts and synovial fibroblasts. As described previously, RANKL acts by binding to RANK on the surface of osteoclast precursors (synovial macrophages), which signals differentiation into osteoclasts [30,32,73]. IL-17 also activates synovial macrophages to release IL-1, IL-6, and TNF $\alpha$ , further upregulating RANKL expression and resulting in massive bone destruction [30,32,73].

Due to the progressive and destructive nature of RA, aggressive drug treatment is implemented as early as possible to prevent major disability. Current therapies are generally very effective at reducing morbidity in patients, but response to individual treatments varies

widely between patients, and can vary over time. Treatment involves drugs to relieve symptoms, as well as disease modifying anti-rheumatic drugs (DMARD), which actually alter the course of the disease to prevent further damage. The DMARDs are divided into those with biologic and non-biologic effects. Biologic effectors act directly on the inflammatory cytokines involved in the progression of the disease. These effectors include TNF $\alpha$ , IL-1, and IL-6 inhibitors, which can very effectively interrupt the progression of the disease [75,76]. Unfortunately, this causes immunosuppression and increases the risk of developing serious infections and some cancers. The non-biologic DMARDs include methotrexate, sulfasalazine, and leflunomide. Methotrexate is one of the mainstays of RA treatment [63]. Its mechanism of action is only partially understood, but it seems to inhibit proliferation of immune cells and interferes with the production of proinflammatory cytokines [77]. Current DMARD therapy is highly effective in most patients, preventing the worst joint disfiguration, but patients often still require joint replacement at some point in the course of the illness.

### **1.5.5 Response to Debris**

As total joint replacement is regularly used in end-stage RA, it is vital to determine if RA alters the response to wear debris. Surprisingly little work has been published at this time. In addition to the detrimental effects of RA on bone metabolism, many of the therapeutic medications used to treat RA, such as methotrexate, can have adverse effects on bone. These effects could increase mechanical failure rates and prevent adequate fixation and osseointegration after implantation, leading to early joint failure. A meta-analysis of cementless hip replacement in RA patients found some increased risk of intra-operative complications including subsidence of the femoral stem and periprosthetic fracture, but overall, found little evidence of long-term adverse effects on implant stability from the altered bone metabolism of

RA. The occurrence of early aseptic loosening was quite low in RA patients, and was comparable to those without inflammatory arthritis [78]. A similar study examined cemented hip replacements in RA patients, and found a small, less than 1% increased risk of failure due to infection, presumably due to immune dysregulation, as well as immunosuppressive treatments to control RA [79].

One recent study analyzed implant wear patterns and histological responses to debris in patients with treated RA, untreated RA, or non-inflammatory arthritis at revision due to aseptic loosening. No differences in the wear patterns or particle volume were observed between any of the patient groups. The biological response to the debris did show some differences between the groups. The patients with untreated RA displayed an interstitial lymphocyte aggregation in the vicinity of wear debris, while the non-RA patients displayed a perivascular aggregation. Interestingly, the treated RA patients showed a mixture of both responses, suggesting that some immune abnormalities remain active during treatment with TNF- $\alpha$  inhibitors [80]. The significance of this altered response remains unknown.

### **1.5.6 Animal Model**

Collagen-induced arthritis (CIA) is a mouse model of rheumatoid arthritis, with many similarities to the human disease. Mice are injected with type II collagen in Complete Freund's Adjuvant, to generate antibodies to collagen. As type II collagen is abundant in synovial joints, these antibodies attack joints in the extremities. About three to four week after injection, most animals develop swelling and erythema in one or more paws, which is the clinical presentation of the arthritis. The disease is self-limiting, as it spontaneously resolves over time, sometimes leading to ankylosis of affect joints. The histopathological appearance of CIA is similar to that seen in RA, with synovitis, pannus, and erosion of bone and cartilage [81].

## **1.6 Animal Model of Inflammation**

The murine air pouch is an experimental mouse model for assessing the inflammatory response to different materials, including metal particles. Sterile air is injected beneath the skin on the back of the mouse to create a pocket for material implantation or injection. Once the pouch is established, the test material is either injected or implanted into the pouch. Two to four weeks after material introduction, the pouch is harvested for molecular and histological evaluation. The membrane thickness, cell number, and cell type are measured to assess the inflammatory response to the implanted material. A thinner membrane composed mostly of fibroblasts would indicate a benign healing response, while a thick membrane containing many mononuclear cells would indicate inflammation. The model provides sufficient tissue to allow molecular evaluation of the pouch tissue to assess levels of inflammatory cytokines, such as IL-1 and TNF- $\alpha$ . A variation of the pouch model includes the surgical implantation of syngeneic bone with particles to examine bone resorption due to the particles [35]. This model will be utilized for this study.

## **1.7 Research Plan**

This study will use the murine air pouch model to investigate the differences in the inflammatory response to cobalt-chromium (CoCr) particles in chromium sensitized or arthritic animals. It is hypothesized that both the chromium sensitized and arthritic animals will display a stronger inflammatory response to the metallic particles than the control animals, suggesting that there may be a stronger inflammatory response around the implant in hypersensitive and arthritic patients. This study will also examine the response to UHMWPE particles (known to be inflammatory) in both chromium sensitized and arthritic animals to determine whether metal hypersensitivity or rheumatoid arthritis can influence the response to non-metallic particles. A

further objective is to assess whether the introduction of UHMWPE or CoCr particles into the air pouch will affect the course of CIA in mice.

This study will investigate three basic questions. First, does the increased metal exposure of patients with failing implants lead to the development of metal hypersensitivity, or does a pre-existing metal hypersensitivity lead to the implant failure by causing a greater response to the implant debris? Secondly, does rheumatoid arthritis, as an autoimmune disorder, affect the biological response to implant debris? Lastly, does the introduction of debris affect the progression of the arthritis? The working hypothesis for this study is that the sensitization to chromium and the collagen induced arthritis will cause an increased inflammatory response to implanted debris and lead to increased resorption of the implanted bone. The secondary hypothesis is that the introduction of debris will increase the severity of the collagen induced arthritis.

## CHAPTER 2

### MATERIALS AND METHODS

#### 2.1 Animals

One hundred and twelve female DBA/1 mice were purchased from The Jackson Laboratory (Bar Harbor, Maine) for this study. Thirty-six underwent metal sensitization, thirty-six underwent collagen arthritis induction, and twenty-four were sensitized to keyhole limpet hemocyanin (KLH) and served as controls. Because the adjuvant utilized in the sensitization process can alter the immune responses in the animals regardless of the specific targets, the controls were sensitized. Since KLH is not found in rodents, the sensitization was not expected to induce an adaptive immune response in the mice. The remaining sixteen mice served as bone donors. The animals were acclimated to the animal facility for one week prior to commencement of the study, and all received a standard rodent diet (5001) supplemented with a higher fat diet (5015) to increase arthritis development. All animals were monitored daily throughout the study for health status. All animal activities were approved by the Wichita State University Institutional Animal Care and Use Committee.

#### 2.2 Conjugate Preparation

A hapten carrier conjugate was prepared for the metal sensitization using glutathione (GSH), chromium, and rabbit serum albumin (RSA) as described by Yang and Merritt. RSA served as the carrier protein while GSH was used to attach chromium to the RSA. GSH is effective in binding metal ions due to the presence of a mercaptan group. To prepare carboxyl groups as additional binding sites, GSH was treated with 1-Ethyl-3-(3-dimethylaminopropyl) Carbodiimide Hydrochloride (EDC) [56].

10 ml of a 5 mg/ml solution of GSH in water was prepared, and combined with 10 ml of a 50 mg/ml solution of EDC. The solution was adjusted to pH 5 with HCl or NaOH as needed, and incubated for 5 minutes at room temperature. Next, 20 ml of a 46 mg/ml solution of RSA was added to the solution and incubated for 4 hours at room temperature. After incubation, 20 ml of a 0.2M sodium acetate buffer was added to stop the reaction, and the solution was incubated for 1 hour at room temperature. In order to separate the unbound GSH from the GSH-RSA compound, the solution was dialyzed overnight with four changes of phosphate buffered saline (PBS). 25 ml of a 1mM solution of chromium chloride was prepared in water, and 3 ml of the GSH-RSA mixture was added dropwise with constant stirring. Next, the solution was again dialyzed overnight with four changes of PBS. The final solution was sterilized by passage through a 0.22  $\mu$ m syringe filter, and stored at 4°C until use. A bicinchoninic acid (BCA) protein assay kit (Pierce, Rockford, IL) was used to determine the protein concentration of the finished conjugate, to determine necessary dilution for injection.

### **2.3 Metal Hypersensitivity Induction and Assessment**

For the metal hypersensitivity group, thirty-six mice received three intraperitoneal injections of 0.2 ml of a 0.25 mg/ml protein solution of the chromium conjugate emulsified in 0.2 ml of Freund's Adjuvant by mixing in glass syringes with a three-way stopcock, with each injection separated by three weeks. The first injection contained Complete Freund's Adjuvant, while the last two contained Incomplete Freund's Adjuvant. Mice were pre-bled to assess baseline serum antibody levels. Blood was further collected ten days after each injection, and again at sacrifice to determine the presence of antibodies to chromium.

Each retro-orbital blood collection procured about 100  $\mu$ l of blood. The blood was collected in glass tubes and allowed to clot. The serum was collected and centrifuged to remove any red blood cells. The serum was stored at  $-20^{\circ}\text{C}$  until analysis by ELISA.

#### **2.4 Preparation of Arthritis Conjugate**

Bovine type II collagen was dissolved in 0.01 M acetic acid to reach a concentration of 1 mg/ml. This solution was emulsified in an equal volume of Complete Freund's Adjuvant by mixing in glass syringes with a three-way stopcock immediately prior to injection.

#### **2.5 Collagen Induced Arthritis Induction and Disease Assessment**

Thirty six mice received an intradermal injection of 100  $\mu$ g of bovine type-II collagen in Complete Freund's Adjuvant at the base of the tail four weeks prior to the establishment of the air pouches. The CIA mice were monitored daily for the development of arthritis, manifested by swelling and redness of one or more paws. Once observed, calipers were used to measure the thickness of all paws and both ankles three times each week for the rest of the study period. The four paws were scored as follows: 0 – normal, no arthritis; 1 – paw swelling and erythema; 2 – swollen paw with limited movement of digits; 3 – ankylosis of joints. Food pellets were placed on the bottom of the cage to facilitate feeding by the mice during the inflammatory portion of the arthritis. Mice were pre-bled prior to the injection to assess levels of collagen specific antibodies present in the serum. Blood was again collected four weeks after injection, and at sacrifice.

#### **2.6 Preparation of Sensitizer for Control Group**

20 mg of KLH (Sigma Aldrich, Springfield, MO) was reconstituted with 2 ml of deionized water per manufacturer's instructions to obtain a 10 mg/ml solution of KLH in sodium phosphate buffer at a pH of 7.4. This was diluted to obtain a concentration of 1 mg/ml. This

solution was emulsified in an equal volume of Complete Freund's Adjuvant by mixing in glass syringes with a three-way stopcock immediately prior to injection.

## **2.7 Control Group Injections**

Twenty-four mice received an intradermal injection of 100 µg of KLH emulsified in Complete Freund's Adjuvant at the base of the tail four weeks before air pouch induction. Because KLH is not found in mice, this injection was not expected to induce autoimmunity.

## **2.8 Air Pouches**

Two days after the final metal sensitization injection, and four weeks after the collagen and KLH injections, air pouches were established on all mice. The animals were anesthetized with an intraperitoneal injection of 90 mg/kg of Ketamine and 8 mg/kg of Xylazine. The back of the animals were shaved and disinfected. Next, 2.5 ml of sterile air was injected subcutaneously to form a pouch under the skin in the middle of the back. The pouch was re-inflated as needed every other day to maintain the pouch size.

Six days later, 16 genetically identical mice were sacrificed and femurs and tibias were harvested under sterile conditions. The same day, all pouch mice had a portion of the proximal femur, proximal tibia, or distal femur from a donor mouse implanted into the air pouch. On the day of surgery, all mice received a subcutaneous injection of 0.05 mg/kg Buprenorphine and 5 mg/kg Carprofen for preventative analgesia. The animals were anesthetized with an intraperitoneal injection of 90 mg/kg of Ketamine and 8 mg/kg of Xylazine, and the pouch area disinfected with Povidone-Iodine. An incision was made into the air pouch, and a portion of the femur or tibia of a donor mouse was implanted into the pouch using sterile surgical technique. The skin and pouch were sutured closed, and the mice were recovered from anesthesia and returned to normal housing.

Two days later, the 3 groups were further divided into 3 groups: saline, cobalt-chromium particles, and UHMWPE particles. According to group, the air pouches were injected with 500  $\mu$ l of saline, 5 mg of cobalt-chromium particles in 500  $\mu$ l of saline, or 5 mg of UHMWPE particles suspended in 500  $\mu$ l of saline. The study outline is displayed in Table 2.1, and a timeline in Table 2.2

Table 2.1: The study groups.

Treatment	Saline	Cobalt-Chromium Particles	UHMWPE Particles
CIA	12	12	12
Metal Hypersensitivity	12	12	12
KLH (Control)	8	8	8

Table 2.2: Study timeline.

Procedure	Sensitization Groups	Day
Pre-Bleed	All	0
1st Metal Injection	Metal Hypersensitivity	5
CIA and Control Injection	CIA and Control	19
2nd Metal Injection	Metal Hypersensitivity	27
Bleed Metal	Metal Hypersensitivity	36
3rd Metal Injection	Metal Hypersensitivity	48
Start Air Pouch	All	50
Implantation Surgery	All	56
Particle Injection	All	58
Bleed All Mice	All	69
Sacrifice/Terminal Bleed	All	84

## 2.9 Harvest

All animals were sacrificed 26 days after the particle injections into the each air pouch. An overdose of pentobarbital was administered intraperitoneally, and the animals underwent terminal bleeding. The air pouches were harvested and divided into two pieces. The portion for histology was fixed in 10% formalin and decalcified using EDTA prior to sectioning. The other half was snap frozen and stored at -80°C for molecular analysis. All CIA mice and two each of

the other two groups had all four feet harvested at the elbow or knee, fixed in 10% formalin, and decalcified using EDTA prior to sectioning.

## **2.10 Metal Antibody ELISA**

An ELISA was performed to detect any serum antibodies against chromium. All reagents were prepared using ultrapure water and without any metal instruments to avoid undesirable binding of glutathione to any metal ions. The plates were coated with 100  $\mu$ l of a coating buffer containing 0.5 mg/ml of GSH, and incubated overnight at 4°C. The next day, 25  $\mu$ l of PBS or 25  $\mu$ l of PBS containing 0.15 mg/ml of CrCl<sub>2</sub> was added to each well, and incubated overnight at 4°C. The plates were washed three times with 300  $\mu$ l of ELISA washing buffer with 0.5% Tween 80 and 0.1% gelatin. The plates were blocked for one hour at 37°C with 200  $\mu$ l of ELISA blocking buffer containing 1% gelatin. The plates were washed six times, then 100  $\mu$ l of a 1:100 dilution of serum samples in blocking buffer were added to the wells. After one hour at 37°C, the plates were washed six times, and 100  $\mu$ l of alkaline phosphatase conjugated goat anti-mouse antibody was added to each well, and incubated for 45 minutes at 37°C. Next, the plates were washed six times, and 200  $\mu$ l of diethanolamine containing the PNPP substrate was added to each well. To discern antibodies against glutathione from those against chromium, half of the wells were coated with glutathione and chromium, and the other half with glutathione only. The plates were read at OD 405 on a microplate reader after 15 minutes of incubation with the substrate. The strength of the antibody response to the metal was determined by the ratio of the OD of the GSH+Cr wells to the OD of the GSH wells, as shown in equation 2.1.

$$OD\ ratio = \frac{OD\ (GSH + Cr)}{OD\ (GSH)} \quad (2.1)$$

## **2.11 Collagen Antibody Assay**

For the assay, 96-well plates were coated with 300  $\mu$ l of the coating buffer containing 3  $\mu$ g of bovine type II collagen, and incubated overnight at 4°C. Next, the plates were washed three times with PBS containing 0.05% Tween 20, and then blocked with 5% of non-fat milk protein overnight at 4°C. Then the plates were dumped and the serum samples were diluted to reach a 1:1000 dilution in blocking buffer. The serum samples were added to the wells, and the plates were incubated at 4° overnight. After three more washes, the plates were developed by addition of a 1:500 dilution of anti-mouse immunoglobulin labeled with alkaline phosphatase. After a two hour incubation period, the plates were washed six times, and the p-nitrophenyl phosphate substrate was added. The plates were incubated at room temperature in the dark for 15 minutes. Next, the optical densities (OD) of each well in the plate were read with a microplate reader at 405 nm. All samples were analyzed in triplicate and the results were averaged. The positive control wells were coated with anti-mouse immunoglobulin. Blanks included non-coated wells and coated wells with and without serum added to define the baseline OD reading. The means of each group were compared using a one-way ANOVA with LSD post-hoc testing with SPSS. The limit of statistical significance was defined as  $p < 0.05$ .

## **2.12 Molecular Analysis of Pouch Tissue**

The other half of the air pouches were frozen and stored at -80°C until analysis. The tissue was homogenized using a Polytron tissue homogenizer. A BCA kit was used to determine the amount of protein in each homogenized sample, which was used to dilute the protein down to 40  $\mu$ g/100  $\mu$ l. 96-well plates were coated with 100  $\mu$ l of capture antibody (IL-1, IL-6, or TNF- $\alpha$ ) in 100  $\mu$ l of 0.1 M sodium bicarbonate buffer in each well and incubated overnight at 4°C. The plates were washed five times with 300  $\mu$ l of PBS containing 0.05% Tween 20. The plates were blocked with 200  $\mu$ l of assay diluent in each well for four hours at room temperature. The

blocking solution was dumped prior to addition of samples. The samples were added in 100  $\mu$ l of assay diluent containing 40  $\mu$ g of protein and the plates were incubated overnight at 4°C. The next day, the plates were washed six times with 300  $\mu$ l of PBS containing 0.05% Tween 20, and blotted dry on paper towels. Next, 100  $\mu$ l of the appropriate biotin-conjugated antibody was added to each well and incubated at 37°C for one hour. The plates were again washed six times, and 100  $\mu$ l of streptavidin-horseradish peroxidase (HRP) was added to each well. After 40 minutes of incubation at room temperature, the plates were washed six more times.

To develop the plates, 100  $\mu$ l of TMB solution was added to each well and the plates were incubated for 5-20 minutes in the dark. Once the reference samples developed sufficient color, the reaction was stopped by the addition of 50  $\mu$ l of 2N H<sub>2</sub>SO<sub>4</sub> stop solution to each well. Within 10 minutes of the addition of the stop solution, the optical density of each well was measured at 450-570 nm with a microplate reader. A reference curve was produced on each plate to determine quantitative cytokine levels in the samples.

### 2.13 Paw Histology

All mouse paws were decalcified and histological sections stained with hematoxylin and eosin (H&E). The carpal and tarsal joints were assessed for synovial inflammation, pannus formation, erosion of cartilage and bone, and fibrous or bony infiltration. Table 2.3 shows the scoring system for the arthritis paw histopathology.

Table 2.3: The scoring system used for the arthritis paw histopathology.

Synovitis	
0	Membrane less than 3 cells thick
1	Membrane 3-5 cells thick
2	Membrane 6-10 cells thick
3	Membrane 10-20 cells thick
4	Membrane 20-30 cells thick
5	Membrane over 30 cells thick

Table 2.3 (continued)

<b>Pannus</b>	
0	No pannus formation
1	Microvilli present
2	Clear pannus attachment to bone or cartilage
3	Marked pannus attachment to bone or cartilage
4	Joint space filled by pannus
5	Extensive pannus proliferation
<b>Marginal Erosions</b>	
0	No erosions visible
1	Minor erosions in area of capsular attachment
2	Clear cartilage erosions
3	Erosions extend into subchondral bone
4	Major erosion of bone and cartilage
5	Loss of visible cartilage and major bone loss
<b>Architectural Changes</b>	
0	Normal joint architecture
1	Edematous changes
2	Minor subluxation of articulating surfaces
3	Major subluxation of articulating surfaces
4	Loss of joint landmarks
5	Complete fibrosis and collagen bridging
<b>Overall Score</b>	
0	Classical normal joint appearance
1	Minor changes; consistent with remission, may be clinically normal
2	Moderate inflammatory disease
3	Major inflammatory disease
4	Destructive, erosive arthritis
5	Destructive, erosive arthritis with major bone remodeling

#### 2.14 Air Pouch Histology

One portion of the pouch was fixed in formalin for histological sectioning and staining with H&E and assessed using ImagePro software for pouch membrane thickness and cellular composition as described by Ottaviani et al [82]. Representative digital photographs were taken of each air pouch and the thickness of the pouch membrane as measured in 6 separate locations for each animal. An example of the thickness measurement is shown in Figure 2.1 below. Figure 2.2 shows an example of the cellularity and percentage of inflammatory cells

measurement. Cellularity was assessed in 3 places on each membrane by cell count and morphology analysis by ImagePro Plus. The cell counts were divided by the measured area to obtain cell density. Mononuclear cells and fibroblasts were differentiated visually by the difference in nuclear aspect ratio. Mononuclear cells have a more rounded nucleus with an aspect ratio close to 1, while fibroblasts are more elongated, and were classified by an aspect ratio of at least 1.8. The software used automatic dark spot detection to count nuclei and display each class of cells with a different false color. Visual inspection was performed for any clearly incorrect assignments and the necessary corrections were made. A high percentage of mononuclear cells in the membrane indicates an inflammatory response, while a high percentage of fibroblasts indicates a benign healing response [82].

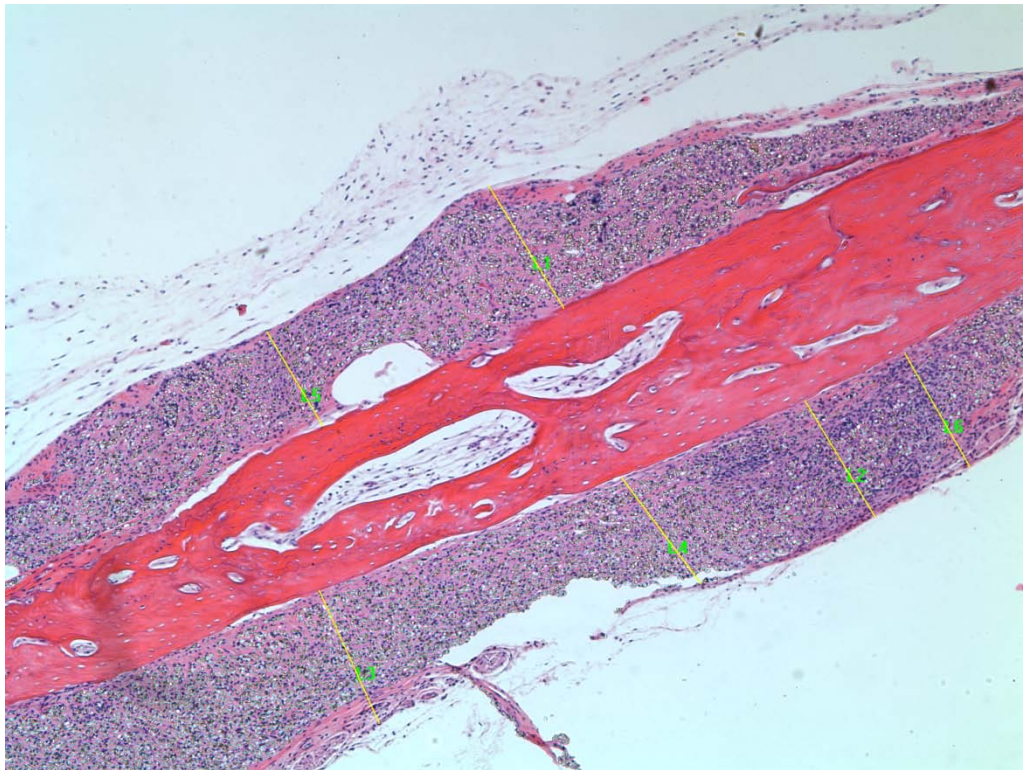


Figure 2.1: An example of the pouch thickness measurements. Six measurements were taken from the edge of the implanted bone to the outside edge of the pouch, as indicated by the yellow lines. H&E staining. 50x magnification.

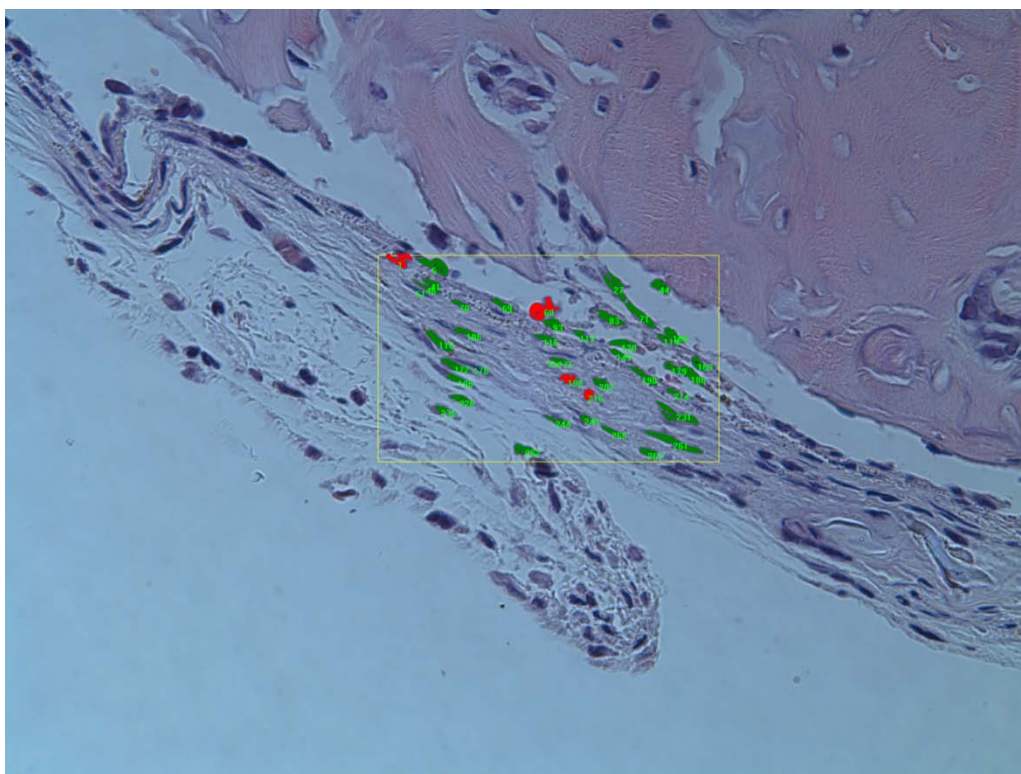


Figure 2.2: An example of the cell count performed on each air pouch. ImagePro Plus applied false color to the cells to separate them based on aspect ratio. The red cells have an aspect ratio of less than 1.8, and are classified as mononuclear cells. The green cells have an aspect ratio of at least 1.8, and are classified as fibroblasts. H&E staining. 400x magnification.

Because of the limitations of the image analysis software to provide an accurate count in highly cellular areas, as well as the complications introduced by the injected particles, the images were also visually inspected and scored by the scale listed in Table 2.4.

Table 2.4: The lymphocyte infiltration scoring system for the air pouch histopathology.

Score	Description
0	Few to no lymphocytes
1	Diffuse scattering of lymphocytes throughout tissue section
2	Focal accumulation of lymphocytes, or diffuse lymphocytes making up 10% or more of the total cells in the section, with or without vascular trafficking
3	Dense accumulation of lymphocytes with perivascular lymphocytic cuffing

### **2.15 Bone Density**

The density of the implanted bone segments was evaluated using the image optical density (IOD) measurement in ImagePro Plus. Density was assessed in three separate areas for each pouch, with an equally sized area of interest (AOI). The more demineralized bone sections had higher IOD scores than the areas with higher density bone, since demineralized bone has a lower staining intensity than normal, dense bone.

### **2.16 Statistical Evaluation**

Statistical evaluation of all results was performed with the SPSS software package. The means of each group were compared using one-way ANOVA and LSD post-hoc analysis for most measurements. Due to high standard deviations in the bone density and mononuclear cell percentages were compared by student t-test to obtain more accurate data. The limit of statistical significance was defined as  $p < 0.05$  for all analyses.

## CHAPTER 3

### RESULTS

In order to examine the effects of metal hypersensitivity and collagen induced arthritis on the inflammatory and osteolytic response to particulate debris, it was first necessary to sensitize the animals to chromium, type II collagen, or KLH using Freund's Adjuvant. To assess the success of the sensitizations, serum samples were analyzed for circulating antibodies using ELISAs.

#### **3.1 Metal Sensitization**

Blood samples from the metal sensitive group were collected before the first injection, 10 days after each of the three injections, and again at sacrifice to track the levels of circulating metal antibodies. Representative samples from the other two groups were also analyzed. An ELISA was used to determine the presence of antibodies to chromium, as described in section 2.10. Because it was possible to induce the formation of antibodies directed toward the GSH instead of the Cr bound to the GSH, and some non-specific antibody binding was expected, half of the wells were coated with GSH with Cr, and half were coated with GSH only. The ratio of the OD readings from the GSH-Cr wells to the GSH wells was used to determine the level of chromium specific antibodies. This calculation assumes that direct binding to GSH was equal in wells with and without Cr, which was considered reasonable due to the great size difference between GSH and Cr. A ratio of 1 or greater would indicate the presence of Cr antibodies.

The changes in serum antibody levels were normalized to the initial pre-bleed values by subtracting the initial OD ratio of each mouse from subsequent blood collections. Most animals showed an increasing antibody level over time, indicating an increasing immune response with each injection, but there was some variability. It is possible that the second and third

sensitization injections acted as antigen depots in some animals, sequestering antibodies out of the blood circulation and preventing accurate measurement. Because of the variability in sequential samples, a positive response was defined as an optical density ratio of 0.4 or higher at any time point, normalized to the pre-bleed ratio. Based on this cut-off 12 of the 36 animals were defined as sensitized to chromium. No representative animals from the CIA and control groups developed metal antibodies. Figure 3.1 shows the highest OD ratio for each metal hypersensitive group mouse by ear tag number and two mice from the CIA and Control groups over all sampling points, normalized to the pre-bleed ratio. Figure 3.2 shows the normalized OD ratio for each animal at each time point. Table 1 shows all animals considered positive for antibodies to chromium. Animals 1022-1033 received a pouch injection of PBS, 1034-1045 received UHMWPE particles, and 1046-1057 received CoCr particles.

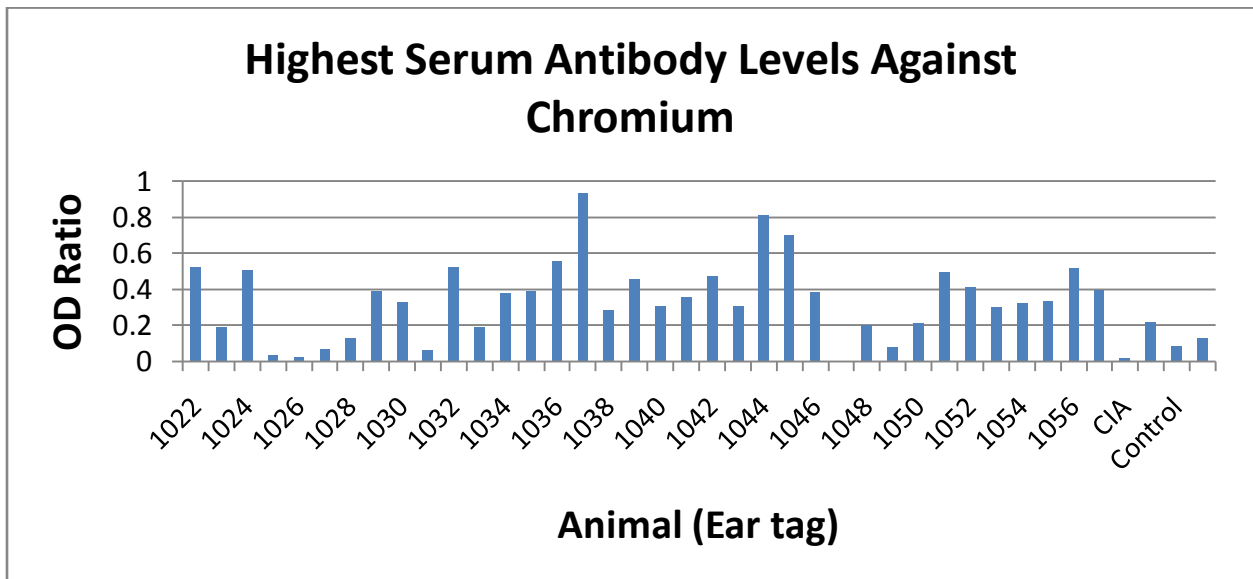


Figure 3.1: The highest normalized OD ratios for all animals in the metal hypersensitive group. Any animal with a ratio of at least 0.4 at any time point was considered to be positive for antibodies to chromium. The highest ratios for each animal are displayed.

Table 3.1: Mice positive for chromium hypersensitivity and the highest normalized OD ratios.

Animal Number	Pouch Injection Groups	Highest Normalized OD Ratio
1022	PBS	0.52
1024	PBS	0.51
1032	PBS	0.52
1036	UHMWPE	0.56
1037	UHMWPE	0.94
1039	UHMWPE	0.46
1042	UHMWPE	0.47
1044	UHMWPE	0.82
1045	UHMWPE	0.70
1052	CoCr	0.41
1056	CoCr	0.52
1057	CoCr	0.40

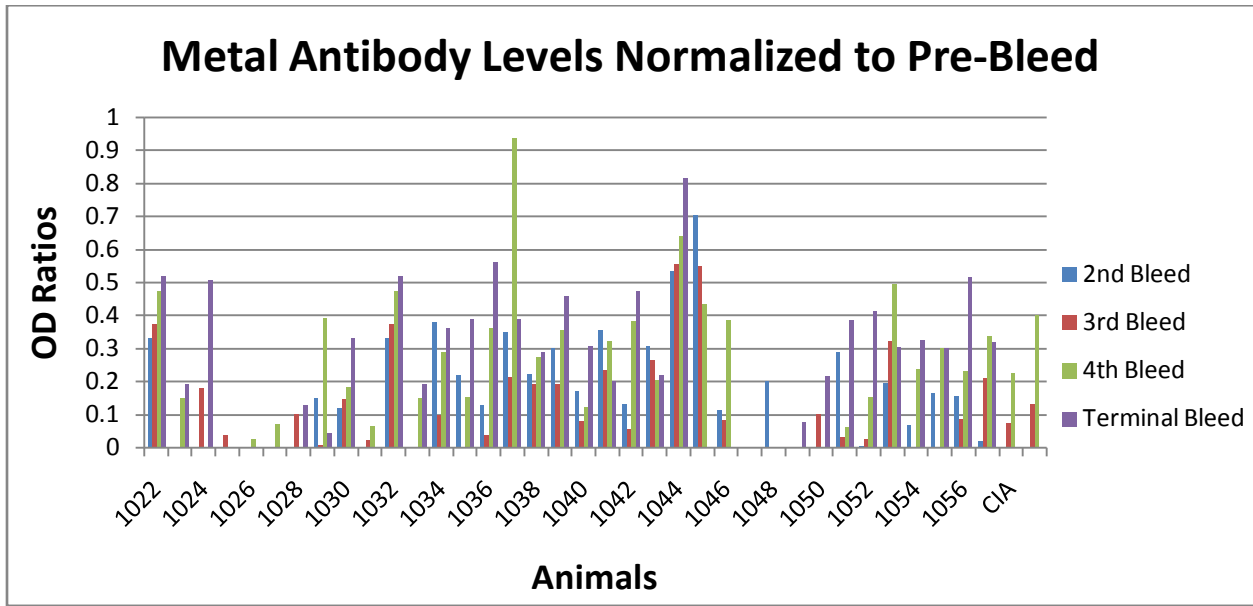


Figure 3.2: The OD ratios for all animals in the metal hypersensitive group at each sampling point, and representative animals from the other treatment groups. None of the tested mice in the other sensitization groups developed antibodies to chromium based on the study criteria. All results were normalized to the pre-bleed ratios, and show high variability between animals and over time. The final rats are the representative animals from the other sensitization groups.

### 3.2 Collagen Sensitization

Blood samples were collected from the collagen arthritis group prior to the sensitization injection, four weeks after the injection, and again at sacrifice. An ELISA was performed on the

serum samples to determine the presence of antibodies to collagen, as described in section 2.11. Successful sensitization was defined as an OD of at least 0.5 after the sensitization. All mice in the CIA group developed antibodies to type II collagen (Figure 3.3). Mice 1058-1069 received a pouch injection of PBS, 1070-1081 received UHMWPE particles, and 1082-1093 received CoCr particles.

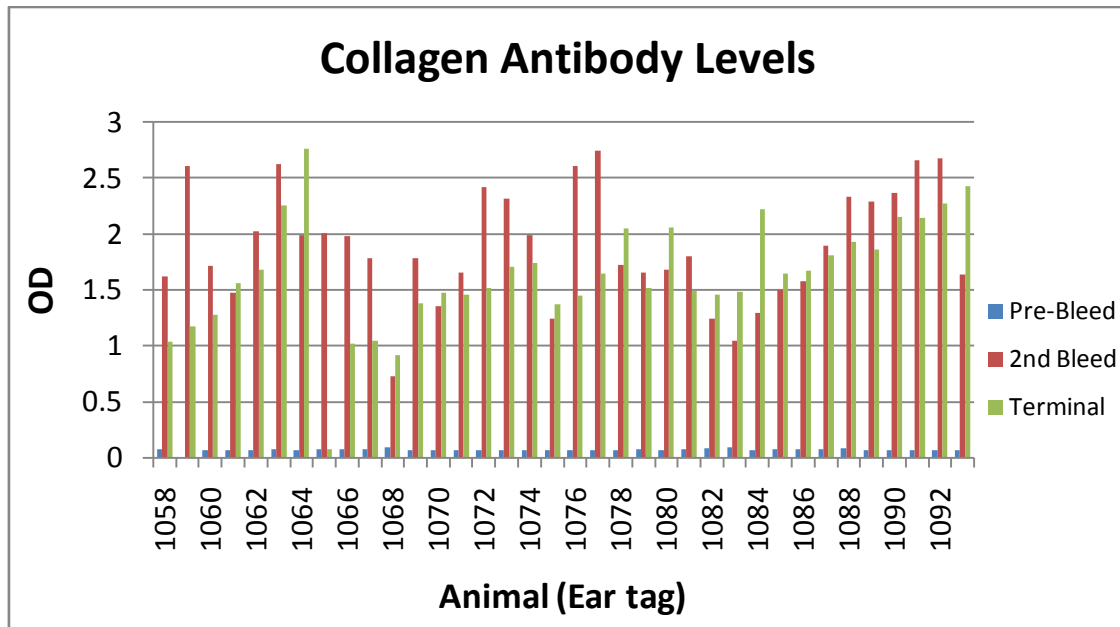


Figure 3.3: The collagen antibody level of each of the collagen sensitized animals at each sampling time point.

### 3.3 Pouch Cytokine Levels

The levels of IL-1, IL-6, and TNF $\alpha$  in the pouch homogenates were assessed by ELISA, as described in section 2.13. A reference standard curve was performed on each plate using the antibodies provided in the kits, and all plates displayed a good curve with correlation coefficient value of at least 0.995. The total protein levels in each homogenate were determined by use of a BCA protein kit, and were adjusted to deliver 40  $\mu$ g of protein to each well. The ELISAs of all samples indicated the complete absence of any of the three tested cytokines. Samples of the homogenates were spiked with the kit cytokine standards to investigate the possibility of an

inhibitor in the sample. The spiked samples showed an amount of cytokine equal to the amount added, indicating that there was no inhibition. No detectable levels of IL-1, IL-6 or TNF $\alpha$  were present in any pouch samples.

### **3.4 Air Pouch Thickness Measurements**

The thickness of each pouch membrane was measured using ImagePro Plus. Six individual measurements were taken for each animal, either from one section or multiple sections. The distance between the edge of the implanted bone and the outside edge of the membrane was measured, and the mean calculated for each animal. Care was taken to avoid sections with large gaps due to tissue separation during histological processing to obtain a more accurate measurement. The pouch thicknesses of all UHMWPE groups were greater than any of the PBS (range  $p < 0.000$  to  $p < 0.001$ ) and CoCr groups (range  $p < 0.000$  to  $p < 0.013$ ). There were no significant differences between any of the groups receiving the same particle injection. In general, the PBS pouches were thinnest, the CoCr pouches were thicker, and the UHMWPE pouches were the thickest. There were no significant differences between metal hypersensitivity group mice that did or did not develop antibodies to chromium. Based on the overall pouch thicknesses of each study group, none of the specific sensitizations made a significant difference in the response to the particle injections. This indicates that the inflammatory response to the particles was more dominant than the adaptive immune response. The mean thicknesses for each group are displayed in Figure 3.4. Figures 3.5-3.7 show representative examples of the pouch membrane thicknesses for animals receiving PBS, UHMWPE, and CoCr.

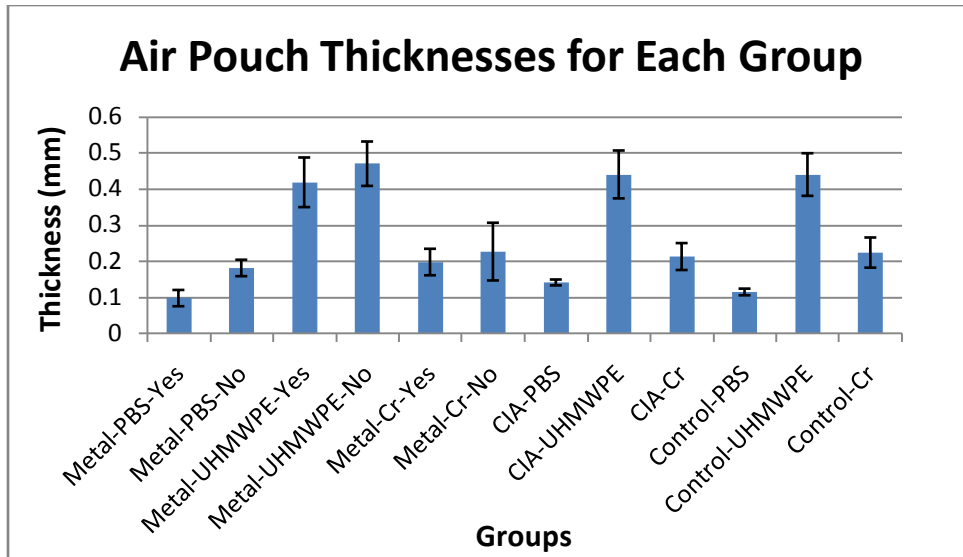


Figure 3.4: The mean pouch thicknesses of each experimental group, with positive and negative metal sensitive animals separated. Each group name indicates the sensitization group (metal, CIA, or Control), the pouch injection (PBS, UHMWPE, or Cr), and the presence or absence of chromium antibodies for the metal hypersensitive group (Yes or No, respectively). The error bars indicate standard error.

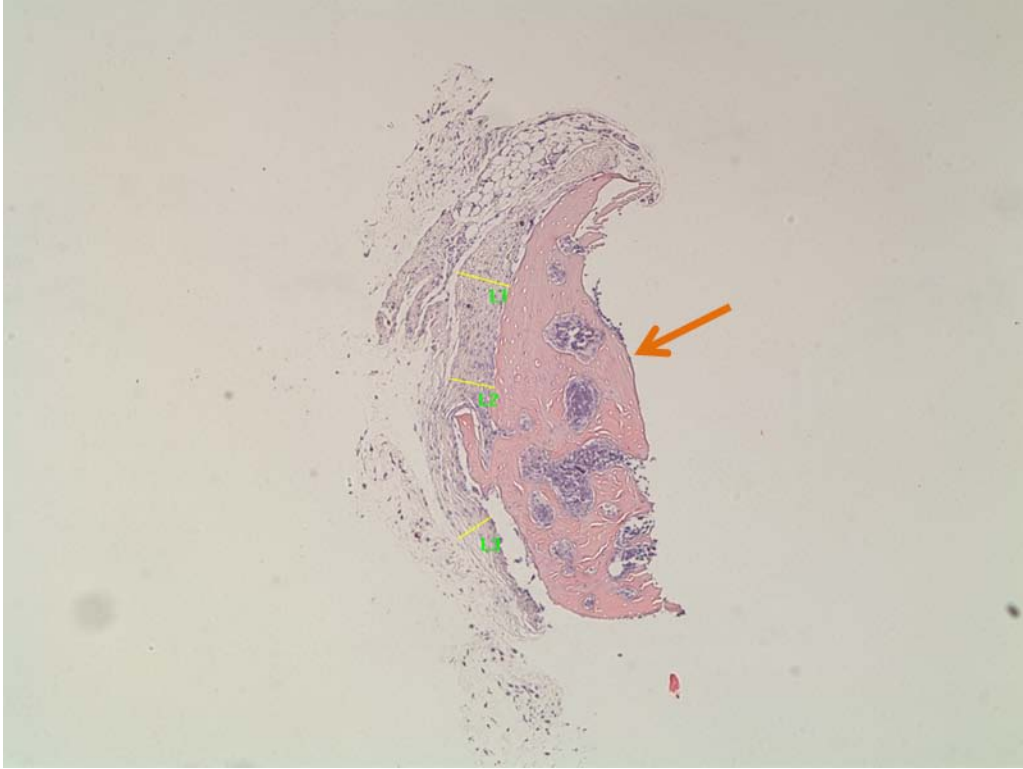


Figure 3.5: A representative animal from the PBS groups. The membrane is relatively thin, indicating a low level of inflammation. The orange arrow indicates the edge of the implanted bone. The yellow lines indicate thickness measurements. H&E staining. 50x magnification.

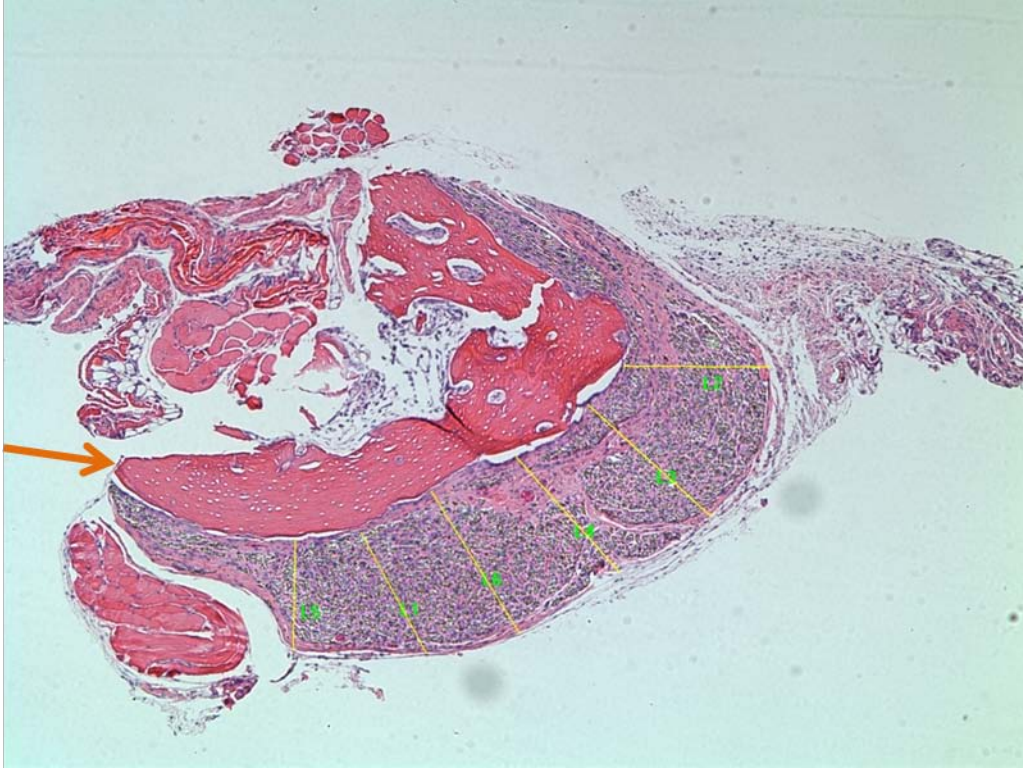


Figure 3.6: A representative animal from the UHMWPE groups. The membrane is quite thick with appreciably high levels of UHMWPE debris. This indicates a relatively high level of inflammation. The orange arrow indicates the implanted bone. The yellow lines indicate thickness measurements. H&E staining. 50x magnification.

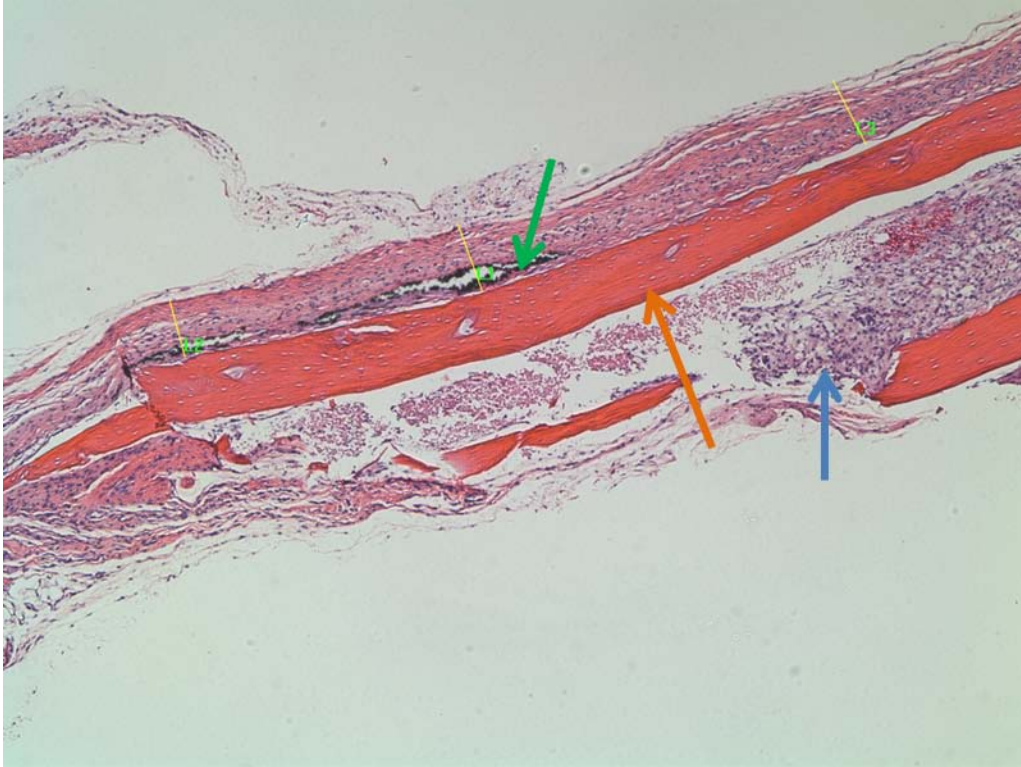


Figure 3.7: A representative animal from the CoCr groups. The membrane is thicker than the PBS groups and thinner than the UHMWPE groups, indicating a moderate level of inflammation. CoCr particles are visible. The orange arrow indicates the implanted bone, the blue arrow indicates the bone marrow of the implanted bone, and the green arrow indicates the CoCr particles trapped in the pouch membrane. The yellow lines indicate thickness measurements. H&E staining. 50x magnification.

### 3.5 Pouch Cell Counts and Inflammatory Percentages

Pouch cell counts were performed using Image Pro Plus image analysis software. Three AOIs with a consistent area were analyzed for each animal, and the mean count for each animal was calculated and divided by the area to obtain cell density. A higher cell density indicates an elevated cellular response in the pouch. Figure 3.8 displays the mean cell density per group. There were no significant trends observed between study groups. It is notable, however, that only three mice in the metal sensitive PBS and CoCr groups that developed antibodies to chromium, decreasing the statistical power of any comparison.

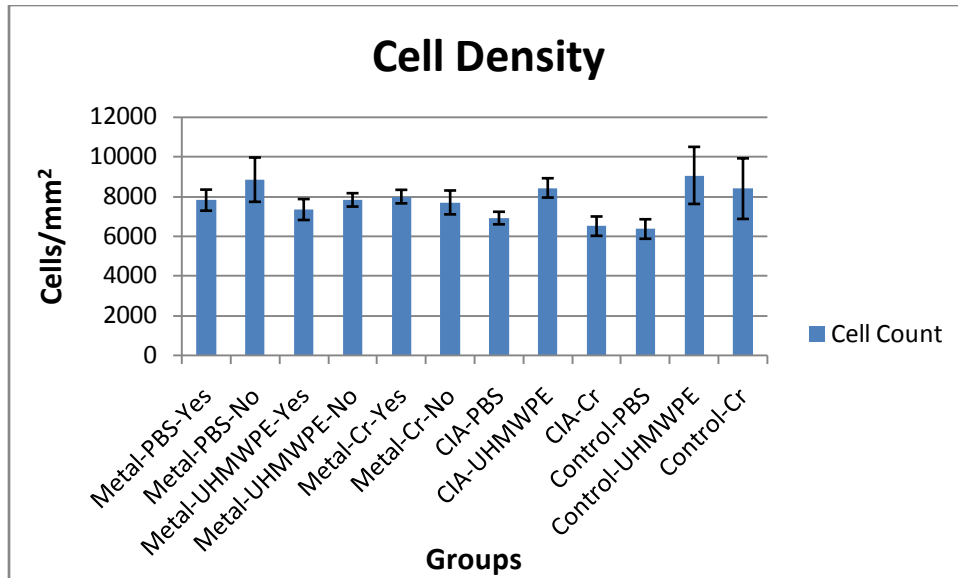


Figure 3.8: The mean cell density for each study group, with the positive and negative metal sensitive animals separated. The error bars indicate standard error.

The nuclei in each AOI were counted and separated based upon the aspect ratio, to separate them into mononuclear cells and fibroblasts. Cells with an aspect ratio of 1.8 or greater were classified as fibroblasts and those with an aspect ratio less than 1.8 were classified as mononuclear cells. A greater percentage of mononuclear cells indicates a more inflammatory response. Figure 3.9 displays the mononuclear cell and fibroblast percentages of each group.

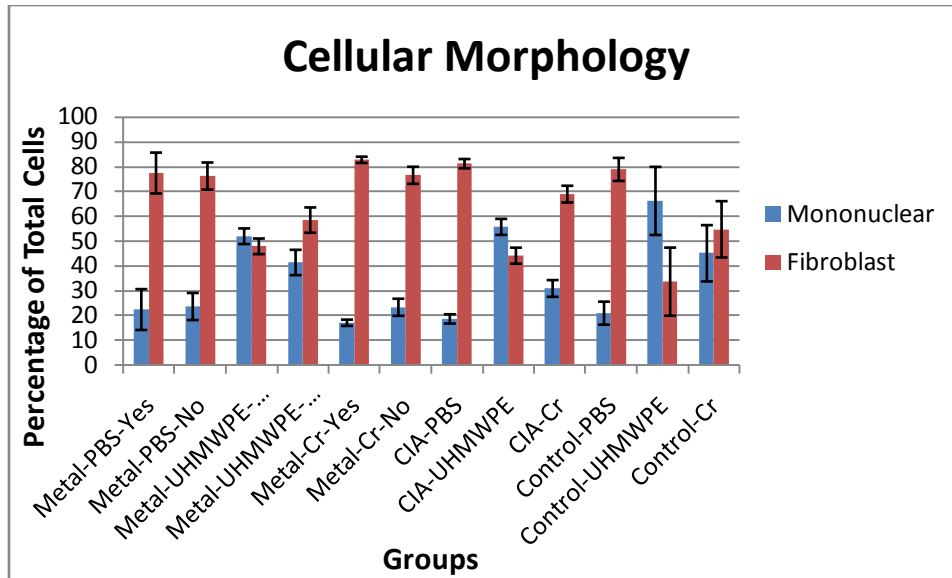


Figure 3.9: The mean mononuclear and fibroblastic cell percentage for each study group, with the positive and negative metal sensitive animals separated. The error bars indicate standard error.

In general, the mononuclear cell percentages of the UHMWPE groups were higher than the PBS and Cr groups, with the exceptions of the negative metal hypersensitive UHMWPE group and the control Cr group. All pouches contained a higher percentage of fibroblasts than mononuclear cells, except for the positive metal hypersensitive, CIA, and control UHMWPE groups. There was no significant difference between the positive and negative metal hypersensitive UHMWPE groups ( $p=0.107$ ). The percentage of mononuclear cells in the positive metal hypersensitive UHMWPE group was significantly higher than in the positive and negative metal hypersensitive PBS groups ( $p<0.004$  and  $p<0.001$ , respectively) the positive and negative metal hypersensitive Cr groups ( $p<0.001$ , both), the CIA PBS and Cr groups ( $p<0.001$ , both), and the control PBS group ( $p<0.001$ ). The CIA UHMWPE group had a percentage of mononuclear cells significantly greater than the positive and negative metal hypersensitive PBS groups ( $p<0.001$ , both), the positive and negative metal hypersensitive Cr groups ( $p<0.001$ , both), the CIA PBS and Cr groups ( $p<0.001$ , both), and the control PBS group ( $p<0.001$ ). The

control UHMWPE group had a higher percentage of mononuclear cells than the positive metal hypersensitive PBS group, but it was not quite statistically significant ( $p=0.078$ ). The control UHMWPE group had a higher percentage of mononuclear cells than the negative metal hypersensitive PBS group ( $p<0.008$ ), the positive and negative metal hypersensitive Cr groups ( $p<0.047$  and  $p<0.009$ , respectively), the CIA PBS and Cr groups ( $p<0.001$  and  $p<0.008$ , respectively), and the control PBS group ( $p<0.011$ ). The control Cr group had a significantly higher percentage of mononuclear cells than the CIA PBS group ( $p<0.015$ ).

The more inflammatory character of the UHMWPE group pouches would be expected given the highly inflammatory nature of UHMWPE particles. The only surprise was the lower inflammation of the negative metal hypersensitive UHMWPE group. Because the pouches contained no metal, it is doubtful that chromium specific antibodies would affect the response to UHMWPE. However, the presence of the antibodies would indicate a higher level of immune activation, potentially leading to more active macrophages to respond to the UHMWPE particles. It would be interesting to determine if the control group had developed measurable antibodies to the KLH. The mononuclear cell percentage of the control CoCr group was also relatively high, suggesting that the Complete Freund's Adjuvant injection by itself may have increased systemic inflammation or immune activity, although that would not explain the low densities in the control PBS group. It is suspected that the long implantation time may have affected the cell densities. Even mice in the PBS groups showed significant inflammation with bone resorption, as discussed later.

### **3.6 Lymphocytic Infiltration**

The pouches were scored on a scale from 0-3, as described previously in section 2.14, based on the level of lymphocyte infiltration, as well as the focal or diffuse nature of the

infiltrate. The nature of the biological response in the air pouches was extremely varied, even within study groups. No discernable pattern or trend was displayed in the groups due to the high intragroup variability. Figure 3.10 shows the mean scores for each study group, with the positive and negative metal sensitive groups separated. Some animals displayed a non-lymphocytic response, either primarily fibroblastic or inflammatory (Figure 3.11). Some of the pouches contained sparse lymphocytes only, with primarily fibrous tissue (Figure 3.12). The mere sensitization, even to KLH, of the animals provoked a generalized lymphocytic response in some animals, even in the non-particle stimulated PBS groups. This was observed as a diffuse lymphocytic infiltrate (Figure 3.13), as opposed to a focal aggregation. In one arthritic animal, a focal lymphocyte aggregate was observed surrounding a piece of UHMWPE debris, suggesting an exaggerated adaptive immune response, potentially initiated by the innate response to particulate debris (Figure 3.14). In many pouches no lymphocytes, or very few, were present. The few lymphocytes seen in these sections were likely simply trafficking through the tissue, rather than collecting to initiate or sustain an immune response to the pouch contents. In those cases, the response was primarily inflammatory, consisting of mostly scattered macrophages and osteoclasts, or fibroblastic, resulting in the formation of a fibrous capsule surrounding the pouch. In some cases, a focal lymphocytic aggregate was observed surrounding one or more blood vessels, consistent with the perivascular lymphocyte cuffing described in patients with ALVAL responses in the periprosthetic tissue at revision surgery [6] (Figures 3.15 and 3.16). One of the positive metal hypersensitive mice which received CoCr particles developed the focal lymphocytic aggregate with possible clonal expansion due to the presence of a mitotic cell in the middle of the aggregate. This suggests an adaptive immune response targeting chromium in a hapten-carrier complex. The fact that this response did not occur in all animals in any group

mirrors the variation observed among implant patients. In several pouches, the majority of the pouch membrane was quite thin and completely fibroblastic, but the area surrounding the sharp, cut end of the implanted bone was often inflamed. This was likely due to mechanical damage to the pouch lining, and/or inflammatory cells originating in the marrow cavity of the implanted bone, as opposed to an immune response. The implanted marrow was visibly active in many of the pouches. Figures 3.11-3.16 show examples of each of the scores to illustrate the grading process.

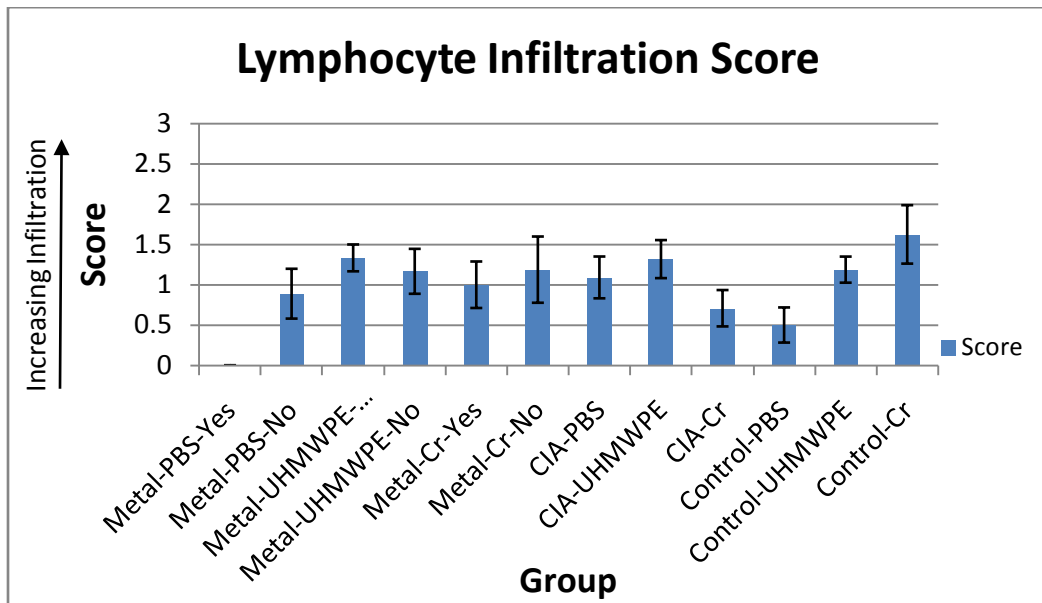


Figure 3.10: Mean lymphocyte infiltration scores for each study group. The error bars indicate standard error.

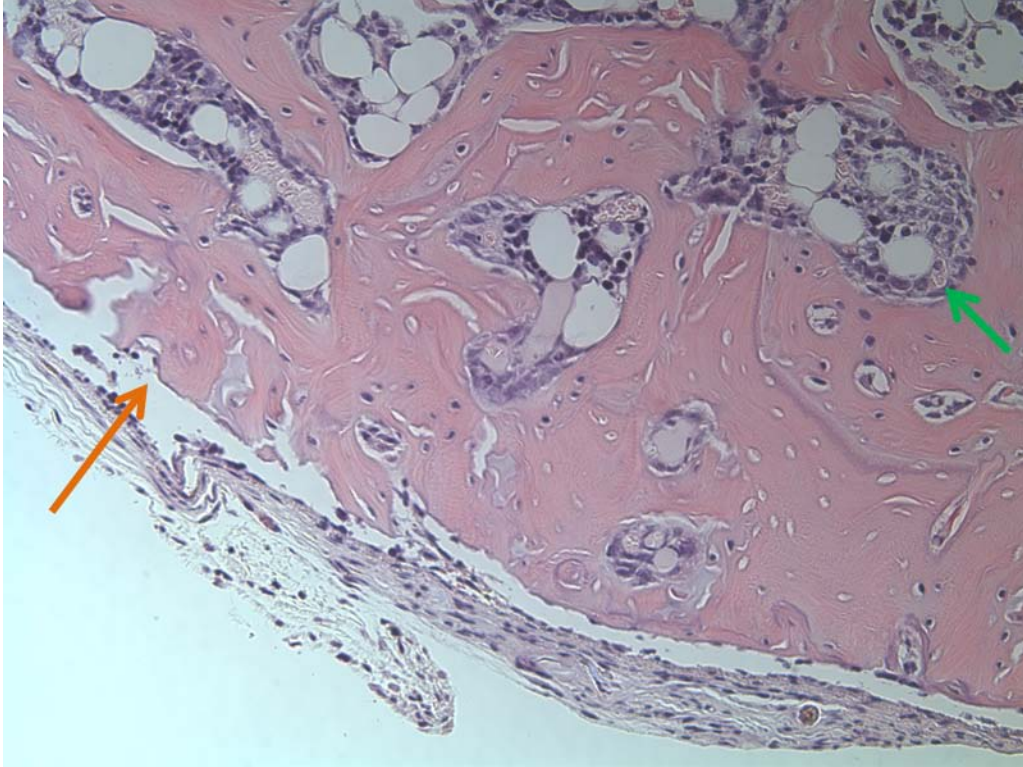


Figure 3.11: A representative air pouch scored as a 0. The membrane itself is quite thin, and nearly all visible membrane cells are fibroblasts. There is no significant mononuclear infiltration. The orange arrow indicates the implanted bone, and the green arrow indicates the bone marrow inside the implanted bone. H&E staining. 200x magnification.

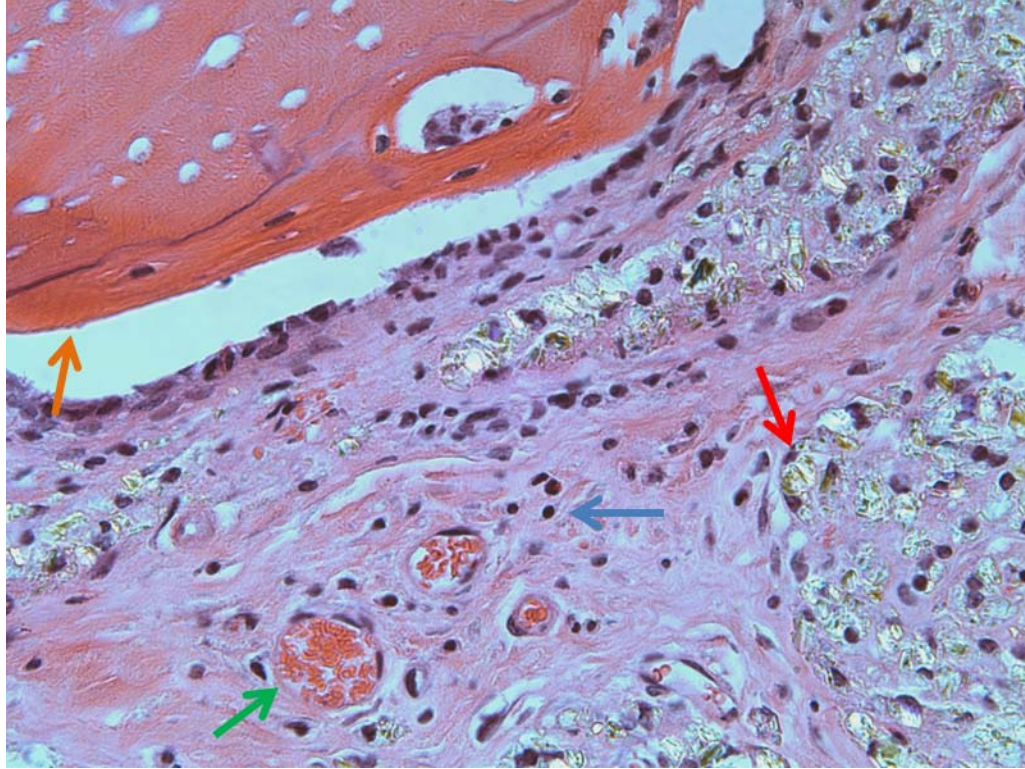


Figure 3.12: A representative animal scored as a 1. This section contains a few lymphocytes, but they are diffuse, with no focal aggregation. Some UHMWPE particles are visible in this section, as well as blood vessels. The majority of the cells in this section are fibroblasts, with considerable acellular fibrous tissue. The orange arrow indicates the implanted bone, the green arrow indicates a blood vessel in the membrane containing erythrocytes, the blue arrow indicates lymphocytes, and the red arrow indicates UHMWPE debris contained within the membrane. H&E staining. 400x magnification.

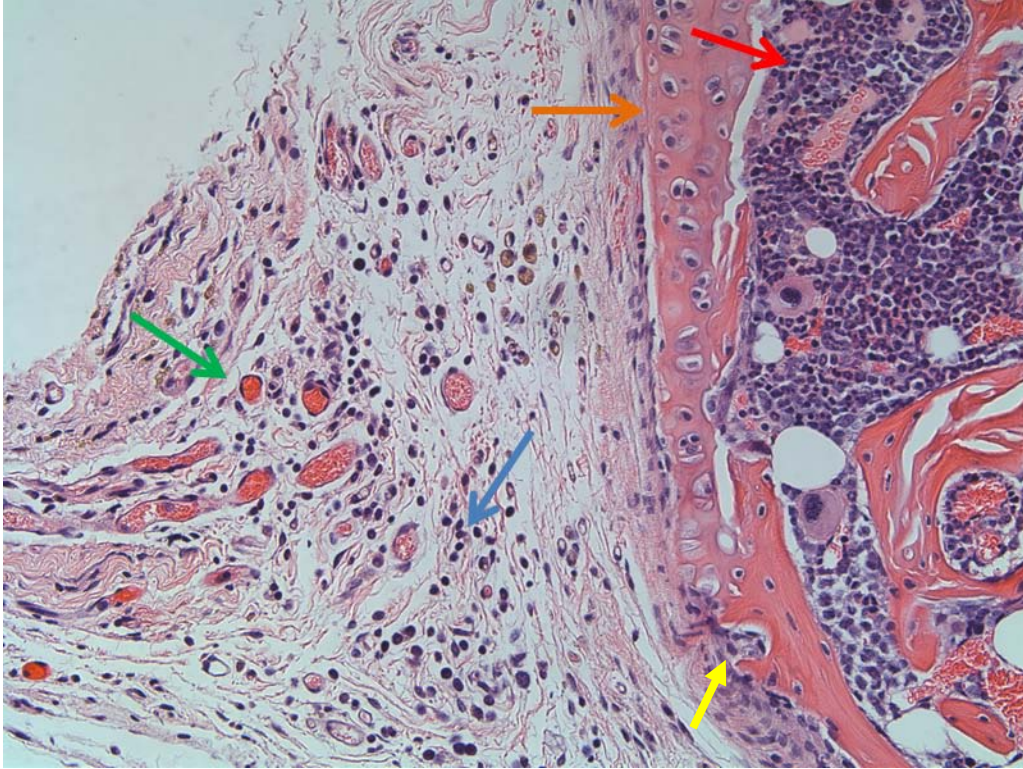


Figure 3.13: A representative air pouch scored as a 2. It contains a diffuse infiltrate of lymphocytes, suggestive of a more systemic lymphocyte response, rather than a focal specific target. This response is consistent with published descriptions of metal hypersensitivity. The orange arrow indicates the articular cartilage surface of the implanted bone, the red arrow indicates the bone marrow within the implanted bone, the green arrow indicates a blood vessel, and the blue arrow indicates the diffuse lymphocytic infiltration. The yellow arrow indicates an erosive pit along the surface of the implanted bone. H&E staining. 200x magnification.

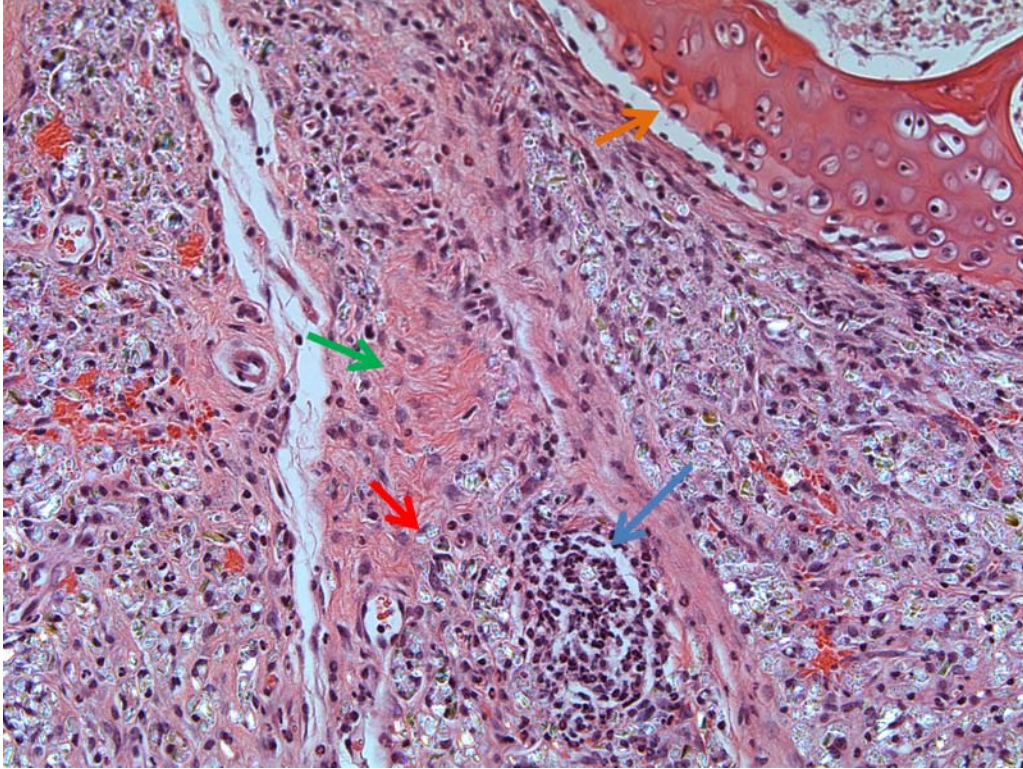


Figure 3.14: A second representative air pouch scored as a 2. Focal lymphocyte aggregation is observed at the lower end of the slide, but no perivascular lymphocytic cuffing. The lymphocyte accumulation appears to surround a piece of UHMWPE, suggesting that the initial response may have been inflammatory, rather than immune. The rest of the slide contains a mixture of mononuclear cells and fibroblasts, with large areas of fibrous tissue running through the section. The orange arrow indicates the articular cartilage surface of the implanted bone, the green arrow indicates an area of fibrous tissue, the red arrow indicates UHMWPE in the pouch, and the blue arrow indicates the focal lymphocyte aggregation surrounding UHMWPE debris. H&E staining. 200x magnification.

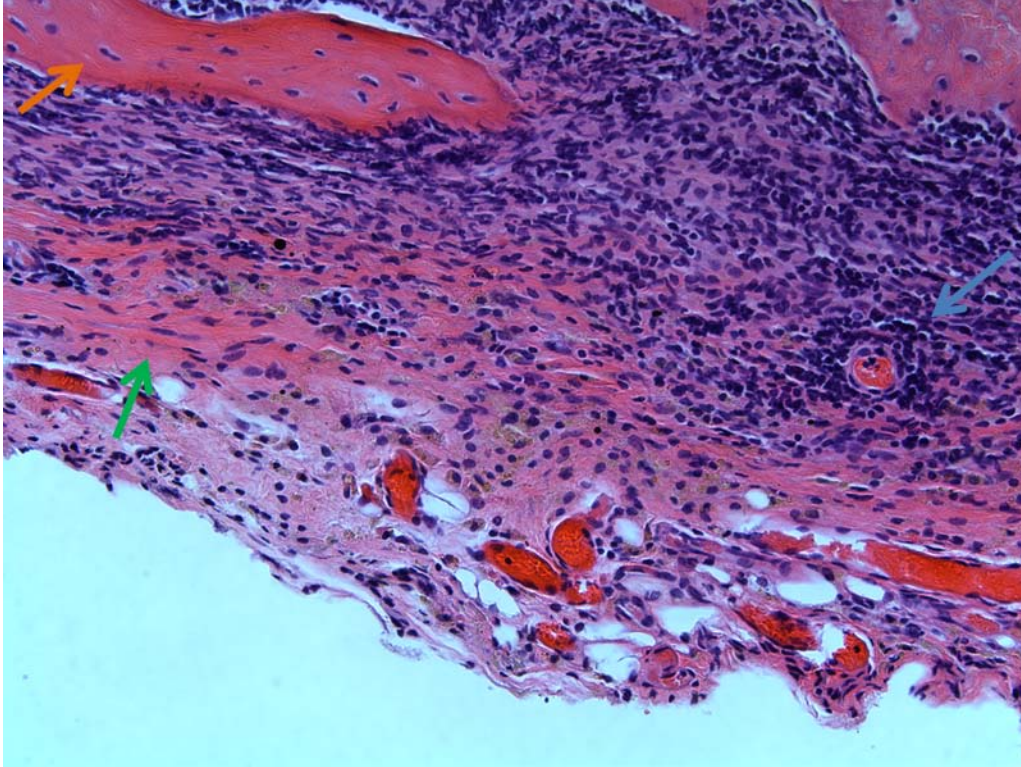


Figure 3.15: A representative air pouch scored as a 3, the maximum level of lymphocytic infiltration. Large numbers of lymphocytes are found throughout the section, with dense collections of inflammatory cells. A dense perivascular lymphocyte cuffing is visible surrounding one blood vessel, presumably due to the extravasation of lymphocytes from the blood circulation into the tissue. Two mononuclear cells are visible within the lumen of the blood vessel. There is also very tight contact between the membrane tissue and the implanted bone, with evidence of bone resorption. The orange arrow indicates the implanted bone, the green arrow indicates fibrous tissue in the pouch, and the blue arrow indicates the perivascular lymphocytic aggregate. H&E staining. 200x magnification.

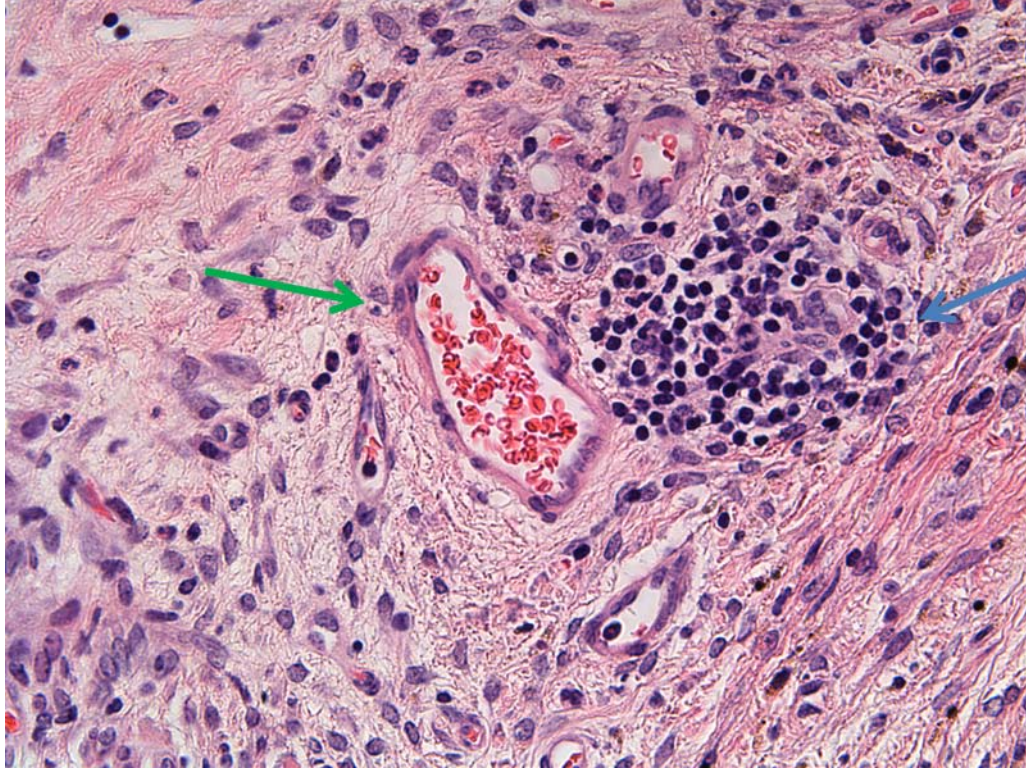


Figure 3.16: A second representative air pouch scored as a 3. There is an intense lymphocyte infiltration near multiple blood vessels. The green arrow indicates a blood vessel, and the blue is a lymphocyte aggregation. There is potential evidence of clonal expansion with visible lymphocyte mitosis. This may be a case of true perivascular lymphocyte cuffing of a blood vessel deeper in the section under the accumulation of lymphocytes, or this may be an early germinal center, in which new lymphocyte development is taking place. This animal was in the metal hypersensitive group and received CoCr particles, suggesting a potential role of chromium sensitivity in the response to the particles. This animal did not develop detectable circulating antibodies to chromium, so it may be a cell-mediated hypersensitivity response. H&E staining. 400x magnification.

The observed results, in which the response to either particulate was typically greater than the response to PBS, indicated that the inflammatory response to either particle was greater than the immunological response, regardless of the sensitization.

Although most pouches showed some degree of fibrous tissue deposition, two animals showed a necrotic response consistent with the definition of necrobiosis by Doorn et al. Unlike conventional necrosis, the fibrous tissue remains intact and the fibroblasts and mononuclear cells die. This response is described in the presence of particulate debris [21]. One animal received

UHMWPE particles (Figure 3.17) and the other received CoCr particles (Figure 3.18), consistent with the description above. This response is non-inflammatory, as evidenced by the lack of cellularity of the membrane in contact with the implanted bone, the loose adherence to the bone, and the lack of erosions of the implanted bone. This appears to be a more benign response, forming a fibrous capsule separating the foreign material from the rest of the body.

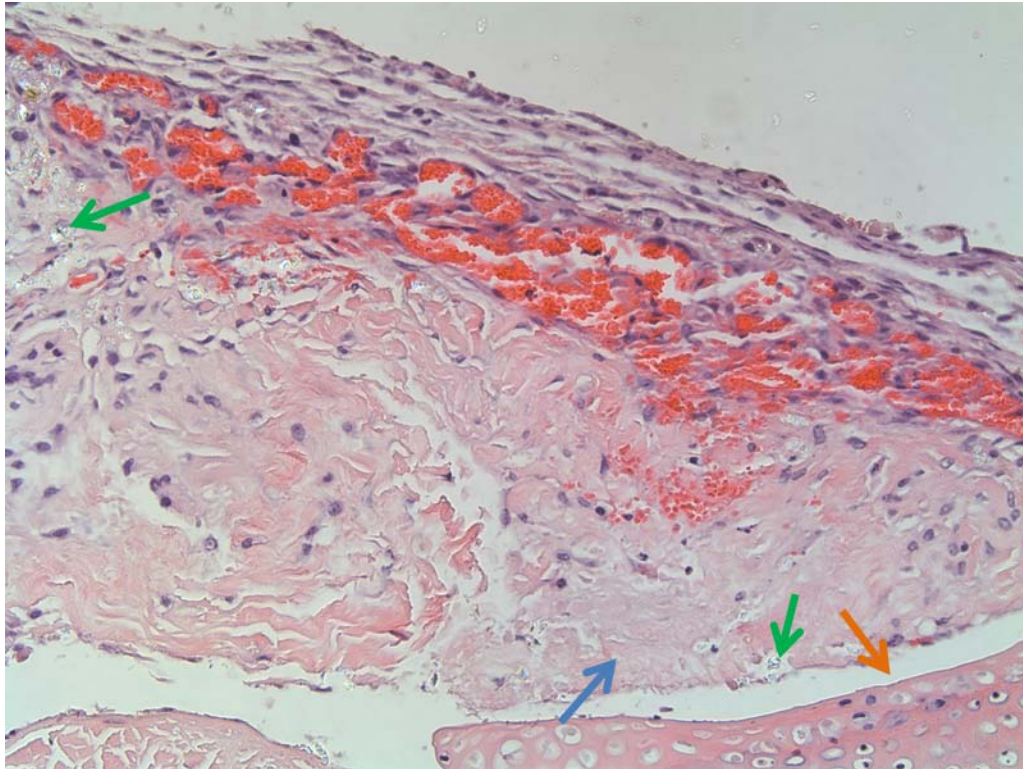


Figure 3.17: An UHMWPE air pouch displaying necrobiosis. This animal was in the positive metal hypersensitive group and received UHMWPE particles. A large fibrous area is located next to the implanted bone, and is mostly acellular. UHMWPE particles are visible within the necrobiotic tissue. Interestingly, the bone surface appears untouched and the necrobiotic pouch tissue is not tightly adherent. This appears to be a non-inflammatory and non-osteoclastic membrane response adjacent to the implanted bone. The orange arrow indicates the intact articular cartilage of the implanted bone, the blue arrow indicates the acellular fibrous tissue, and the green arrows indicate UHMWPE inside the necrobiotic tissue. H&E staining. 200x magnification.

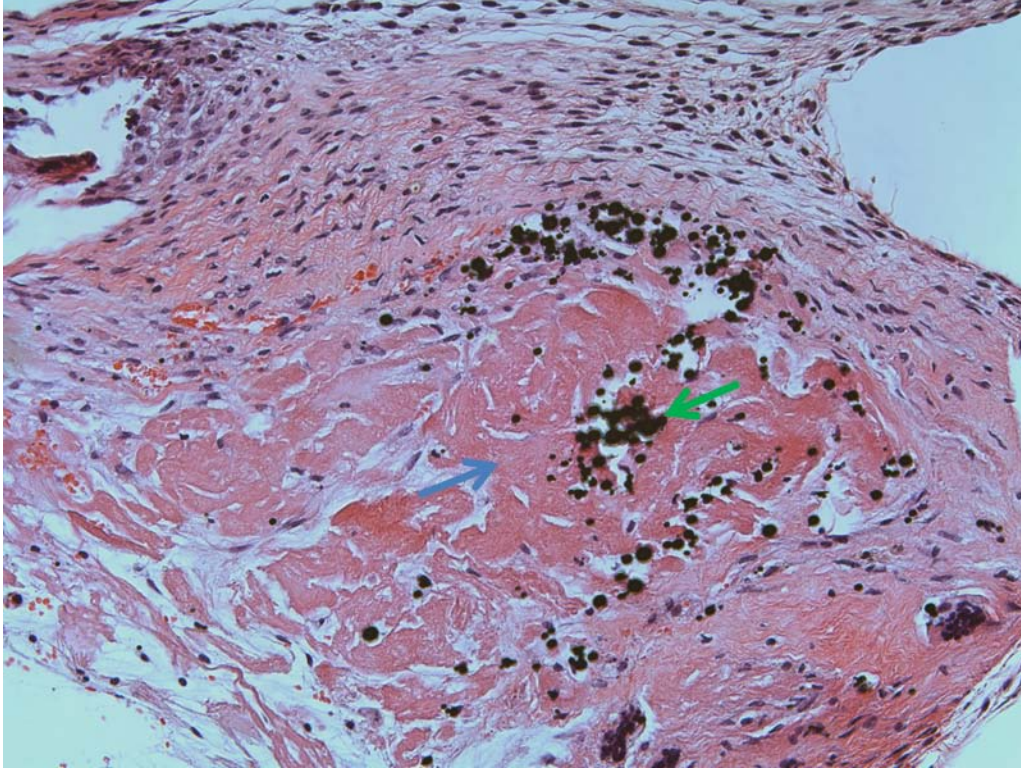


Figure 3.18: A CoCr air pouch displaying necrobiosis. This animal was in the CIA group and received CoCr particles. A large, mostly acellular fibrous area is surrounded by fibroblasts. Numerous CoCr particles are visible within the necrobiotic tissue. The blue arrow indicates an acellular area of necrobiosis, and the green arrow indicates CoCr particles contained in the necrobiotic tissue. H&E staining. 200x magnification.

### 3.7 Implanted Bone Density

#### 3.7.1 Image Optical Density

The IOD values were assessed using three AOIs of the same size to measure the density of the implanted bone, as described in section 2.15. There was an inverse relationship between the IOD value and the bone mineral density with H&E staining. Figure 3.19 shows the mean IOD values for all study groups. The hypothesis was that the metal hypersensitive and arthritic animals would display lower bone densities than the control animals, and that the animals receiving particles in the air pouch would have lower bone densities than those receiving only PBS, but this was not observed. Interestingly, the positive metal hypersensitive animals that received CoCr particles showed a greater bone density decrease than the positive and negative

metal hypersensitive groups receiving PBS ( $p<0.02$  and  $p<0.001$ , respectively), and the positive and negative metal hypersensitive groups receiving UHMWPE ( $p<0.03$  and  $p=0.085$ , respectively), although the difference from the negative metal hypersensitive group with CoCr was not quite significant. The difference between the positive and negative metal hypersensitive groups with UHMWPE was not significant ( $p=0.11$ ). The three arthritic groups showed similar levels of bone demineralization, which was significantly greater than both metal hypersensitive groups receiving PBS. The control group that received only PBS showed the greatest amount of bone demineralization, significantly greater than all other groups ( $p<0.001$ ) except for the positive metal hypersensitive group with CoCr and the control group receiving UHMWPE particles. These results indicate that there was significant bone loss even in the absence of injected particles.

The air pouch itself is mildly inflammatory, and inflammation can lead to bone loss, as described in aseptic osteolysis and rheumatoid arthritis. It is likely that the extended implantation period for the pouches contributed to bone loss. Based on other studies, major osteolysis of implanted bone in this model is observed in all animals regardless of treatment after 28 days, and this study ended at 26 days. More significant trends would likely be observed in a 14-21 day implantation. The chromium sensitive animal response to CoCr was interesting, suggesting that the sensitivity could play a role bone loss in metal hypersensitive patients with metallic implants. The fact that the positive CoCr group showed a greater degree of bone loss ( $p=0.122$ ) than the negative CoCr, although not statistically significant, suggests that metal antibodies could play a role in osteolysis, but this would have to be verified with further work. The negative metal hypersensitive mice received the same treatment as the positive animals, but did not develop sensitivity. This is consistent with the relationship between sensitive and non-

sensitive patients with the same type of implant. This lends support for the role of the individual immune system in the response to debris. Figures 3.20 and 3.21 display examples of demineralized bone sections.

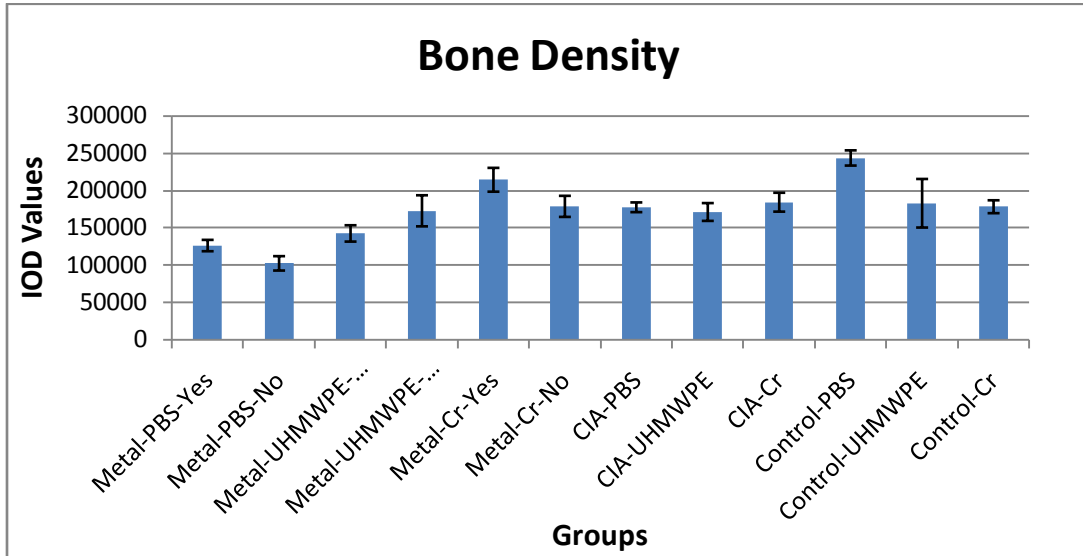


Figure 3.19: The mean IOD values for each study group, with the positive and negative metal sensitive groups separated. The higher the IOD value, the lower the bone density, so the higher IOD values indicate a higher amount of bone resorption. The error bars indicate standard error.

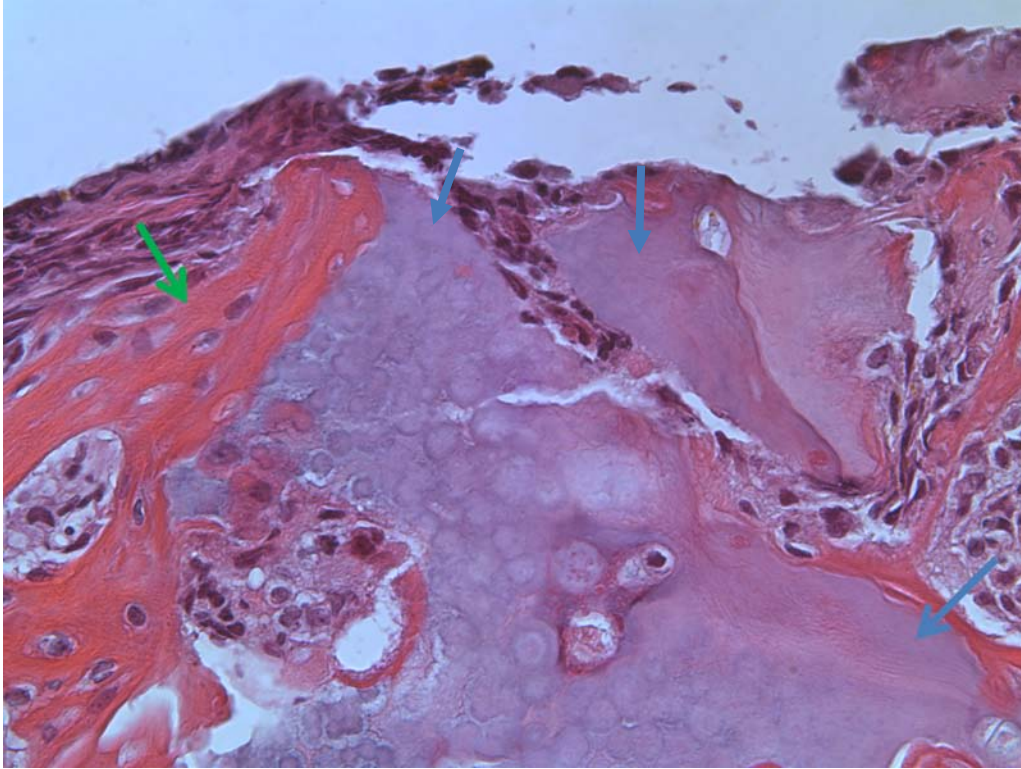


Figure 3.20: A representative section showing demineralization and resorption of the implanted bone. The discoloration indicates a lower density of bone, and pits have formed in the bone, infiltrated with osteolytic cells. The outlines of non-viable osteocytes or chondrocytes are visible in the demineralized area, consistent with the continuing bone resorption. The green arrow indicates the interface between the implanted bone and the tightly adherent pouch membrane, and the blue arrows indicate demineralized sections of bone. H&E staining. 200x magnification.

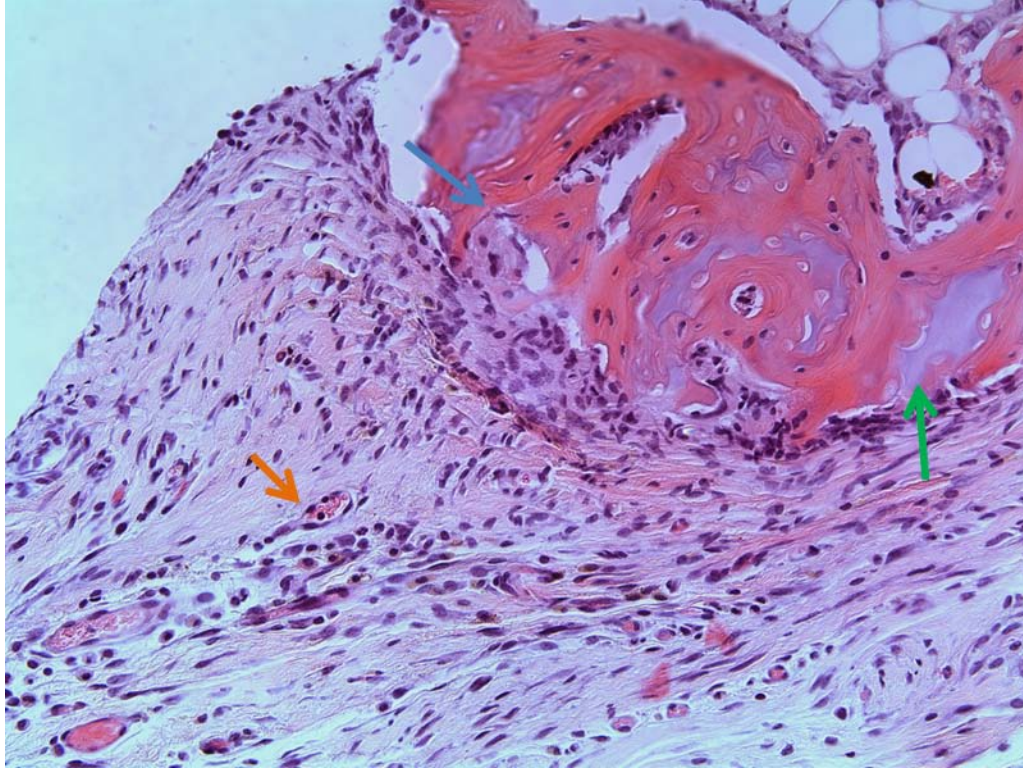


Figure 3.21: A second representative section showing demineralization and resorption of the implanted bone. The discoloration indicates a lower density of bone, and pits have formed in the bone, infiltrated with osteolytic cells. The orange arrow indicates a blood vessel with some streaming lymphocyte bands running through the pouch tissue, the green arrow indicates a demineralized area of the implanted bone with a tightly adherent pouch membrane, and the blue arrow indicates an erosive pit in the bone. H&E staining. 200x magnification.

### 3.7.2 Osteoclastic Osteolysis

In many sections multinucleated cells consistent with the appearance of osteoclasts were observed either near or in contact with the implanted bone (Figures 3.22-3.25). In many cases, the cells were observed attached to erosions in the implanted bone. About 25% of the sections showed presumptive osteoclasts, and they were observed in all groups except for the metal hypersensitive PBS groups, potentially due to lower levels of inflammation and immune responses.

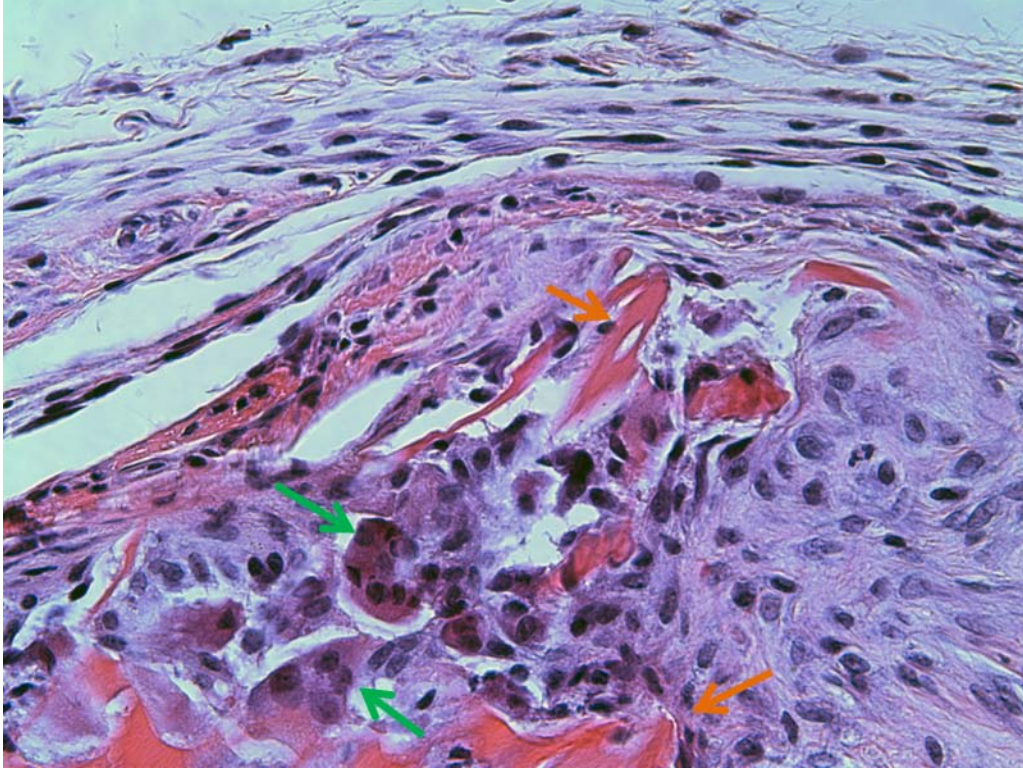


Figure 3.22: A representative section showing several multi-nucleated cells consistent with the morphology of osteoclasts attached to an eroded area in the implanted bone. These cells appear to be actively eroding the implanted bone. The orange arrows indicate the implanted bone, and the green arrows indicate the multinucleated cells morphologically consistent with osteoclasts. H&E staining. 400x magnification.

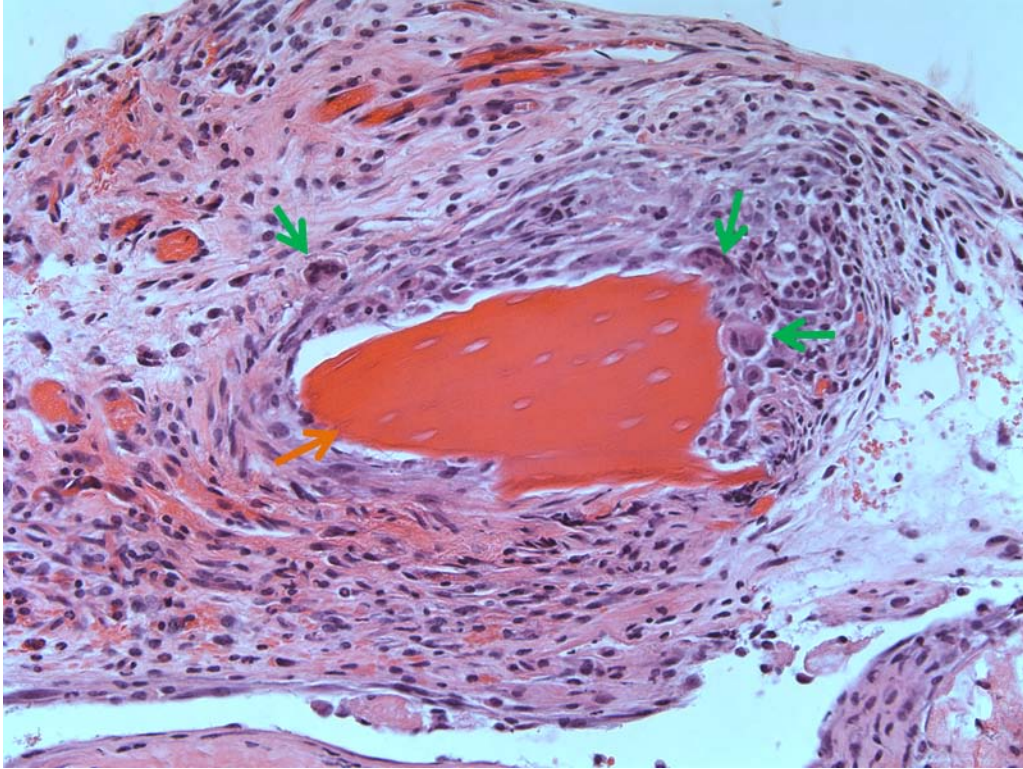


Figure 3.23: A second representative section showing several multi-nucleated cells consistent with the morphology of osteoclasts attached to an eroded area in the implanted bone. These cells appear to be actively eroding the implanted bone. The orange arrow indicates the implanted bone. The green arrows indicate several suspected osteoclasts. H&E staining. 400x magnification.

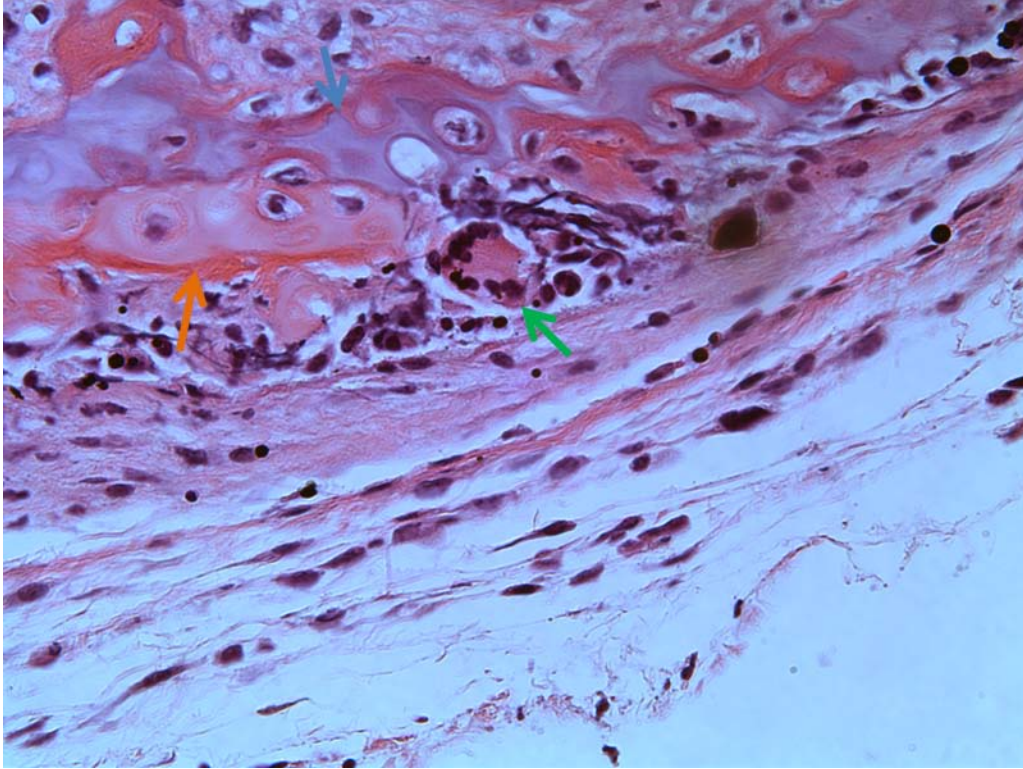


Figure 3.24: A representative section showing a multi-nucleated cell consistent with the morphology of an osteoclast next to an area of bone resorption. The orange arrow indicates an area of articular cartilage, the blue area indicates a demineralized area of either bone or cartilage, and the green arrow indicates a cell suspected to be an active osteoclast in close contact with the implanted bone. H&E staining. 400x magnification.

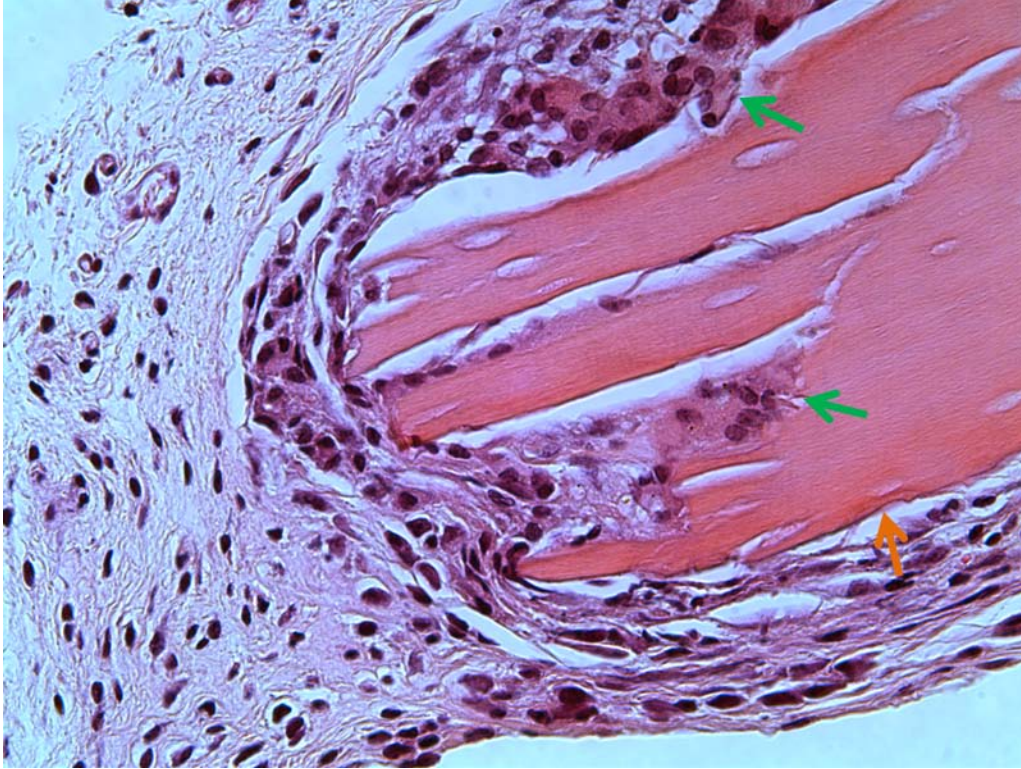


Figure 3.25: A representative section showing several multi-nucleated cells consistent with the morphology of osteoclasts. These cells appear to be actively eroding the implanted bone. The orange arrow indicates an intact surface of the implanted bone, and the green arrows indicate suspected osteoclasts in close contact with the bone, and within erosive pits. H&E staining. 400x magnification.

### 3.8 CIA Progression

All mice in the arthritis groups were evaluated daily for the presence and extent of arthritis. The paws were scored from 0-3 based on the scale described previously in section 2.5. The appearance, joint mobility and thickness of the paws were used to determine the paw score. The initial onset of arthritis is characterized by redness and swelling. As the paw moves into the second stage, the gross inflammation subsides and the swelling decreases. Some ankylosis is also typically observed. The final stage of the disease is characterized by ankylosis of most joints in the ankle or wrist, as the damaged joints are filled with fibrous tissue.

All animals developed arthritis except for one mouse in the UHMWPE group. There was no significant difference in the arthritis scores or paw numbers between the groups receiving PBS, UHMWPE, or CoCr in the air pouch, indicating that none of these injections had any effect on the development and severity of the arthritis. Figure 3.26 shows the mean arthritis scores for each particle group over the study period. Figure 3.27 shows the mean number of affected paws for each particle group over the study period. Figure 3.28 shows the percentage of affected paws in each group.

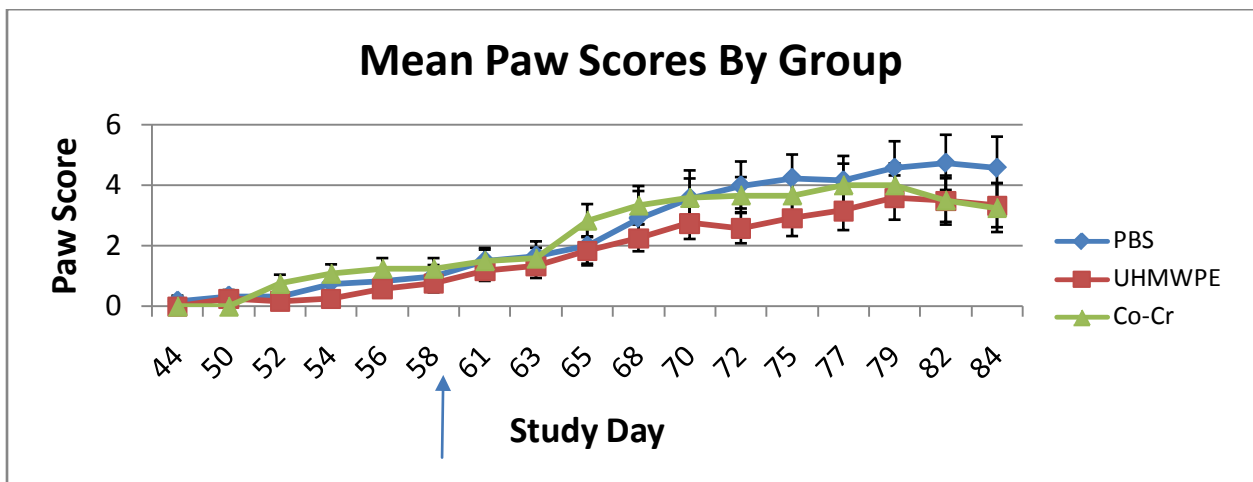


Figure 3.26: The mean paw scores by particle group of the arthritic animals by study day. No significant differences were observed between any of the groups at any time point. The arrow indicates the day of the particle injections into the air pouches.

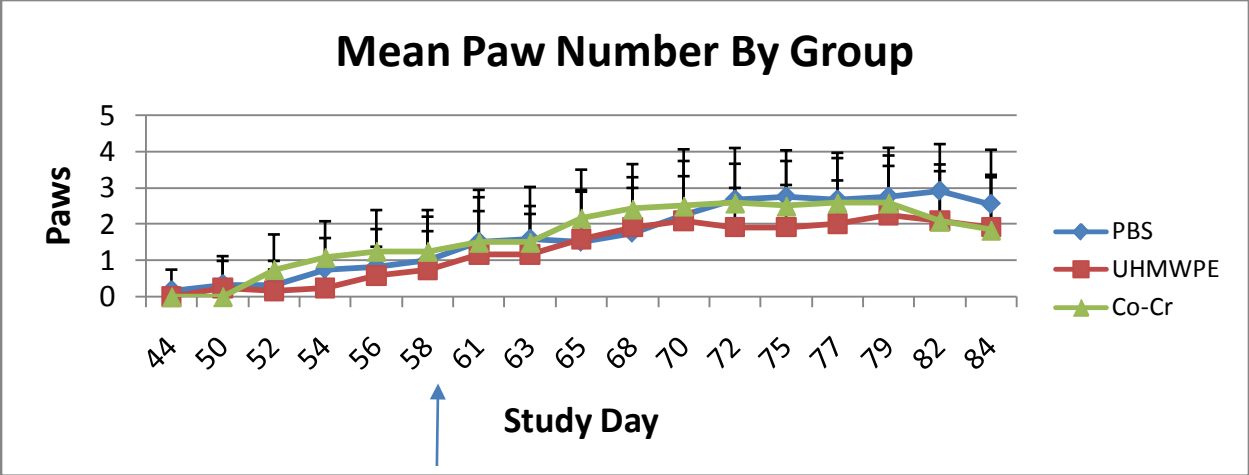


Figure 3.27: The mean number of affected paws by particle group of the arthritic animals by study day. No significant differences were observed between any of the groups at any time point. The arrow indicates the day of the particle injections into the air pouches.

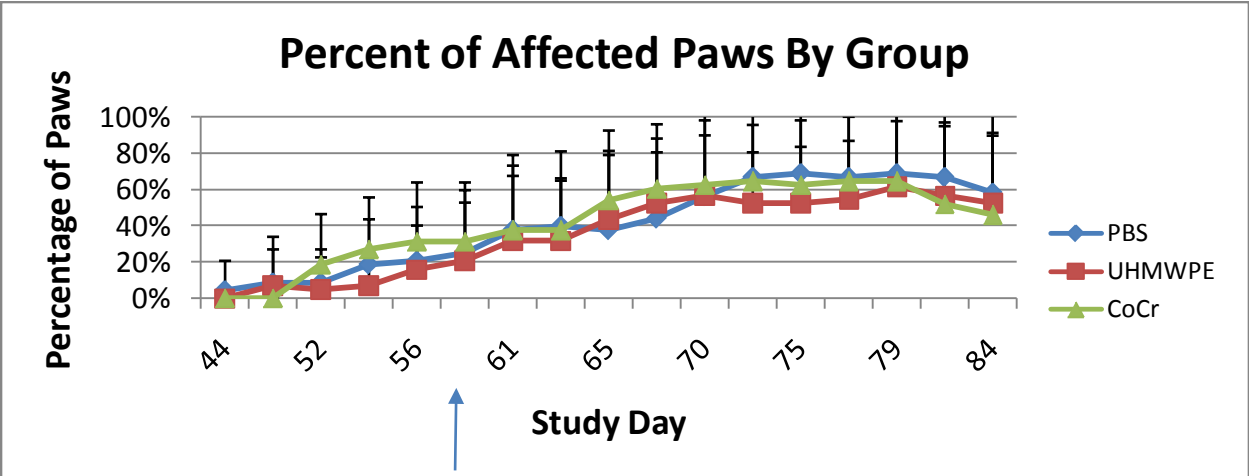


Figure 3.28: The percentage of total paws affected in each group throughout the study. The error bars indicate standard error. The arrow indicates the day of the particle injections into the air pouches.

### 3.9 Arthritis Histopathology

The pathology scores were assessed visually based on the scale described previously in section 2.5. Synovitis was assessed based on the thickness and mononuclear cell infiltration of the synovial membrane. In the early stages of the arthritis, the hypertrophied synovial membrane forms microvilli which attach to the articular cartilage and form a pannus. Once the pannus attaches, cartilage erosions begin, and some marginal erosion occurs in the bone and cartilage

near the synovial membrane attachment site. As the joint swells, edematous changes appear, distorting the joint architecture. The swelling and inflammatory infiltration can cause misalignment of the joints, interfering with joint articulation. The final stage of severe disease involves the complete destruction of joint mobility, with full bridging of the joints with fibrous tissue.

Some of the study animals showed possible germinal centers in the inflammatory infiltrate, suggesting a local continuation of the immune response in the joint. In a chronic inflammatory process, it is possible to develop tissue that mimics a tertiary lymphoid organ in the inflamed tissue. This is similar to a lymph node, and contains APCs which activate B-cells with receptors specific for local antigens. In this manner, a more efficient maturation and activation process for lymphocytes can take place, in addition to antigen transport to regional lymph nodes [47].

There were no statistically significant difference in the histopathology scores of the animals at sacrifice. The mean histopathology scores for each group are displayed in Figure 3.29. Figures 3.30-3.36 show examples of each of the overall scores.

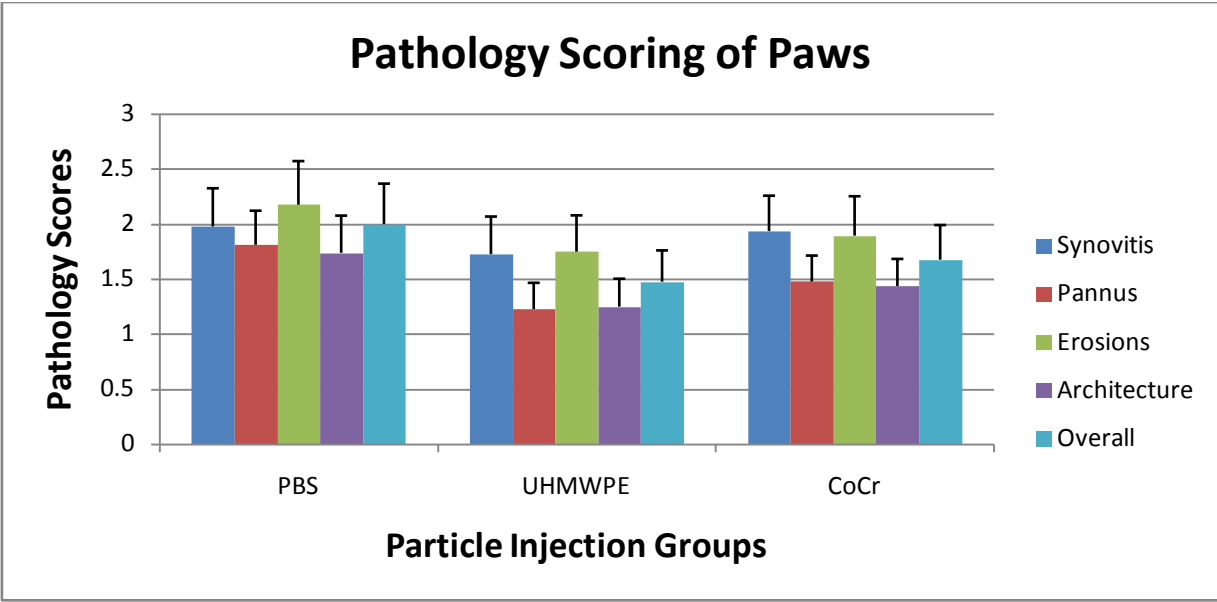


Figure 3.29: The mean histopathological scores for each particle group. No significant differences were observed between the groups for any measurement. The error bars indicate standard error.

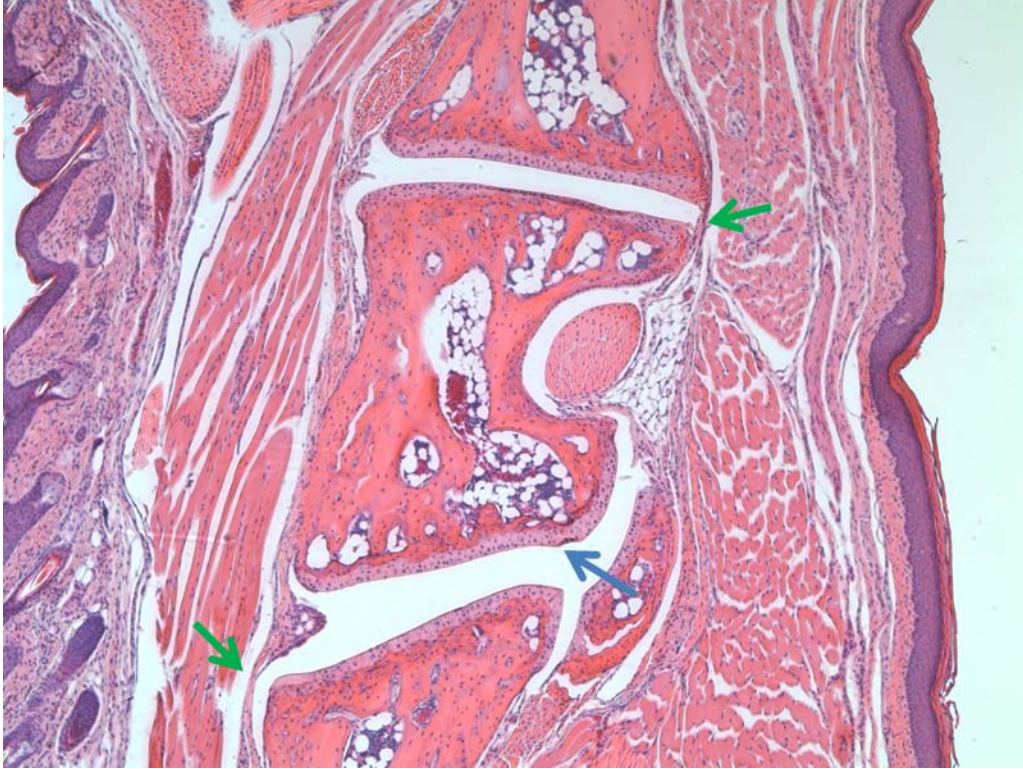


Figure 3.30: A representative section of a normal animal scored as a 0. This section received a score of 0 for all parameters. The blue arrow indicates smooth, intact articular cartilage. The green arrows indicate the thin synovial membrane. All joint spaces are visible and the bones are well-aligned. H&E staining. 50x magnification.

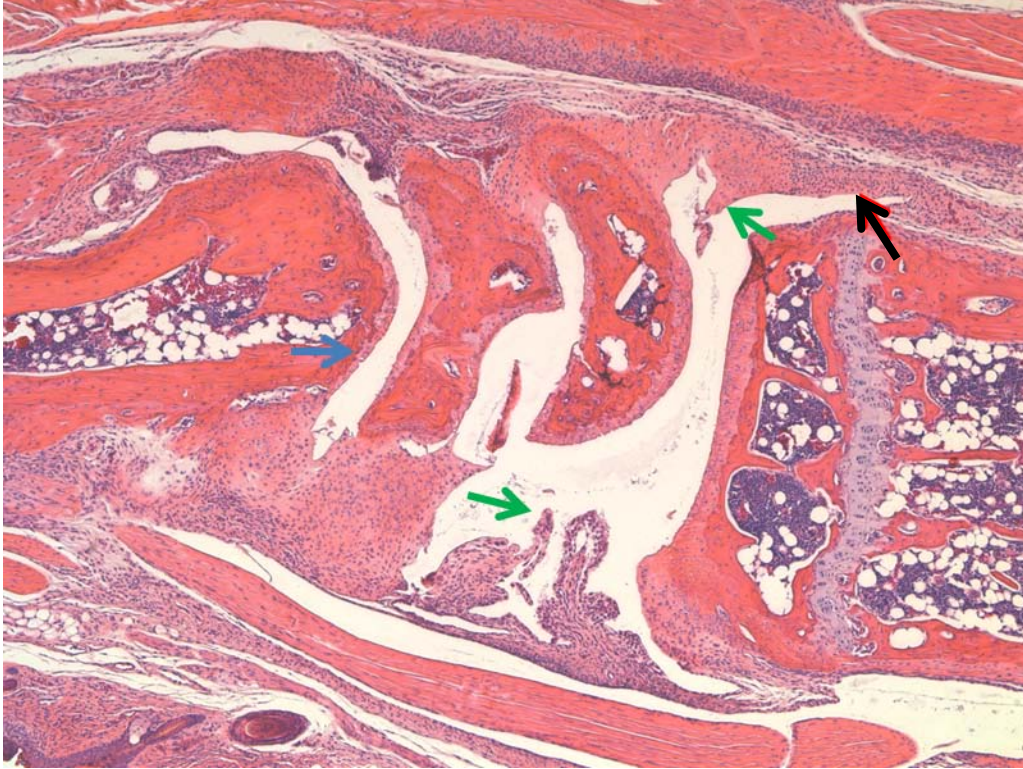


Figure 3.31: A representative section of an animal given an overall score of 1. There is slight cartilage and bone erosion for an erosion score of 1. Synovitis score is 2, and microvilli are present for a pannus score of 1. The architecture score was also 1, since the joint spaces are still present. The green arrows indicate microvilli. The blue arrow indicates cartilage erosion. The black arrow indicates a thickening of the synovial membrane, or synovitis. H&E staining. 50x magnification.

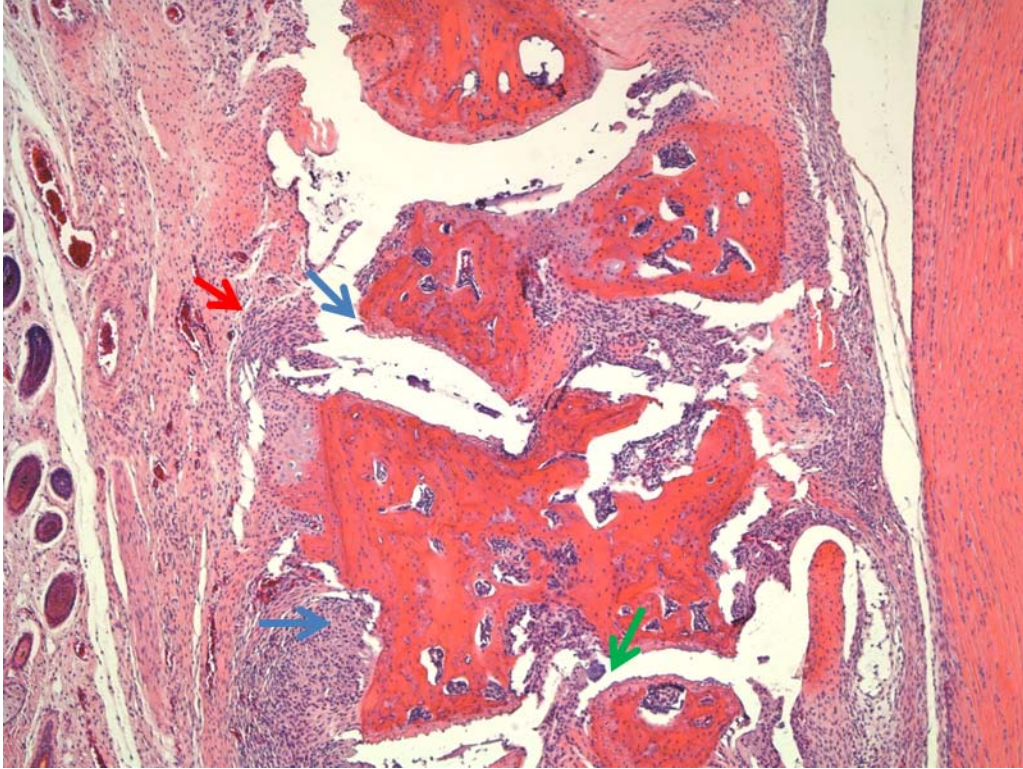


Figure 3.32: A representative section of an animal given an overall score of 2. There is some cartilage and bone erosion for an erosion score of 2. Moderate synovitis is present and some of the joints have pannus attachments, so both were scored as 2. The architecture score was a 2, since the basic joint spaces are still present. The blue arrows indicate areas of bone and cartilage erosion. The green arrow indicates an area of pannus attachment, separated by sectioning. The red arrow indicates an area of synovitis. H&E staining. 50x magnification.



Figure 3.33: A representative section of an animal given an overall score of 3. There is some cartilage and bone erosion for an erosion score of 3. Synovitis is present and the pannus is attached to some of the articular surfaces, so both were scored as 3. The architecture score was a 2, since the basic joint spaces are still present. The blue arrows indicate cartilage and bone erosions. The green arrow indicates pannus, detached by sectioning. The red arrows indicate synovitis. H&E staining. 50x magnification.

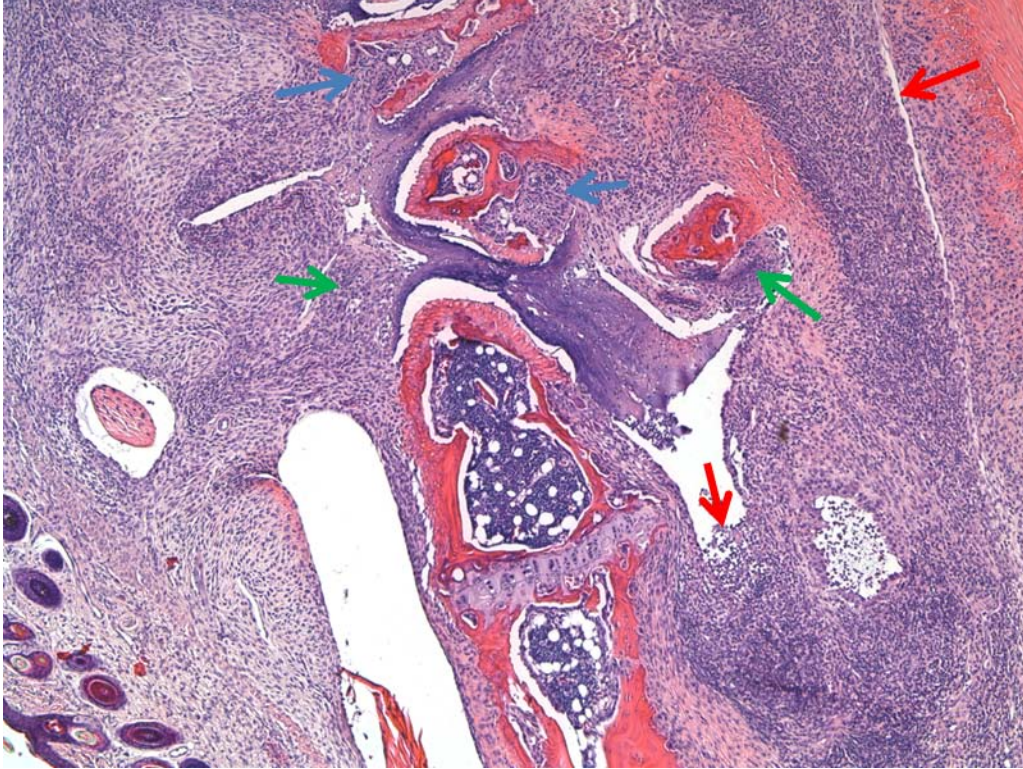


Figure 3.34: A representative section of an animal receiving an overall score of 4. The synovitis is clearly a 5, but some cartilage remains and joint spaces are still discernable. The marginal erosions are 5 and the architecture is a 4. The red arrows indicate areas of synovitis. The blue arrows indicate areas of bone and cartilage erosions. The green arrows indicate areas of pannus filling the joint spaces. H&E staining. 50x magnification.

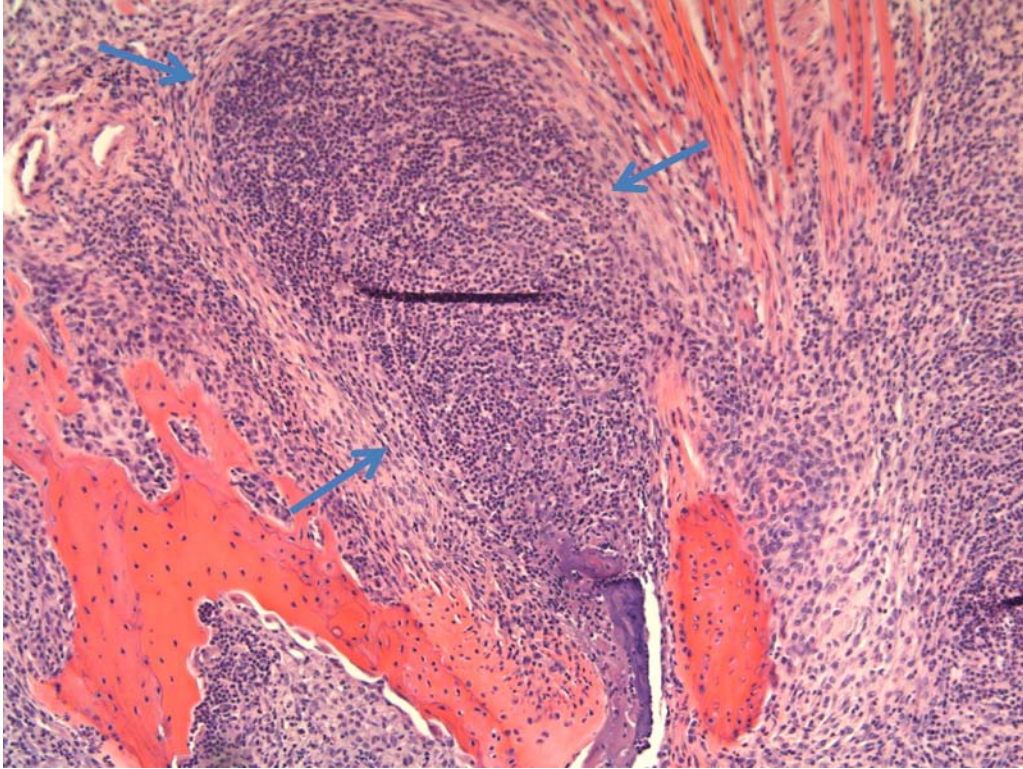


Figure 3.35: A possible germinal center adjacent to eroded bone. The blue arrows delineate a possible germinal center. The horizontal line is a folding artifact from histological sectioning. H&E staining. 100x magnification.

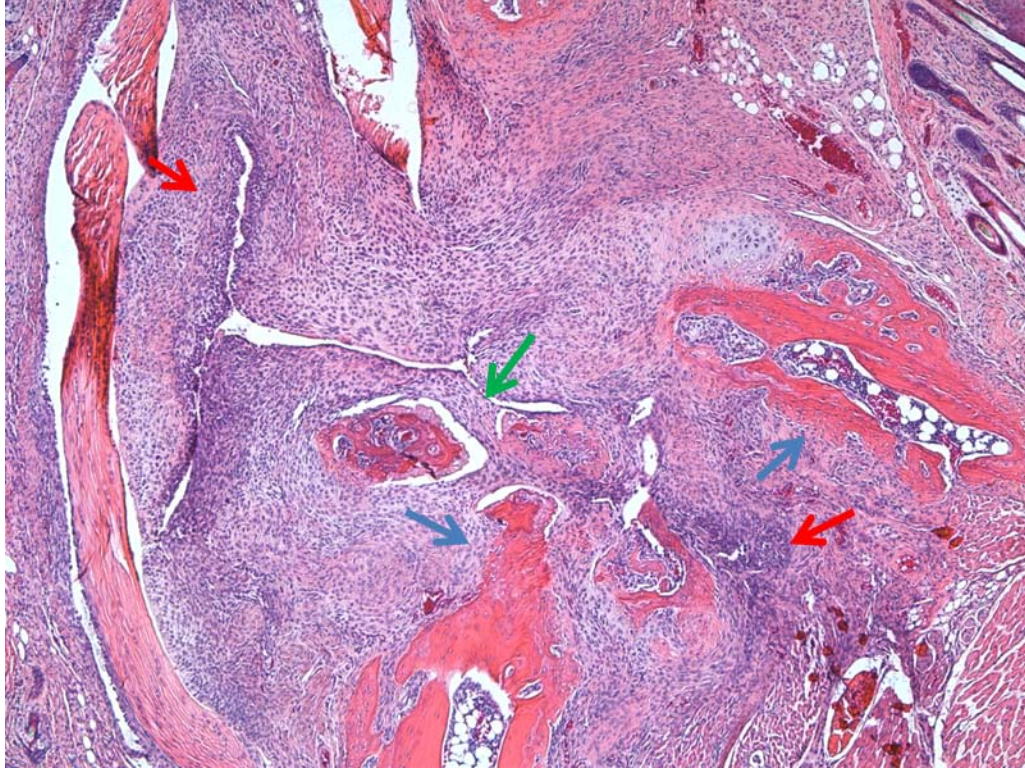


Figure 3.36: A representative section of an animal given an overall score of 5. This severely arthritic animal received a score of 5 for all parameters. The pannus has filled the joint spaces and fibrous tissue has immobilized the joints. The red arrows indicate synovitis. The blue arrows indicate areas of bone erosion. The green arrow indicates pannus filling the joint spaces, although most of the tissue is actually pannus. H&E staining. 50x magnification.

## CHAPTER 4

### DISCUSSION

The objectives of this study were 1) to investigate the effects of chromium hypersensitivity and collagen induced arthritis on the inflammatory, immunological, and osteolytic response in an air pouch containing bone with either CoCr or UHMWPE particles and 2) to determine the effects, if any, of CoCr or UHMWPE particles on the progression of collagen induced arthritis.

#### **4.1 Metal Sensitization**

Metal hypersensitivity is relatively common among the general population, due to environmental exposure to metals such as nickel, cobalt, and chromium. These sensitivities primarily manifest as a cutaneous type IV hypersensitivity reaction [57]. The incidence of metal hypersensitivity to medical implants is less well known, and the relevance of it to implant success is still being investigated. This topic has gained in importance due to the premature failures of the recent MOM hip prostheses. The overall prevalence of implant failures directly attributable to metal hypersensitivity varies by study, but is suspected to be less than 1% [48]. It is unknown, however whether the hypersensitivity may contribute to more failures typically attributed to other causes. About 25% of patients with well-functioning implants display a hypersensitivity to one or more metals, as opposed to 10-15% of the general population. This risk rises to 60% with a failing implant, but the cause and effect relationship is unclear [48]. It is important to emphasize the individual variability in the development of metal hypersensitivity among patients with the same implant under similar conditions. This indicates that individual variation exists in response to similar metal exposures, implicating a potential genetic component of the risk of metal hypersensitivity. It is known that there is a genetic predisposition toward the

development of drug allergies [83], so it is reasonable to expect a genetic component of metal hypersensitivity.

To study the effects of a hypersensitivity to metal on the response to metal debris, the mouse model developed by Yang and Merritt was utilized [56]. Because metal corrosion products are atomic, they must complex with proteins (albumin primarily) to form hapten-carrier complexes in order to be recognized by the adaptive immune system [56]. This is observed in the case of dermal hypersensitivity. To provide for the carrier, chromium was bound to glutathione and rabbit serum albumin. The glutathione is ideal for the binding of metals due to the presence of mercaptan groups [56]. Since metal is a “weak” antigen three separate injections were required, with the use of both Complete and Incomplete Freund’s Adjuvants. The low antigenicity of chromium is also exemplified by the low prevalence of successful induction of hypersensitivity (33%) among mice receiving the same treatments, as shown in section 3.1.

The low percentage of animals successfully sensitized in the metal group reflects the low prevalence of metal hypersensitivity in humans [9]. The original study conducted by Yang and Merritt had a successful sensitization rate of 33%, which was identical to this study [56]. However, compared to that study, the degree of sensitization in this study measured by OD ratio was quite low, which could compromise the assumptions made based on hypersensitivity to chromium. Since this study utilized an inbred strain, DBA/1, genetic variability between animals was minimized, indicating that susceptibility to metal hypersensitivity is not purely genetic. In the pilot work, Balb/c mice were utilized in the metal sensitization process, and the results were more positive, suggesting that Balb/c mice may be more prone to the generation of a hypersensitivity response to metal than DBA/1 mice. This difference was unforeseen, so DBA/1 mice were used in this study due to their improved susceptibility to collagen induced arthritis

[81]. For a more informative investigation of chromium hypersensitivity, it would be advisable to perform this experiment using Balb/c mice.

One limitation to the use of circulating antibodies to chromium to define metal hypersensitivity is that the prevailing theory of metal hypersensitivity in humans is that it resembles a type IV response primarily mediated by T-cells and macrophages [56], not antibody secreting plasma cells. Although the relevance of an antibody mediated response to a primarily cell-mediated response is uncertain, antibodies to Co, Cr, and Ni were detected in patients after implantation of a metallic implant [56]. This suggests a possible contribution of humoral immunity in the response to metals.

## **4.2 CIA Induction**

CIA is a rodent model of RA with significant similarities to human RA, including the initial onset of inflammation with joint swelling and redness. Bone erosions are also mediated by an erosive pannus formed from synovitis. CIA also often results in ankylosis of affected joints, leading to a permanent deformity [81]. Germinal centers can arise in the synovium of CIA affected joints [47,84] as well as in RA, and are believed to promote continuation of the inflammatory response. Circulating antibodies to type II collagen are present in CIA, and lead to erosions of hyaline cartilage which is primarily composed of type II collagen [81]. As with all animal disease models, there are some variations from the human disease which must be considered when drawing conclusions from animal studies. In RA, the specificity of autoantibodies is more variable and uncertain, as antibodies to citrullinated proteins [68], collagen [66], heat shock proteins [66,71], the Rheumatoid Factor [66,85], and other targets [66] have all been detected in RA patients. CIA is also typically a self-limiting disease which

resolves spontaneously even without treatment [86]. While RA can resolve, it often persists as a chronic disease for decades [83,86].

The induction of collagen induced arthritis is much more predictable than the metal sensitization procedure. This is likely at least partially due to the increased antigenicity of collagen as a protein, over chromium bound to a carrier protein. All mice in this study developed circulating antibodies to type II collagen after the type II collagen and Complete Freund's Adjuvant injection.

The development of clinical arthritis is less predictable, with an average of 80-100% of animals developing arthritis in one or more paws [86]. The extent of the arthritis is much more variable, as observed in this study and others from our lab. Some animals develop low level disease in only one paw, while others develop severe disease in all four paws. The number and extent of paw inflammation showed no relationship to the level of antibodies to collagen. The cause of this variability is unknown. Because the antibodies are measured in the general circulation, they presumably pass through all paws equally. In this study, 97% of the mice developed arthritis, providing large samples for statistical analysis.

### **4.3 Pouch Cytokine Levels**

Wooley et al. demonstrated that UHMWPE and CoCr particles introduced into the air pouch stimulated the production of IL-1 and TNF- $\alpha$ , perpetuating an inflammatory response [35], so elevation of these cytokines was expected in this study. CIA causes high levels of IL-1 and TNF- $\alpha$  [81], so those animals were predicted to have high levels in the pouches. The specimen collection, preparation, and ELISA for IL-1, IL-6, and TNF- $\alpha$  were carried out in the established method in our lab, except that half of the implanted bone was homogenized with the pouch membrane. Bone tissue contains numerous proteinases [87], which likely degraded the

cytokines in the samples, since no inhibitors were employed in the tissue processing. It would be expected that all three cytokines would be elevated in the thicker pouches and the ones with significant mononuclear infiltration, since all three are released by activated macrophages and attract further mononuclear cells [7]. As TNF- $\alpha$  is responsible for much of the bone destruction observed in RA and aseptic loosening [7,72], this cytokine would likely be more elevated in pouches with greater degrees of bone demineralization.

#### **4.4 Pouch Reactivity**

The murine air pouch is a widely used model for the assessment of biological responses to particulate debris and potential biomaterials. The membrane allows implanted materials and inflammatory cells and cytokines to remain contained in place, allowing convenient tissue harvest for histological sectioning, as well as molecular analysis for inflammatory mediators [35]. A modified version of the murine air pouch with implanted bone was utilized in this study to examine the inflammatory and immune responses to particulate chromium and UHMWPE debris, as well as the degree of osteolysis of the implanted bone.

The thickness of the air pouch membrane is directly related to the level of the inflammatory response to the pouch contents, with more inflammatory or immunostimulative contents causing an increase in thickness [13]. In this study, shown in section 3.3, there were no significant differences between any PBS groups, any UHMWPE groups, or any CoCr groups. This indicates that the specific sensitization targets did not cause a variation in pouch thicknesses in response to the same particles. It is possible that the adjuvant injection itself caused an alteration in the pouch thicknesses, but unsensitized controls were not examined. The differences in pouch thickness between groups with different particle injections appeared to be due only to the particles. As expected, the groups receiving the control PBS injections had the

thinnest membranes. The pouches containing CoCr particles were of intermediate thickness, and the UHMWPE pouches had the greatest thicknesses. This suggests that UHMWPE particles induce a greater pouch thickening than CoCr, regardless of sensitization. This trend differs from the finding of Wooley et al, when comparing the pouch reaction to various particles, in which CoCr particles produced a thicker pouch than UHMWPE, but that implantation was only 2 days, a much shorter duration than in the present study [35]. That was an acute study, while this was a chronic model, and the adjuvant injections here may have also induced a more aggressive response to the UHMWPE particles. An adaptive immune response would be much less likely in the case of the acute study, given the shorter exposure time, since the development of adaptive immunity takes several days.

Although the cell density measurements showed little variation among the study groups, the percentage of inflammatory cells making up the membranes did vary based on the particle injection. In general, the UHMWPE groups showed higher percentages of inflammatory cells than the PBS and CoCr groups, with the exception of the negative metal hypersensitive UHMWPE particle group. Because the response to UHMWPE is primarily innate, the higher level of inflammatory cells in those pouches is logical. It was unexpected that the negative metal hypersensitive UHMWPE group did not achieve statistical significance over any of the other groups. The value did not vary significantly from the positive metal hypersensitivity UHMWPE group, so it is likely that the lower value of the negative group was simply due to intragroup variation. It would be interesting to determine to whether the control group developed measureable antibodies to KLH. If so, it could potentially show an effect of a positive sensitization on the biologic response to UHMWPE, which is considered to be a non-specific innate response. However, von Domarus et al. described the appearance of lymphocytes in

periprosthetic tissue surrounding MOP implants at revision for aseptic loosening, so some uncertainty remains regarding the exact nature of biological responses to debris [88].

Because the air pouch is an inflammatory tissue, some level of inflammation is expected in all pouches, regardless of stimulation [13,35]. In addition, the implanted bone was observed to mechanically irritate the membrane and contains viable bone marrow, which could provide osteoclastic and mononuclear cells in addition to those generated by the implanted mice. Significant bone destruction was observed in most of the pouches, which is an inflammatory process on its own, potentially leading to mononuclear cell infiltration regardless of particle addition. A shorter implantation time might have yielded more intergroup difference, as the bone demineralization was evident even in the groups receiving only PBS, which were expected to display the least bone resorption of all the pouch injections. The longer implantation time was used in order to allow for observation of the effects of the particle stimulation on the progression of the arthritis. Since this study indicated a lack of influence of the particle injections on the arthritis course, a 10-14 day implantation is more likely to provide a more robust comparison of the pouch responses [13].

Since the metal hypersensitivity reactions are typically lymphocytic [4], the pouch membranes were also assessed for lymphocyte infiltration. No significant trends were observed between the groups in terms of lymphocyte infiltration, although the PBS groups tended to show less lymphocyte infiltration than the particle-stimulated groups, as described in section 3.5. High intragroup variability was observed in all study groups, which mirrors the high variability of patient response to similar biomaterial exposure. Some animals had very little mononuclear infiltration, while others had high levels of perivascular lymphocyte infiltration. The observation of the lymphocyte cuffing is presumably the result of extravasation of lymphocytes into the

tissue surrounding the inflammatory material, in this case, both the particles and the implanted bone. The high density of these cells suggests that the tissues contain high levels of inflammatory cytokines and chemokines, stimulating a large influx of immune cells. The innate immune system (macrophages) is primarily involved in the response to UHMWPE, as opposed to the adaptive system (lymphocytes) [19], so the observation of a lymphocytic response in these groups was unexpected. All animals received at least one injection of Complete Freund's Adjuvant, however, which likely led to alteration of the immune surveillance even in the KLH groups. The majority of the lymphocytes in all groups were relatively scattered throughout the pouches, presenting a more diffuse lymphocyte infiltration, suggesting a potentially systemic increase in non-specific inflammatory and immune responses. Von Domarus et al. described lymphocytic infiltration in the periprosthetic tissue surrounding loose MOP hip and knee replacements, suggesting that they may be involved in the aseptic osteolysis, but their presence in the tissue was unexplained [88].

Multiple case studies describe necrotic tissue surrounding MOM implants, primarily in the form of pseudotumors [4,15,20,21]. The exact cause of these masses is unclear, but may be chronic inflammation and immune activation or local toxicity due to the presence of a large volume of debris. Another type of necrosis, necrobiosis, is observed in periprosthetic tissue and involves the loss of cellularity with the preservation of the fibrous tissue matrix. In conventional necrosis, collagenases degrade the fibrous matrix, leaving unstructured acellular tissue [21]. Von Domarus et al. described necrobiosis in the synovial tissue in 23 out of 28 patients undergoing revision of MOP implants due to aseptic loosening, indicating that it is not simply associated with MOM implants [88]. That is consistent with the observation of necrobiosis in one mouse receiving UHMWPE, shown in section 3.5. Both of these results are consistent with the results

of Doorn et al, in which debris was implicated in the development of necrobiosis [21]. Von Domarus et al. states that this necrobiosis is not a sign of metal hypersensitivity [88], which is supported by the fact that none of the UHMWPE group mice received any metal in the pouch, excluding that as a possibility.

Some pouches contained multinucleated cells, often in close contact with the bone surface, which appeared consistent with osteoclasts, although specific staining, such as TRAP, would be necessary for definite identification. The identity of the lymphocytes as B-cells or T-cells could not be determined without immunohistochemical staining for markers such as CD3, CD4 or CD8, but given the general description of the adaptive metal responses as type IV hypersensitivities [57], they are expected to be primarily T-lymphocytes. The close attachment of the pouch membranes to the implanted bone, especially in erosion pits, is consistent with the appearance of inflammatory bone resorption described in Wooley et al. [35]. Wooley et al. observed a significant increase in osteoclasts and bone resorption pits in particle-stimulated pouches over those only receiving PBS [35], which would be expected in a more acute implantation period.

#### **4.5 Bone Density Measurements**

The IOD measurement itself is highly dependent on the consistency of staining intensity of the histological sections, which was somewhat variable in this study. However, visual inspection for areas of demineralization in each air pouch section supported the IOD measurement results of the different treatment groups, ameliorating the confounding effects of staining inconsistency.

There was little statistically significant difference in the implanted bone densities between the different groups. This may be due to the long implantation time. Several of the

PBS mice showed decreased bone density and increased inflammation related to bone resorption, indicating that a shorter implantation time might show more variation. The air pouch itself is inflammatory [82], and the relationship of chronic inflammation and osteolysis is recognized [3,19,89]. Therefore, the eventual destruction of the implanted bone is expected in an extended implantation, regardless of particle stimulation. The cut ends of the bone fragments were also observed to cause mechanical damage to the pouch membrane, which would further increase inflammation surrounding the bone independent of injected particles. Another possible cause would be the sensitization injections. If a systemic change in inflammatory and/or immune responses occurred, it would be reasonable that osteoclastic activity could also be upregulated, given the close relationship between bone metabolism and immunology [19].

#### **4.6 Effects of Particles on CIA Progression**

The development of arthritis was assessed throughout the study based on paw redness, swelling, and ankylosis. The onset and progression of arthritis in mice in each particle group was compared to determine whether the particles had any effect on the arthritis. There were no significant differences in arthritis progression between the groups receiving PBS, CoCr, or UHMWPE particles. No differences were seen in affected paw number or total paw score. This is not surprising, given that no major differences in cementless implant survival after successful osseointegration, are recorded between patients with rheumatoid arthritis and patients without inflammatory arthritis [78].

There are known differences between osteoarthritis and RA patients in the degree of osseointegration of an implant after insertion, which led to the recommendation of only placing cemented implants in RA patients [78,79]. RA disrupts bone homeostasis and causes decreased bone density and bone quality in affected joints. This poor quality bone, together with the

inhibited formation of new bone complicates the development of osseointegration with joint replacements, so bone cement is generally used to achieve a more stable junction at the bone-implant interface [78,79]. Another limitation of this study is that the particles were not introduced into any affected joint, so no definite correlation can be made to patients with TJA in arthritic joints, in which there would be local introduction of debris. A more relevant model would involve repeated intra-articular particle injections into affected joints, as this would better mirror the situation in RA patients with joint prostheses, in which the debris is generated over time in the arthritic joint. The intra-articular debris generation would be expected to cause more inflammation in the affected joint than in non-articular areas. It is unknown whether this intra-articular debris can exacerbate the course of the arthritis.

A second factor potentially influencing the relevance of this study was the fact that none of the animals were receiving any sort of treatment for the arthritis. Patients with RA are typically aggressively treated with DMARDs as soon as the diagnosis is reached [75,76], which has been shown to alter the biological response to debris [80]. Theoretically, it could be expected that untreated animals would be more likely to experience an alteration in arthritis progression, given the potentially unrestricted expression of pro-inflammatory cytokines, so the lack of the difference in untreated animals would be more definitive than the results of treated animals. It would be interesting to compare mice treated with DMARDs such as methotrexate or a TNF inhibitor. Because those treatments have similar effects on CIA as on RA, the animal responses would likely be relevant to those experienced in human patients.

## CHAPTER 5

### CONCLUSIONS

Hypersensitivity to metallic medical implant components is believed to be a relatively rare and poorly understood cause of implant failure. The pathological characteristics of metal hypersensitivity and other ARMDs remain unclear, but improved understanding is vital to improvements in implant longevity. The perceived rarity of implant failure due to metal hypersensitivity is supported by the low success of chromium sensitization in this study. The recent metal-on-metal implant failures and recalls have only increased the need for more information regarding the biological responses to metallic implants.

The inflammatory responses in the air pouches in this study showed more correlation with the type of particle introduced than whether they were sensitized to chromium, type II collagen, or KLH. The pouch thicknesses of all of the UHMWPE groups were consistently higher than the thicknesses of the CoCr groups, and the thicknesses of the PBS groups were consistently lower than either particle. The cell densities showed no significant differences between any of the study groups with large standard deviations, and some infiltration due to osteolysis. The mononuclear percentage of the membrane cells was significantly greater in the UHMWPE groups than the other groups with, aside from the control CoCr group, which had a large standard deviation. There was no significant difference between the different UHMWPE groups, indicating that none of the sensitizations affected the mononuclear cell response. The negative metal hypersensitive UHMWPE was not significantly elevated over the other particle groups, but this appeared to be due to a large standard deviation. The UHMWPE groups were the only animals with mononuclear cell percentages greater than 50%.

In contrast with the inflammatory response, the lymphocyte infiltration response in the pouches was much more variable. High variability led to a lack of significant differences between groups, which correlates well with clinical observations. The immune response was unpredictable regardless of sensitization. Importantly, perivascular lymphocyte cuffing was observed in some animals, showing that this model is capable of producing ALVAL-like pathologies.

The bone demineralization analysis, which is relevant to clinical osteolysis, was likely biased by the long implantation period, since even pouches without particles showed appreciable bone loss. The positive and negative metal hypersensitive CoCr group had a higher level of bone resorption than the positive and negative metal hypersensitive PBS groups, although the negative metal hypersensitive CoCr group was less significantly elevated. This result suggests that antibodies to chromium could encourage bone loss in the presence of CoCr particles, and potentially, that the sensitization injections alone may increase bone resorption. In general, the pouches without particles showed lower bone resorption than particle-laden pouches, except for the control PBS group. It is unknown why the control PBS group had the highest level of bone resorption of any group, suggesting that in the presence of particles, KLH antibodies are potentially anti-osteolytic. This is unlikely, and further study is required to verify this finding, as well as to test for the presence of antibodies to KLH. The level of bone resorption was equivalent between the CIA groups, indicating that CIA itself determines bone resorption, and that the presence and type of particles do not measurably affect the amount of resorption. To obtain more comparative data, this study should be repeated with a 10-14 day implantation, as this should allow evaluation prior to the generalized resorption occurring around day 28.

Based on this study, the overall inflammatory response was largely unaffected by any of the sensitizations. This suggests that the presence of material sensitivities or autoimmunities does not affect the inflammatory response to UHMWPE or CoCr particulate debris. The large variation in the immune responses as determined by histopathology precluded conclusions regarding the effects of metal hypersensitivities and autoimmune diseases on the immune responses to particles. This study showed a higher prevalence of perivascular lymphocyte cuffing among animals receiving either UHMWPE or CoCr particle injections, as opposed to PBS, which is consistent with the pathological description of ALVAL in periprosthetic tissue.

Although no clear effect of metal hypersensitivity on immune response to particles was observed, it is logical to assume that patient metal hypersensitivity could adversely impact the success of an implant, so patients should be tested for material sensitivities prior to insertion of joint prostheses. The presence of material sensitivity should be considered a contraindication for implantation of a metal-on-metal implant due to the metal particulate and corrosion product generation.

No effect of particle introduction was observed on the progression or severity of collagen arthritis, with regard to overall arthritis score or number of paws affected. These results suggest that rheumatoid arthritis likely does not cause decreased longevity of joint replacements, and the introduction of metal or UHMWPE particles does not appear to affect the course of the arthritis. Further work is required to assess the response to intra-articular debris in arthritic joints, as that is more likely to affect joint inflammation. It is important to realize, as well, that the results of a rodent study may or may not translate well to the conditions in humans. The lack of any effect of the particle injections on the course of the arthritis suggests that RA need not be a

contraindication for the use of joint replacements to improve quality of life in end-stage RA patients.

The results of this study did not confirm either of the working hypotheses. The inflammatory and immune responses to the particles did not vary between the different sensitization groups, suggesting that the sensitizations did not have a statistically significant effect on those responses. There was also no variation in bone resorption between the sensitization groups. Finally, the particles had no statistically significant effect on the progression of the arthritis.

## REFERENCES

## REFERENCES

- [1] Hosman AH, van der Mei HC, Bulstra SK, Busscher HJ, Neut D. Effects of metal-on-metal wear on the host immune system and infection in hip arthroplasty. *Acta Orthop.* 2010; 81(5): 526-534.
- [2] Rahaman MN, Yao A, Bal SB, Garino JP, Ries MD. Ceramics for prosthetic hip and knee joint replacement. *J Am Ceram Soc.* 2007; 90(7): 1965-1988.
- [3] Wooley PH, Schwarz EM. Aseptic loosening. *Gene Therapy.* 2004; 11: 402-407.
- [4] Watters TS, Eward WC, Hallows RK, Dodd LG, Wellman SS, Bolognesi MP. Pseudotumor with superimposed periprosthetic infection following metal-on-metal total hip arthroplasty. *J Bone Joint Surg Am.* 2010; 92(7): 1666-1669.
- [5] Edwards S. *Current concepts in total hip arthroplasty.* Accessed 12 March 2014. Available from: <http://www.hipandkneesurgery.ie/hips-conditions.html#bearing-options>
- [6] Watters TS, Cardona DM, Menon KS, Vinson EN, Bolognesi MP, Dodd LG. Aseptic lymphocyte-dominated vasculitis-associated lesion. A clinicopathologic review of an underrecognized cause of prosthetic failure. *Am J Clin Pathol.* 2010; 134: 886-893.
- [7] Ingham E, Fisher J. The role of macrophages in osteolysis of total joint replacement. *Biomaterials.* 2005; 26: 1271-1286.
- [8] Goodman SB. Wear particles, periprosthetic osteolysis and the immune system. *Biomaterials.* 2007; 28(34):5044-5048.
- [9] Langton DL, Jameson SS, Joyce TJ, Gandhi JN, Sidaginamale R, Mereddy P, Lord J, Nargol AVF. Accelerating failure rate of the ASR total hip replacement. *J Bone Joint Surg Br.* 2011; 93(8): 1011-6.
- [10] Haddad FS, Thakrar RR, Jart AJ, Skinner JA, Nargol AVF, Nolan JF, Gill HS, Murray DW, Blom AW, Case CP. Metal-on-metal bearings. The evidence so far. *J Bone Joint Surg [Br].* 2011; 93-A: 572-9.
- [11] Langton DJ, Jameson SS, Joyce TJ, Hallab NJ, Natsu S, Nargol AVF. Early failure of metal-on-metal bearings in hip resurfacing and large diameter total hip replacement. *J Bone Joint Surg Br.* 2010; 92-B(8): 38-46.
- [12] Migaud H, Putman S, Combes A, Berton C, Bocquet D, Vasseur L, Girard J. Metal-on-metal bearing: is this the end of the line? We do not think so. *HSSJ.* 2012; 8:262-269.

## REFERENCES (continued)

- [13] Nikoiaou VS, Petit A, Debiparshad K, Huk OL, Zukor DJ, Antoniou J. Metal-on-metal total hip arthroplasty. Five- to 11-year follow-up. *Bull NYU Hosp Jt Dis.* 2011;69: S77-83.
- [14] Langton DJ, Joyce TJ, Jameson SS, Lord J, Van Orsouw M, Holland JP, Nargol AVF, De Smet KA. Adverse reaction to metal debris following hip resurfacing. The influence of component type, orientation, and volumetric wear. *Bone Joint Surg Br.* 2011; 93-B(8): 164-71.
- [15] Pandit H, Vlychou M, Whitwell D, Crook D, Luqmani R, Ostlere S, Murray DW, Athanasou NA. Necrotic granulomatous pseudotumours in bilateral resurfacing hip arthroplasties: evidence for a type IV immune response. *Virchows Arch.* 2008; 453: 529-534.
- [16] Mabillean G, Kwon Y-M, Pandit H, Murray DW, Sabokbar A. Metal-on-metal hip resurfacing arthroplasty. A review of periprosthetic biological reactions. *Acta Orthop.* 2008; 79 (6): 734-747.
- [17] Matthies AK, Skinner JA, Osmani H, Henckel J, Hart AJ. Pseudotumors are common in well-positioned low-wearing metal-on-metal hips. *Clin Orthop Relat Res.* 2013; 470(7): 1895-1906.
- [18] Savarino L, Baldini N, Ciapetti G, Pellacani A, Giunti A. Is wear debris responsible for failure in alumina-on-alumina implants? Clinical, histological, and laboratory investigations of 30 revision cases with a median follow-up time of 8 years. *Acta Orthop.* 2009; 80(2): 162-167.
- [19] Catelas I, Wimmer MA, Utzschneider S. Polyethylene and metal wear particles: characteristics and biological effects. *Semin Immunopathol.* 2011; 33: 257-271.
- [20] Campbell P, Ebramzadeh E, Nelson S, Takamura K, De Smet K, Amstutz. Histological features of pseudotumor-like tissues from metal-on-metal hips. *Clin Orthop Relat Res.* 2010; 468: 2321-2327.
- [21] Doorn PF, Mirra JM, Campbell PA, Amstutz HC. Tissue reaction to metal on metal total hip prostheses. *Clin Orthop Relat Res.* 1996; 329S: S187-S205.
- [22] Hallab NJ, Jacobs JJ. Biologic effects of implant debris. *Bull NYU Hosp Jt Dis.* 2009; 67(2): 182-188.
- [23] Jazrawi LM, Bogner E, Della Valle CJ, Chen FS, Pak KI, Stuchin SA, Frankel VH, Di Cesare PE. Wear rates of ceramic-on-ceramic bearing surfaces in total hip implants. A 12-year follow-up study. *J Arthroplasty.* 1999; 14(7): 781-787.

## REFERENCES (continued)

- [23] Wimmer MA, Fischer A, Buscher R, Pourzal R, Sprecher C, Hauert R, Jacobs JJ. Wear mechanisms in metal-on-metal bearings: the importance of tribochemical reaction layers. *J Orthop Res.* 2010; 28: 436-443.
- [24] Archibeck MJ, Jacobs JJ, Roebuck KA, Glant TT. The basic science of periprosthetic osteolysis. *J Bone Joint Surg.* 2000; 82A: 1478–1497.
- [25] Park YS, Moon YW, Lim SJ, Yang JM, Ahn G, Choi YL. Early osteolysis following second-generation metal-on-metal hip replacement. *J Bone Joint Surg Am.* 2005; 87: 1515-1521.
- [26] Savarino L, Granchi D, Ciapetti G, Stea S, Donati ME, Zinghi G, Fontanesi G, Rotini R, Montanaro L. Effects of metal ions on white blood cells of patients with failed total joint arthroplasties. *J Biomed Mater Res.* 1999; 47(4): 543-50.
- [27] Cadosch D, Chan E, Gautschi OP, Filgueira L. Metal is not inert: role of metal ions released by biocorrosion in aseptic loosening—current concepts. *J Biomed Mater Res A.* 2009; 91.4: 1252-1262.
- [28] Hip Solutions. Zimmer. Accessed 12 March 2014. Available from: <http://www.zimmer.com/en-US/hcp/hip.jsp>
- [29] Harada S-I, Rodan G. Control of osteoblast function and regulation of bone mass. *Nature.* 2003; 423: 349-355.
- [30] Takayanagi, H. Inflammatory bone destruction and osteoimmunology. *J Periodont Res.* 2005; 40:287-293.
- [31] Pajevic PD. Regulation of Bone Resorption and Mineral Homeostasis by Osteocytes. *IBMS BoneKEy.* 2009; 6(2): 63-70.
- [32] Adamopoulos IE, Bowman EP. Immune regulation of bone loss by Th17 cells. *Arthritis Res Ther.* 2008; 10(5): 225.
- [33] Aderem A, Ulevitch RJ. Toll-like receptors in the induction of the innate immune response. *Nature.* 2000; 406: 782-787.
- [34] Medzhitov R, Janeway Jr CA. Innate immune recognition: mechanisms and pathways. *Immunol Rev.* 2000; 173: 89-97.
- [35] Wooley PH, Morren R, Andary J, Sud S, Yang S-Y, Mayton L, Markel D, Sieving A, Nasser S. Inflammatory responses to orthopaedic biomaterials in the murine air pouch. *Biomaterials.* 2002; 23: 517-526.

## REFERENCES (continued)

- [36] Anderson JM, McNally AK. Biocompatibility of implants: lymphocyte/macrophage interactions. *Semin Immunopathol.* 2011; 33: 221-233.
- [37] Pals ST, Horst E, Scheper RJ, Meijer CJLM. Mechanisms of human lymphocyte migration and their role in the pathogenesis of disease. *Immunol Rev.* 1989; 108: 111-133.
- [38] Norman MU, Hickey MJ. Mechanisms of lymphocyte migration in autoimmune disease. *Tissue Antigens.* 2005; 66: 163-172.
- [39] Medzhitov R, Janeway Jr CA. Innate immunity: the virtues of a nonclonal system of recognition. *Cell.* 1997; 91: 295-298.
- [40] Yano T, Kurata S. Intracellular recognition of pathogens and autophagy as an innate immune host defence. *J. Biochem.* 2011; 150(2): 143-49.
- [41] Yokota K, Miyazaki T, Hemmatazad H, Gay RE, Kolling C, Fearon U, Suzuki H, Mimura T, Gay S, Ospelt. The pattern-recognition receptor nucleotide-binding oligomerization domain-containing protein 1 promotes production of inflammatory mediators in rheumatoid arthritis synovial fibroblasts. *Arthritis Rheum.* 2012; 64(6): 1329-1337.
- [42] Schlesinger MJ. Heat shock proteins. *J Biol Chem.* 1990; 265(21): 12111-12114.
- [43] Kolev M, Towner L, Donev R. Complement in cancer and cancer immunotherapy. *Arch Immunol Ther Exp.* 2001; 59: 407-419.
- [44] Hao H-N, Zheng B, Nasser S, Ren W, Latteier M, Wooley P, Morawa L. The roles of monocytic heat shock protein 60 and toll-like receptors in the regional inflammation response to wear debris particles. *J Biomed Mater Res A.* 2010; 92(4): 1373-81.
- [45] Vermes C, Glant TT, Hallab NJ, Fritz EA, Roebuck KA, Jacobs JJ. The potential role of the osteoblast in the development of periprosthetic osteolysis. *J Arth.* 2001; 16(8): 95-100.
- [46] Boehm T. Design principles of adaptive immune systems. *Nature.* 2011; 11: 307-317.
- [47] Drayton DL, Liao S, Mounzer RH, Ruddle NH. Lymphoid organ development: from ontogeny to neogenesis. *Nat Immunol.* 2006; 7: 344-353.
- [48] Hallab N, Merritt K, Jacobs JJ. Metal sensitivity in patients with orthopaedic implants. *J Bone Joint Surg Am.* 2001; 83: 428-436.

## REFERENCES (continued)

- [49] Sidaginamale RP, Joyce TJ, Lord JK, Jefferson R, Blain PG, Nargol AVF, Langton DJ. Blood metal ion testing is an effective screening tool to identify poorly performing metal-on-metal bearing surfaces. *Bone Joint Res.* 2013; 2: 84-95.
- [50] Kim PR, Beaulé PE, Dunbar M, Lee JKL, Birkett N, Turner MC, Yenugadhati N, Armstrong V, Krewski D. Cobalt and chromium levels in blood and urine following hip resurfacing with the conserve plus implant. *J Bone Joint Surg Am.* 2011; 93 Suppl 2: 107-17.
- [51] Smolders JMH, Hol A, Van Susante JLC. Metal ion trend may be more predictive for malfunctioning metal-on-metal implants than a single measurement. *Hip Int.* 2013; 23 (5): 434-440.
- [52] Hart AJ, Satchithananda K, Liddle AD, Sabah SA, McRobbie D, Henckel J, Cobb JP, Skinner JA, Mitchell AW. Pseudotumors in association with well-functioning metal-on-metal hip prostheses. A case-control study using three-dimensional computed tomography and magnetic resonance imaging. *J Bone Joint Surg Am.* 2012; 94: 317-25.
- [53] Henderson RA, Lachiewicz PF. Groin pain after replacement of the hip: aetiology, evaluation, and treatment. *J Bone Joint Surg Br.* 2012; 94-B(2): 145-51.
- [54] Beaulé PE. A survey on the prevalence of pseudotumors with metal-on-metal hip resurfacing in Canadian academic centers. *J Bone Joint Surg Am.* 2011; 93(2): 118-21.
- [55] Merritt K, Rodrigo JJ. Immune response to synthetic materials. Sensitization of patients receiving orthopaedic implants. *Clin Orthop Relat Res.* 1996; 326: 71-79.
- [56] Yang J, Merritt K. Production of monoclonal antibodies to study corrosion products of co-cr biomaterials. *J Biomed Mater Res.* 1996; 31: 71-80.
- [57] Yang J, Merritt K. Detection of antibodies against corrosion products in patients after co-cr total joint replacements. *J Biomed Mater Res.* 1994; 28(11): 1249-58.
- [58] Jacobs JJ, Campbell PA, Kontinen YT. How has the biologic reaction to wear particles changed with newer bearing surfaces? *J Am Acad Orthop Surg.* 2008; 16(1): S49-S55.
- [59] Gao X, He R-X, Yan S-G, Yu L-D. Dermatitis associated with chromium following total knee arthroplasty. *J Arthroplasty.* 2011; 26(4): 665.e13-6.
- [60] Baeck M, Marot L, Nicolas J-F, Pilette C, Tennstedt D, Goossens A. Allergic hypersensitivity to topical and systemic corticosteroids: A review. *Allergy.* 2009; 64: 978-994.

## REFERENCES (continued)

- [61] Gawkrödger DJ. Metal sensitivities and orthopaedic implants revisited: the potential for metal allergy with the new metal-on-metal joint prostheses. *Brit J Dermatol.* 2003; 148: 1089-1093.
- [62] Mikhael MM, Hanssen AD, Sierra RJ. Failure of metal-on-metal total hip arthroplasty mimicking hip infection. A report of two cases. *J Bone Joint Surg Am.* 2009; 91:443-446.
- [63] Clements JN. Treatment of rheumatoid arthritis: a review of recommendations and emerging therapy. *Formulary.* 2011; 46: 532-545.
- [64] Steenbergen HW, Huizinga TWJ, van der Helm-van Mil AHM. The preclinical phase of rheumatoid arthritis, what is acknowledged and what needs to be assessed? *Arthritis Rheum.* 2013; 65(9): 2219-2232.
- [65] Schmidt EM, Davies M, Mistry P, Green P, Giddins G, Feldmann M, Stoop AA, Brennan FM. Selective blockade of tumor necrosis factor receptor I inhibits proinflammatory cytokine and chemokine production in human rheumatoid arthritis synovial membrane cell cultures. *Arthritis Rheum.* 2013; 65(9): 2262-2273.
- [66] Firestein GS. Evolving concepts of rheumatoid arthritis. *Nature.* 2003; 423: 356-361.
- [67] Aho K, Koskenvuo M, Tuominen J, Kaprio J. Occurrence of rheumatoid arthritis in a nationwide series of twins. *J Rheumatol.* 1986; 13: 899-902.
- [68] Klareskog L, Stolt P, Lundberg K, Kallberg H, Bengtsson C, Grunewald J, Ronnelid J, Harris HE, Ulfgren A-K, Rantapaa-Dahlqvist S, Eklund A, Padyukov L, Alfredsson L. A new model for an etiology of rheumatoid arthritis. Smoking may trigger HLA-DR (shared epitope)-restricted immune reactions to autoantigens modified by citrullination. *Arthritis Rheum.* 2006; 51(1): 38-46.
- [69] Jonsson T, Steinsson K, Jonsson H, Geirsson AJ, Thorsteinsson J, Valdimarsson H. Combined elevation of IgG and IgA rheumatoid factor has high diagnostic specificity for rheumatoid arthritis. *Rheumatol Int.* 1998; 18(3): 119-22.
- [70] Moore TL, Dorner RW. Rheumatoid factors. *Clin Biochem.* 1993; 26: 75-84.
- [71] Huang Q-Q, Sobkoviak R, Jockheck-Clark AR, Shi B, Mandelin II AM, Tak PP, Haines III GK, Nicchitta CV, Pope RM. Heat shock protein 96 is elevated in rheumatoid arthritis and activates macrophages primarily via tlr2 signaling. *J Immunol.* 2009; 182: 4965-4973.
- [72] Choy EHS, Panayi GS. Cytokine pathways and joint inflammation in rheumatoid arthritis. *N Engl J Med.* 2001; 344(12): 907-916.

## REFERENCES (continued)

- [73] Kwok S-K, Cho M-L, Park M-K, Oh H-J, Park J-S, Her Y-M, Lee S-Y, Youn J, Ju JH, Park KS, Kim S-I, Kim H-Y, Park S-H. Interleukin-21 promotes osteoclastogenesis in humans with rheumatoid arthritis and in mice with collagen-induced arthritis. *Arthritis Rheum.* 2012; 64(3): 740-751.
- [74] Kim S-J, Chen Z, Chamberlain ND, Volin, Swedler W, Volkov S, Sweiss N, Shahrara S. Angiogenesis in rheumatoid arthritis is fostered directly by toll-like receptor 5 ligation and indirectly through interleukin-17 induction. *Arthritis Rheum.* 2013; 65(8): 2024-2036.
- [75] Klareskog L, Van der Heijde D, De Jager JP, Gough A, Kalden J, Malaise M, Mola EM, Pavelka K, Sany J, Settas L, Wajdula J, Pedersen R, Fatenejad S, Sanda M. Therapeutic effect of the combination of etanercept and methotrexate compared with each treatment alone in patients with rheumatoid arthritis: double-blind randomized controlled trial. *Lancet.* 2004; 363: 675-81.
- [76] Korela M, Laasonen L, Hannonen P, Kautiainen H, Leirisale-Repo M, Hakala M, Paimela L, Blafield H, Puolakka K, Mottonen T. Retardation of joint damage in patients with early rheumatoid arthritis by initial aggressive treatment with disease-modifying antirheumatic drugs. *Arthritis Rheum.* 2004; 50(7): 2072-2081.
- [77] Cutolo M, Sulli A, Pizzorni C, Serio B. Anti-inflammatory mechanisms of methotrexate in rheumatoid arthritis. *Ann Rheum Dis.* 2001; 60: 729-735.
- [78] Zwartele RE, Witjes S, Doets HC, Stijnen T, Poll RG. Cementless total hip arthroplasty in rheumatoid arthritis: a systematic review of the literature. *Arch Orthop Trauma Surg.* 2012; 132: 535-546.
- [79] Zwartele R, Poll RG. Cemented total hip arthroplasty in rheumatoid arthritis. A systematic review of the literature. *Hip Int.* 2013; 23(2): 111-122.
- [80] Vasudevan A, DiCarlo EF, Wright T, Chen D, Figgie MP, Goldring SR, Mandl LA. Cellular response to prosthetic wear debris differs in patients with and without rheumatoid arthritis. *Arthritis Rheum.* 2012; 64(4): 1005-1014.
- [81] Wooley PH, Dutcher J, Widmer MB, Gillis S. Influence of a recombinant human soluble tumor necrosis factor receptor fc fusion protein on type II collagen-induced arthritis in mice. *J Immunol.* 1993; 151(11):6602-6607.
- [82] Ottaviani R, Wooley PH, Song Z, Markel DC. Immunological responses to hyaluronan preparations. *J Bone Joint Surg.* 2007; 89A: 148-157.

## REFERENCES (continued)

- [83] Pirmohamed M. Genetic factors in the predisposition to drug-induced hypersensitivity reactions. *The AAPS Journal*. 2006; 8 (1): E20-E26.
- [84] Dong W, Li X, Liu H, Zhu P. Infiltrations of plasma cells in synovium are highly associated with synovial fluid levels of APRIL in inflamed peripheral joints of rheumatoid arthritis. *Rheumatol Int*. 2009; 29: 801-806.
- [85] Kyburz D, Corr M, Brinson DC, Von Damm A, Tighe H, Carson DA. Human rheumatoid factor production is dependent on CD40 signaling and autoantigen. *J Immunol*. 1999; 163: 3116-3122.
- [86] Brand DD, Latham KA, Rosloniec EF. Collagen-induced arthritis. *Nat Protoc*. 2007; 2(5): 1269-1275.
- [87] Kanzaki S, Hilliker S, Baylink DJ, Mohan S. Evidence that human bone cells in culture produce insulin-like growth factor-binding protein-4 and -5 proteases. *Endocrinology*. 1994; 134(1): 383-392.
- [88] Von Domarus C, Rosenberg JP, Ruther W, Zustin J. Necrobiosis and t-lymphocyte infiltration in retrieved aseptically loosened metal-on-polyethylene arthroplasties. *Acta Orthop*. 2011; 82 (5): 596-601.
- [89] Aggarwal S, Gurney A. IL-17: prototype member of an emerging cytokine family. *J Leuk Biol*. 2002; 71: 1-8.